CHANGES IN CYTOSKELETAL ORGANIZATION DURING MYOTUBE FORMATION *IN VITRO*

A thesis submitted to the University of East Anglia
for the degree of Doctor of Philosophy

By
Melih Zeytinoğlu

School of Biological Sciences,
University of East Anglia,
Norwich, U.K.

1992

ACKNOWLEDGEMENTS

Throughout my postgraduate training I have benefitted from the help and guidance of so many people. Of course to my supervisor, Richard Warn who introduced me to the worlds of cell culture and immunofluorescence so many thanks for his infinite patience care and support throughout my time in his laboratory; In particular my thanks are also due to: Alan Prescott for considerable help, hints, techniques and advice; Eric Olson (U.S.A.) for his kind gift of CO25 and C2 cell lines; Alba Warn for her support, and understanding throughout this study; and Rick Gowing for bring me closer to the mysteries of electronmicroscopy. I would finally like to many thank all the staff of cell biology for their friendship.

DEDICATION

I would like to give thanks to the Turkish people who supported my study by generously paying their taxes. For this reason, this thesis is dedicated to Anadolu on which my genial people live.

ABSTRACT

The cytoskeletal changes accompanying CO25 myoblast differentiation, and transformation have been investigated using various techniques.

A very significant change in microtubule organization was found to occur upon inducing differentiation by transferring the cells into a medium containing horse serum. Elongation of the cells was accompanied by a change in microtubule distribution such that all the microtubules ran parallel to the long axis of the cells and the radial organization from centrosomes was lost.

The transient formation of primary cilia in the elongating cells was proceeded by an aggregation and fusion of all the centrioles within the cells. There seemed to be an apparent shift in microtubule nucleation centres from the centrosomes in myoblasts to a perinuclear distribution in myotubes. The capacity of these structures to nucleate microtubules was studied by allowing repolymerization after nocodazole treatment. The possible significance of these rather string changes in centriole organization, and in MTOC capacity, and the possible role of the primary cilia in myogenesis are discussed.

During the course of the research the antibody MPM-13, supposed to be a centrosomal marker, was used. A very variable distribution of peri-centrosomally located granules was identified in myoblasts with MPM-13. Double immunostaining experiments demonstrated that MPM-13 stained elements of the Golgi rather than a supposed centrosomal component.

Study of the distribution of actin cables showed that stress fibres were very rich in myoblasts, but decreased markedly in number as the myoblasts elongated. After fusion, an increase of F-actin cables occurred in newly formed myotubes, F-actin finally became highly organised in a periodic distribution along the myofibrils *in vitro* .

In transformed CO25 myoblasts, the distribution of F-actin was very variable. A few actin cables were seen in some cells which were attached to the substratum, but stress fibres were lacking in most cells, which were rounded cells in foci and not attached to the substratum. A possible relationship of these changes to the focal contacts is considered.

TABLE OF CONTENTS

REFERENCES :

CHAPTER 1

GENERAL INTRODUCTION

1.1. INTRODUCTION TO THE CYTOSKELETON

The cytoskeleton permeates the cytoplasm with an intricate three-dimensional array of interconnected filaments and tubules (Reviews, Amos and Amos, 1991; Bershadsky and Vasiliev, 1988). In the cytoplasm of eukaryotic cells, the three major types of structure forming the cytoskeleton are: microfilaments (5-10 μm in diameter), microtubules (22-25 μm), and intermediate filaments (7-11 μm).

Cytoskeletal fibres carry out a very wide spectrum of functions. These include: all the types of movements performed by and taking place within eukaryotic cells (e.g. Changes in cell shape, beating of cilia or flagella); they maintain the integrity of cell shape and form and also tissue integrity; provide a scaffold for cellular activities; form transport systems for the movement of organelles within the cell; divide chromosomes at mitosis, and separate daughter cells at cytokinesis, and many others. These and other sorts of movement arise through the activities of two basic systems, one of them involving microtubules and the other involving microfilaments.

The polymerisation of fibres from the protein subunits and the reverse process, depolymerisation, constitute one class of molecular reaction responsible for the rapid reorganisation of cytoskeletal structures. The second general mechanism for change and also force production is one filament sliding past another. Cytoskeletal fibres can be reversibly attached to a variety of types of other cellular structures. Thus the cytoskeleton can be regarded as part of a dynamic cytoplasmic matrix, surrounding and embedding other intracellular structures. This matrix may determine the position and movements of other cellular structures as well as the shape of the whole cell. The matrix may also be actively involved in the control of the metabolic activity of other organelles and of the whole cell.

This thesis considers the changing pattern of cytoskeleton organisation during myogenesis, and the roles of constituent in muscle cell differentiation, paying particular attention to microtubules and associated structures. A detailed description of each constituent of the cytoskeleton will be given in the Introduction of the appropriate Chapter.

1.2. INTRODUCTION TO SKELETAL MUSCLE

1.2.1. DEVELOPMENT OF SKELETAL MUSCLE

Limbs develop from mesenchyme that has its origin in the somatic layer of the lateral plate mesoderm in mammals (Charles, 1968; Gerald

and Berrill, 1981; Gray, 1989). At first, the segmented myotome appears as a discrete layer of cells between the dermatome and scleretome. In a short time, cells begin to leave this dorsal situated layer and invade the vertical and lateral plate region of the embryo. After the myotome has separated from the dermatome the individual myoblasts begin to line up with their long axes parallel and to stretch out into spindle-shaped cells and then form motubes and myofibrils. This bipolar shape distinguishes the myoblasts from the associated fibroblasts, which form the connective tissue elements of the muscle.

Myoblasts in tissue culture undergo the same morphological transformations as *in vivo*. During this process, fibres and granules within the cytoplasm of the myoblasts become aligned in rows lying parallel to the long axis of the cell. Myofibrils running the length of the cell then appear and become increasingly numerous until they fill the muscle cell, pushing the nuclei into eccentric positions against the cell membranes (Gerald and Berrill, 1981).

Mammalian myogenesis is characterised by four stages:

1- Determination, in which the muscle precursor cell population is generated;
2- Proliferation, in which the myogenic population is expanded;
3- Differentiation, in which the myoblasts become post-mitotic, fuse into multinucleated cells, and initiate synthesis of specialised contractile proteins;
4- Maturation, in which innervation and the final differentiation of muscle sarcomeres occur. This stage in characterised by the appearance of muscle specific forms of actin, myosin and related protein (Quinn *et al.*, 1990).

Developmental biologists often use the term determination to describe an event the complexities of which are little known. One of the paradoxes of developmental biology is that a given event may be interpreted either as an increase in specialised cell function or, conversely, as a decrease in the ability to perform alternative functions. It is believed that each cell of an organism is endowed with an equal genome potential, and that differences among embryonic cells occur as a cell or group of cells begin to show a limited capacity to express the full genomic potential. The cells of the primary germ layers are already determinated to a considerable extent and the event that causes such

determination must have occurred during gastrulation, or earlier (Review, Gurdon, 1977).

The earliest stages of differentiation remain poorly understood, but at some point during development a population of mesenchymal cells, which are capable of differentiating into a variety of tissue types such as cartilage, blood, or connective tissue, undergoes a further restriction in their ability to express their total content of genetic information and become channelled into the muscle-forming line of cells as myoblasts (Review, Gurdon, 1989). Myoblasts are spindle-shaped, mononucleated cells that develop the capability of producing some of the characteristic proteins of muscle. In these cells one can identify large polyribosome complexes on which myosin will be synthesised.

The next major phase in the cytodifferentiation of muscle is the fusion of individual myoblasts into myotubes. Originally it was not known if myotubes developed by fusion or by the internal multiplication of the nucleus of a single myoblast. The fusion model was shown to be correct by both cytospectrophotemetric studies of the DNA content of the nuclei in developing muscle and by studying the isoenzyme pattern of hybrid muscle fibres formed by fusion within early allophenic embryos from two different strains of mice (Nathanson, 1988).

A single myotube can be 10-15 μm in diameter and over 300 μm in length (Lin *et al.*, 1987). Mononucleated myoblasts fuse a forming syncytial myotube. The preparation of individual myoblasts for fusion appears to be coupled to a withdrawal from the cell-division cycle and fusion occurs only during the G1 phase (Bruce *et al.*, 1983). Myotubes engage intensively in the synthesis of contractile proteins and the contractile proteins assemble into regularly arranged myofilament arrays (Babai *et al.*, 1990; Schaper *et al.*, 1989).

The differentiation of myotubes into mature skeletal muscle fibres involves changes at a number of different levels. New nuclei are added to the myotube by the fusion of additional myoblasts. The nuclei of a myotube are large and contain prominent nucleoli, as would be expected of cells intensively engaged in RNA and protein synthesis (Review, Muntz, 1990). The contractile proteins of the myotube undergo a process of self-assembly into myofibrillar units, starting at the periphery of the myotube. As the myotube matures and a greater proportion of its volume is occupied by contractile proteins, the nuclei become more compact, the nucleoli lose their prominence, and the nuclei migrate from the centre of the myotubes toward the periphery. Only when the nuclei become

peripherally located, can the differentiating myotube be properly called a muscle fibre (Carlson and Faulkner, 1983).

1.2.2. THE REGENERATION OF SKELETAL MUSCLE

The satellite cell was first identified and named by Katz (1961) and also by Mauro and Adams (1961). It has been suggested that satellite cells may be the source of nuclei added to myofibres during tissue regeneration (Bischoff, 1986; Campion, 1984). The satellite cells have mitogenic potential and are involved in both the growth and regeneration of skeletal muscle. Following a variety of insults, skeletal muscle fibres break down and replacement of the damaged tissue is achieved by the development of these myogenic precursor cells. The sequence of events in many ways resembles the embryonic development of a muscle fibre (Carlson and Faulkner, 1983).

Skeletal muscle regenerates after a wide variety of injuries. There are several types of response. One type of regeneration, epimorphic regeneration, is found mainly in those amphibians capable of regenerating an entire limb after amputation (Carlson and Faulkner, 1983; Feldman and Stockdale, 1991). In epimorphic regeneration the tissues near the plane of amputation lose their adult structure and form a regeneration blastema, which is roughly the equivalent of the embryonic limb bud. A new limb develops from the blastema, and within that limb a new musculature develops in a manner that is both grossly and cytologically very similar to the normal ontogenetic sequence of events.

In mammals skeletal muscle regenerates in a manner different from that seen in the regenerating limbs of amphibians. A major difference is that regenerating mammalian muscle utilises the remnants of the original muscle fibre complex (Carlson and Faulkner, 1983). Mammalian muscle regeneration has been classically divided into two types, discontinuous and continuous. In discontinuous regeneration the entire muscle fibre or a portion thereof is completely destroyed, and a new muscle fibre is formed from myoblastic cells. Continuous muscle regeneration is described as the budding or outgrowth from the end of a partially damaged muscle fibres.

Muscle regeneration begins with some type of damage to the muscle fibre. The initial event consists of an intrinsic degeneration within the muscle fibre itself. This process is characterised by the breaking up of the myofibrils into individual sarcomeric units, the disruption of the mitochondria and the sarcoplasmic reticulum, and the

interruption of the continuity of the sarcolemma. After some types of initial damage such as ischaemia essentially all of the myofibrils and cell nuclei die and ultimately undergo dissolution. Whether all myonuclei die after all form of initial trauma has not been determined and remains controversial. Satellite cells, which are located beneath the largely intact basal lamina, then undergo an initial activation reaction (Bischoff, 1986). The activation reaction involves enlargement of the nuclei and increases in DNA synthesis, in cytoplasmic mass, and in the density of cytoplasmic organelles. A major difference between regenerating and embryonic muscle is the persistence of the basal lamina of the original muscle fibre (Carlson and Faulkner, 1983).

Cell division requires a precisely controlled re-organisation of the cell with co-ordinated changes in the organisation of the nucleus and of the cytoplasm. The process would be much more complex and difficult a task for a skeletal muscle cell, which contains many nuclei instead of one, and also has its cytoplasm crammed with highly ordered arrays of actin and myosin. In fact, skeletal muscle cells do not divide. Most skeletal muscle cells probably survive for the lifetime of the animal, but some are likely to be destroyed in one way or another. Replacements can be produced only by a reactivation of the process by which skeletal muscle is formed in the embryo (Bruce *et al.*, 1983). This process involves the action of precursor cells, also known as satellite cells (Nathanson, 1986).

1.3. INTRODUCTION TO THE CO25 CELL LINE

To investigate changes in the cytoskeletal organisation of differentiating muscle cells, it was decided to use the CO25 cell line. CO25 is derivative of a mouse line capable of differentiating into striated muscle cells, originally isolated by Yaffe and Saxel (1977) and called C2. C2 was derived as follows: the cell line was established from primary cultures taken from thigh muscle of 2-month-old mice 70 hours after injury. Whether it was derived from satellite cells or some other cell type was not known.

The CO25 line was obtained from C2 cells by transfection with a plasmid containing several copies of the human N-ras oncogene under transcriptional control of the steroid-sensitive promoter of the mouse mammary tumor virus long terminal repeat (MMTV-LTR) (Olson and Capetanaki, 1989). This promoter renders myoblasts sensitive to the induction of a transformed state and the inhibition of differentiation by

dexamethasone. Non-transformed CO25 cells have been found to be morphologically indistinguishable from nontransfected C2 myoblasts. In the absence of dexamethasone, fusion and induction of muscle-specific gene products were found to occur with kinetics indistinguishable from C2 myoblasts (Olson *et al.*, 1987). The induction of *ras* proteins in terminally differentiated myotubes was without effect on myotube morphology and on the expression of muscle-specific genes (Gossett *et al.*, 1988). *Ras* inhibited myogenic differentiation through a transient and reversible mechanism and this ras-dependent pathway interfered with an early step in the process of muscle-specific gene activation (Gossett *et al.*, 1988).

CHAPTER 2

MORPHOLOGICAL CHANGES DURING THE DIFFERENTIATION OF CO25 CELLS

2.1. INTRODUCTION TO MYOBLAST MORPHOLOGY

In order to investigate the roles of the cytoskeleton in the shape changes which accompany differentiation of muscle cells, it was first necessary to briefly characterize the manner in which CO25 cells differentiate. At the same time some study was made of the effects of transformation upon the cells as the result of the switch on of the N-*ras* gene using dexamethasone. The changes which occur during myoblast differentiation and transformation, are described in this chapter and compared with what is known for other cell types. An introductory description of myotube and myofibril formation has already been given in the General Introduction.

2.2. MATERIALS AND METHODS

2.2.1. CELL CULTURE

2.2.1.1. CELL TYPE

The CO25 myoblast cell line, which contains a few copies of the human N-*ras* oncogene encoded on a plasmid, was originally obtained from Dr. E. N. Olson (The University of Texas, U.S.A.).

2.2.1.2. CULTURE MEDIA

Cells were cultured in Dulbecco's Modification of Eagles Medium (DMEM) (Gibco) supplemented with 10% Foetal Calf Serum (FCS) (Gibco), which is described as the growth medium, in 10% Horse Serum (HS) (Gibco) which is described as the fusion medium, or in 10% Foetal Calf Serum or in 10% Horse Serum with 1μM dexamethasone (Sigma). Both these media were used to cause transformation of the cultures. 100 U/ml penicillin, and 100 mg/ml streptomycin were added to the media which were stored at 4 °C.

2.2.1.3. CELL CULTURE

The cells were cultured in either the growth medium or the fusion medium. In both media, the cells were grown in an atmosphere of 90% air, 10% carbon dioxide at 37 °C. After cells reached 70-80% confluence in the growth medium, it was replaced with fusion medium to allow differentiation to occur. Cells grew and differentiated only very slowly if they were seeded directly into fusion medium containing 10% horse serum. Cells were cultured in flasks (25 cm^2, 5 ml, Gibco) or plastic

petri dishes (30 mm diameter, Sterilin) and the medium was changed once per day.

2.2.1.4. TRYPSIN SOLUTION

Trypsin solution consisted of 10 ml Puck A saline (0.7 ml 5% $NaHCO_3$, 0.33 ml 300 mM EDTA in 100 ml sterile distilled water), plus 25 ml 10X Trypsin/EDTA (Gibco). It was stored at -20 ^{o} C.

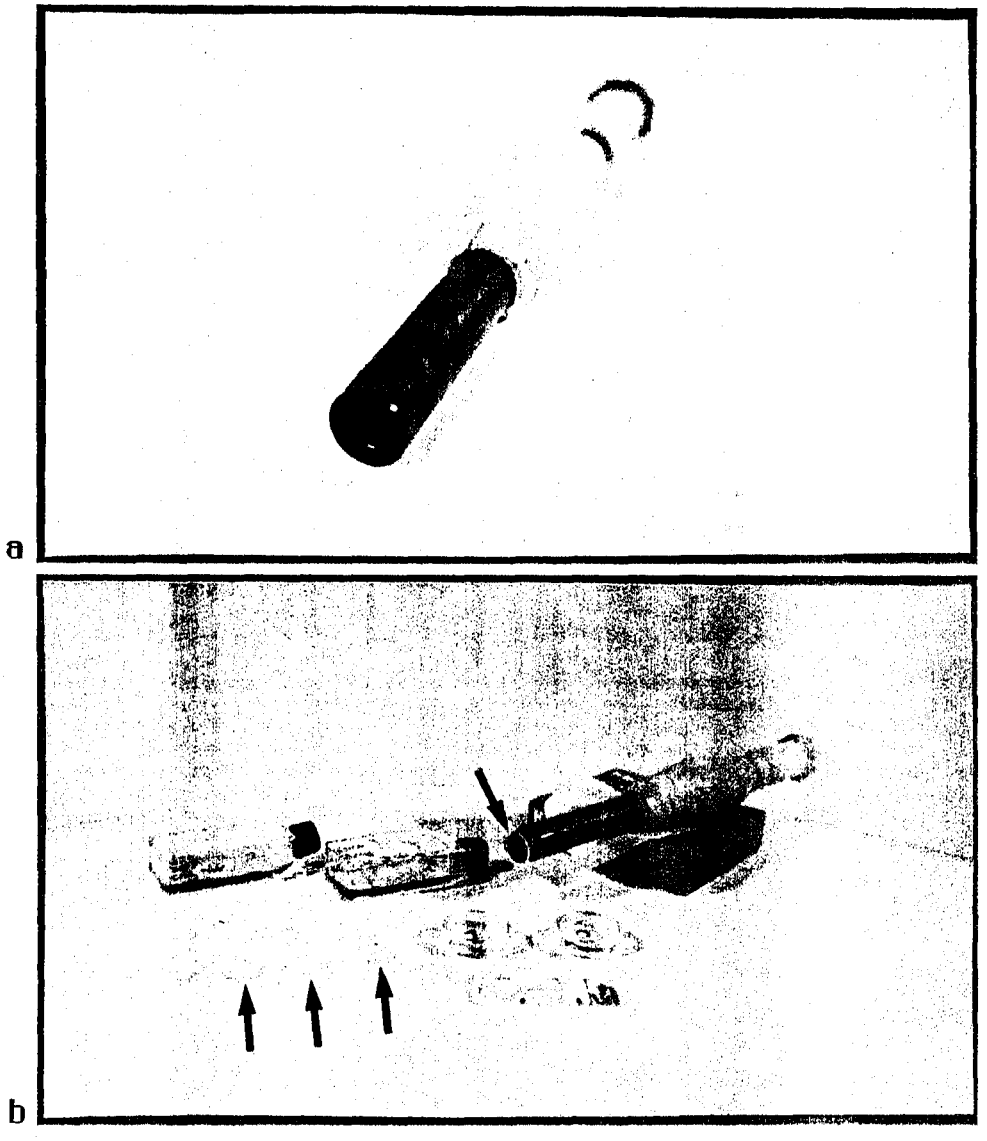

FIG.-1 : The cork borer (a and b) and plastic discs (arrows on b) are obtained by melting the flasks.

2.2.1.5. PREPARATION OF PLASTIC DISCS

After growing the cells in a flask, pieces of the flask were removed by melting through the flask surface with a heated cork borer (30

seconds heating with a bunsen) to remove a disc (2 cm diameter). The cork borer and some plastic discs made from the flasks are shown in Fig. 1 . This method was adopted after attempts to grow the cells on glass coverslips, covered with a variety of substrates, did not succeed in eliminating the problem of cell loss during preparation for fluorescence microscopy.

2.2.2. BUFFERS

2.2.2.1. PBS

Phosphate buffered saline (PBS) consisted of 137 mM NaCl, 2.7 mM KCl, 1.5 mM KH_2PO_4, 8 mM Na_2HPO_4, at pH 7.3. PBS/BSA contains 0.02% bovine serum albumin (BSA) in the solution.

2.2.3. FIXATIVES AND FIXATION

2.2.3.1. GLUTARALDEHYDE

Cells grown on glass or on plastic coverslips were washed with PBS and then fixed with 2.5% glutaraldehyde in PBS (pH 7.2) at room temperature for 15 minutes. After fixing the cells were washed with 3 changes of PBS.

2.2.4. MICROSCOPY

2.2.4.1. INVERTED MICROSCOPY

Cells were examined directly in the flasks or petri dishes using a Nikon TMS inverted microscope equipped with optics as described in section 2.2.5.. Photographs were taken as described in section 2.2.6..

2.2.4.2. SCANNING ELECTRON MICROSCOPY

Cells were grown on round glass coverslips (13 mm diameter) and washed with PBS for 3 X 30 seconds at room temperature. They were fixed with 2.5% glutaraldehyde in PBS described in section 2.2.3.1., then washed with PBS for 15-30 minutes at room temperature, and postfixed with 1% osmium tetroxide in PBS for 5-10 minutes at room temperature. After washing with distilled water for 3 X 30 seconds, they were then dehydrated with an ethanol series (50%, 70%, 90%, 100%) for 5 minutes. The cells on the coverslips were placed in the chamber of a pressure bomb using a Poleron critical point drier. The bomb was filled with liquid carbon dioxide and the temperature of the pressure bomb was raised. The critical pressure was approximately 1081 lb/m^2 for carbon dioxide in the Poleron critical point drier. After critical point drying, the

samples were coated with a thin layer of gold (approximately 200 angstroms thick) in an argon atmosphere for 5 minutes. An Edwards S 150 B Sputter Coater was used to coat with gold.

Samples were examined in a Hitachi S 800 scanning electron microscope. Photographs were taken as described in section 2.2.6..

2.2.5. LENSES AND FILTERS

2.2.5.1. LENSES AND FILTERS FOR INVERTED MICROSCOPY

X10/0.25 Ph1 DL, X20/0.4 Ph2 DL, and X40/0.55 Ph3 DL objectives and a condenser with N.A. 0.1, N.A. 0.2, or N.A. 0.3 were used with the inverted microsope. A green filter was used to enhance resolution and visualization of the cells.

2.2.6. PHOTOMICROSCOPY

2.2.6.1. CAMERAS

Photographs were taken using a Nikon F-301 camera for inverted microscopy, and Mamia 50A roll film holder for transmission and scanning electron microscopy.

2.2.6.2. FILMS

The following films were used: Kodak Tri X-Pan 400 for inverted microscopy, and Ilford FP4 120 and FP5 (6.5X9.0 cm) for SEM,

2.2.6.3. PHOTOGRAPHIC SOLUTIONS

A- Developer solutions; 12.5% Acuspeed, 87.5% distilled water. The films were washed with developer solution for 8 minutes at room temperature, and shaken every 20 seconds for 20 seconds.

B- Stopper solution; 20% Hypam, 2% Hardener, 78% distilled water. The films were washed with developer solution for 5 minutes at room temperature, and shaken every 20 seconds for 20 seconds.

After processing, all films were washed with warm water for 30 minutes. 3 drops of anti-static were added to the last rinse.

2.2.6.4. PHOTOGRAPHIC PAPER

Ilford multigrade III RC rapid photographic paper was used.

2.3. RESULTS

2.3.1. INDUCTION OF MYOTUBE FORMATION

2.3.1.1. RESOLUTION OF CULTURE PROBLEMS WITH CO25 CELLS TO INDUCE DIFFERENTIATION

Cells were seeded onto glass coverslips in petri dishes and allowed to proliferate in growth medium (as described in section 2.2.1.). CO25 cells grew rapidly in this medium when supplemented with 10% FCS but did not differentiate. After the cells reached until 70-80% confluence, this medium was replaced with the fusion medium (as described in section 2.2.1.2.), and the medium was changed once a day. Under these conditions, cells ceased proliferation but did not form myotubes. The problem was not due to either the pH or to problems with particular batches of horse serum, since a variety of pHs and horse sera were examined. A further approach to stimulate differentiation was the use of DNA replication inhibitors (Tomasz *et al*, 1987; Lin *et al.*, 1989; Hinterberger and Barald, 1990). Mitomicin-C (Sigma) at a concentration of 0.05 mg/ml or Cytosine β -D- Arabinofuranoside -5'-Monophosphate (Sigma) at a concentration of 15 mM were added to the myoblasts in the fusion media. No myotubes were formed as the result of the addition of these molecules.

A further problem was the lack of adhesion of the cells to the surfaces. After 2-3 days incubation on glass coverslips in the fusion medium the cells totally covered the surface of the coverslips. However when the medium was changed or while the cells were washed during immunostaining the cells became detached in sheets. It was an evident that the normal way of growing cells for immunofluorescence microscopy was not satisfactory for this cell type.

One possibility was that coating the coverslips might overcome the adhesion problem and also provide a better anchorage of the cells for differentiation. Coverslips were coated with one of the following: poly-L lysine (0.01% w/v; Sigma; Leifer *et al.*, 1984), type IV collagen (0.1% in 0.1 N acetic acid; Sigma; Goldberg *et al*, 1989; Sanderson *et al*, 1986), gelatin (2%; Sigma; Yaffe, 1973), or fibronectin (1-5 mg/cm^2; Sigma; Grant and Tseng, 1986) before the cells were seeded. However better adhesion of the cell was not obtained and no formation of myotubes was observed using any of the above.

Eventualy the cells were grown in tissue culture flasks in the presence of 10% horse serum in DMEM, and the medium was changed 7-10 times a week. Under these condition, the cells formed myotubes

without coming off from surface of the plastic flasks during fixation or washing. It was therefore decided to grow cells in plastic flasks and to prepare cells for fixation by punching out a disc from the base as described in section 2.2.1.5. Thus positive results were obtained simply with uncoated flasks. So, cells seeded into flasks were mainly used in this study.

2.3.1.2. OBSERVATIONS OF CELL GROWTH IN DIFFERENT MEDIA

Approximately $3.5x10^3$ of cells in 1 ml. volume were seeded into flasks to examine the effects of four different media on cell grown . These media were: DMEM, DMEM with 10% foetal calf serum, DMEM with 10% horse serum, DMEM with 10% horse serum plus 1µM dexamethasone. Cells were then fed for up to two weeks in these media. The medium was replaced to fresh medium every day. The numbers of the cells grown in these different media were counted after one, three, five, ten, and fourteen days (Table-1; Graph-1). Counting of cells was done five times for each sample and the average was taken.

Medium / Time	DMEM	Growth medium	Fusion medium	Fusion medium + Dexame-thasone
At start	36.864	36.864	36.864	36.864
After 1 day	74.400	110.080	61.520	98.768
After 3 days	13.520	218.896	103.040	236.816
After 5 days	15.136	463.008	103.856	504.688
After 10 days	17.568	578.112	104.016	768.736
After 14 days	19.584	621.024	104.128	965.232

TABLE-1 : Growth characteristics of CO25 cells grown in the different media. The cells were counted 5 times for each sample and the average taken.

In the first day in the media, no significant differences were observed in the proliferation of the cells and all cultures showed significant cell doubling. However, during consecutive days in culture, the effects of the media on cell proliferation became clear; proliferation increased by over approximately twofold on the second day in all media.

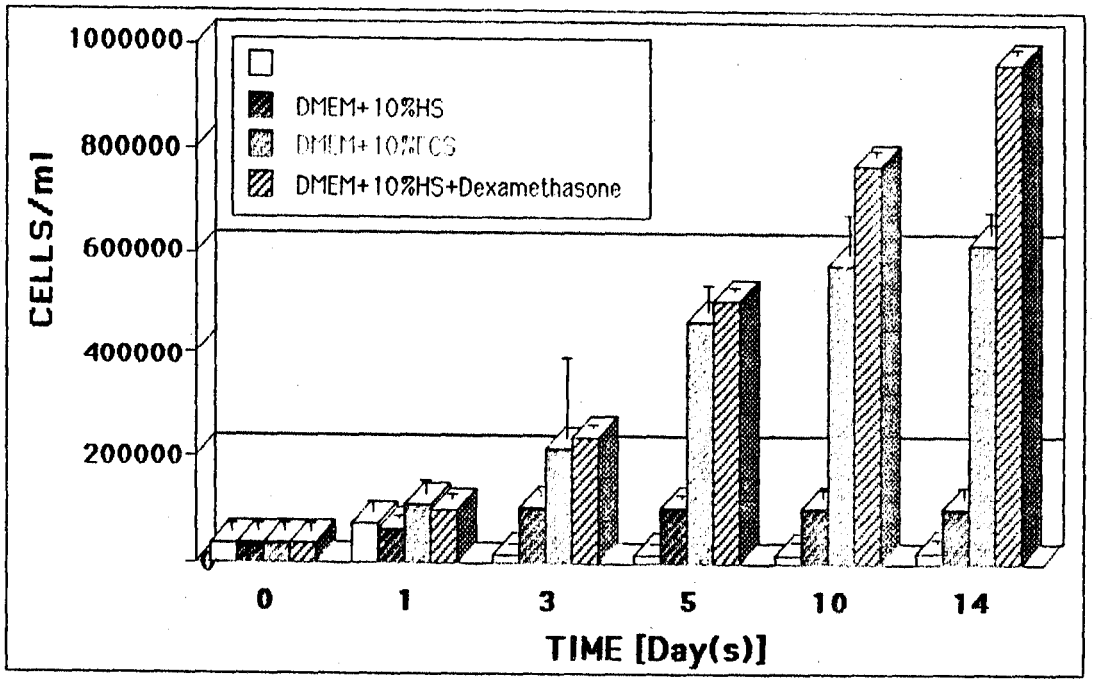

GRAPH-1 : Growth characteristics of CO25 cells grown in different media. Data for graph taken from Table-1. Bars indicate maximum values found.

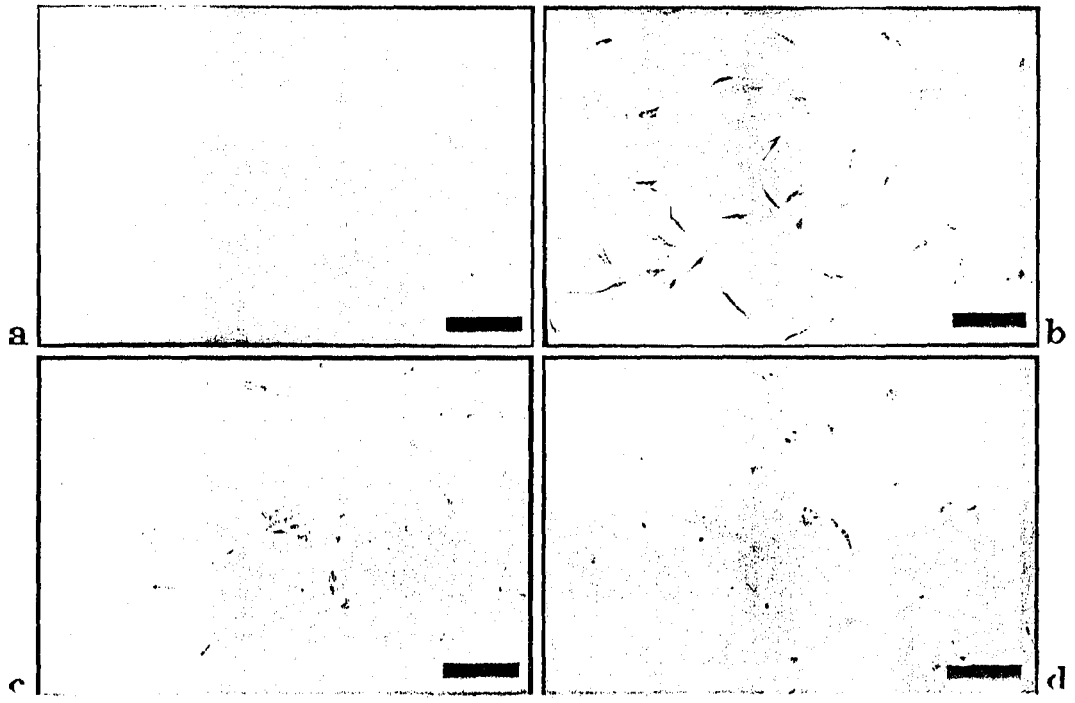

FIG.-2 : Culture of CO25 cells in DMEM alone,. Cells were directly observed in the inverted phase microscope (a) soon after plating out, (b) after 24 hours, (c) 3 days, and (d) 14 days; Bars= 100 µm .

Graph-1 demonstrates that little growth occurred in the medium containing only DMEM, as would be expected. In DMEM, the number of cells only increased on day 1, significant cell death occurred by three days(Fig. 2). After 3 days, some cells became sticky and formed clump or colonies (Fig. 2b). These clumps of the cells stayed together in the clumped form. The morphology of the surviving cells became aberrant after three days. Suprisingly some odd clumped cells were still present after 14 days culture in DMEM alone (Fig.2d). Individual cells had no processes, and also many dead cells were seen in cells cultured in DMEM alone (Fig. 2c, d). When the cells were cultured in DMEM with 10% foetal calf serum, the number of cells was increased approximately ten-fold after four days (Table-1; Graph-1; Fig. 3). Cell proliferation continued until they reached confluence, which occurred between 4-7 days, after which growth reached a plateau but continued up more slowly (Table-1; Graph-1).

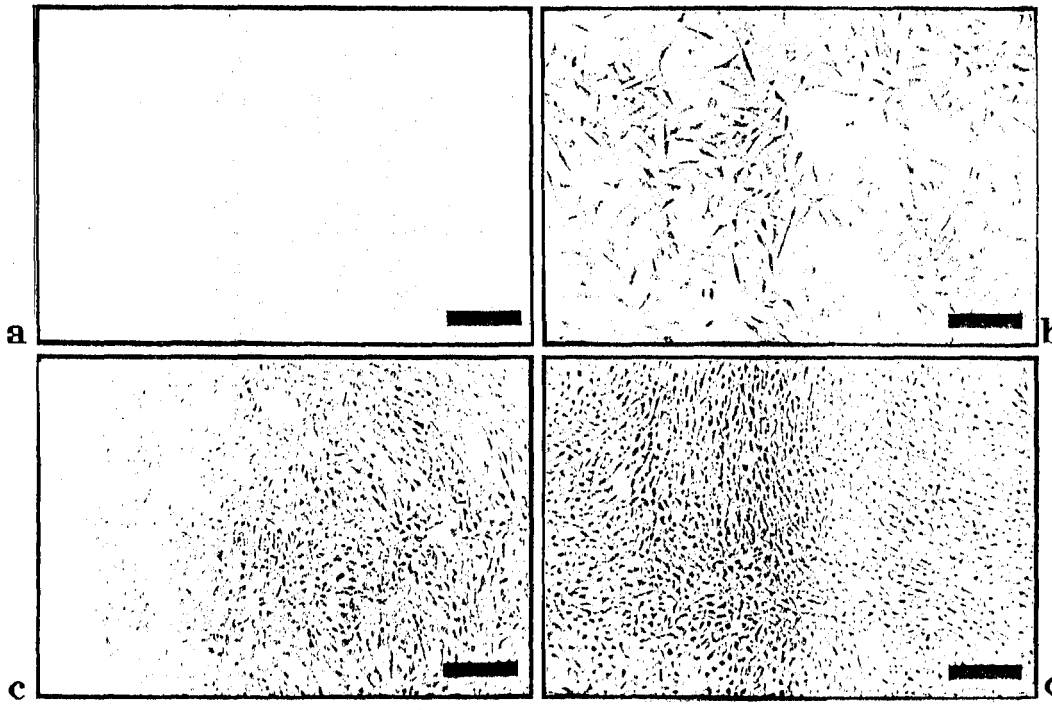

FIG.-3 : Culture of CO25 cells in the growth medium (DMEM + 10% foetal calf serum), (a) soon after plating out, (b) after 24 hours, (c) 3 days, and (d) 2 weeks; Bars= 100 µm.

The cells were polygonal in shape (Fig. 3b), and they had one or more long processes (Fig. 3b). In the growth medium, the cells became

smaller when they reached confluence in the culture (Fig. 3c). At high cell densities there was some cell overgrowth (Fig. 3d).

The number of cells in the horse serum, increased rapidly over the first three days and then reached a clearcut plateau, representing cessation of growth. The cells were dividing rapidly for the first 3 days, they then stopped dividing (Table-1; Graph-1; Fig. 4). This cessation of division corresponds to the onset of differentiation (Fig. 4c). Fusion medium is proposed to stimulate mitogenic activity that supports the growth of cells at low densities. After 3 days this was halted completely. The shape of the cells was polygonal and they also had processes after 3 days when they became confluent (Fig. 4c). Their shapes changed from polygonal to ovoid, and they became progresively localized parallel to each other (arrow on Fig. 4c). Then they fused to form myotubes in the culture (arrow on Fig. 4d).

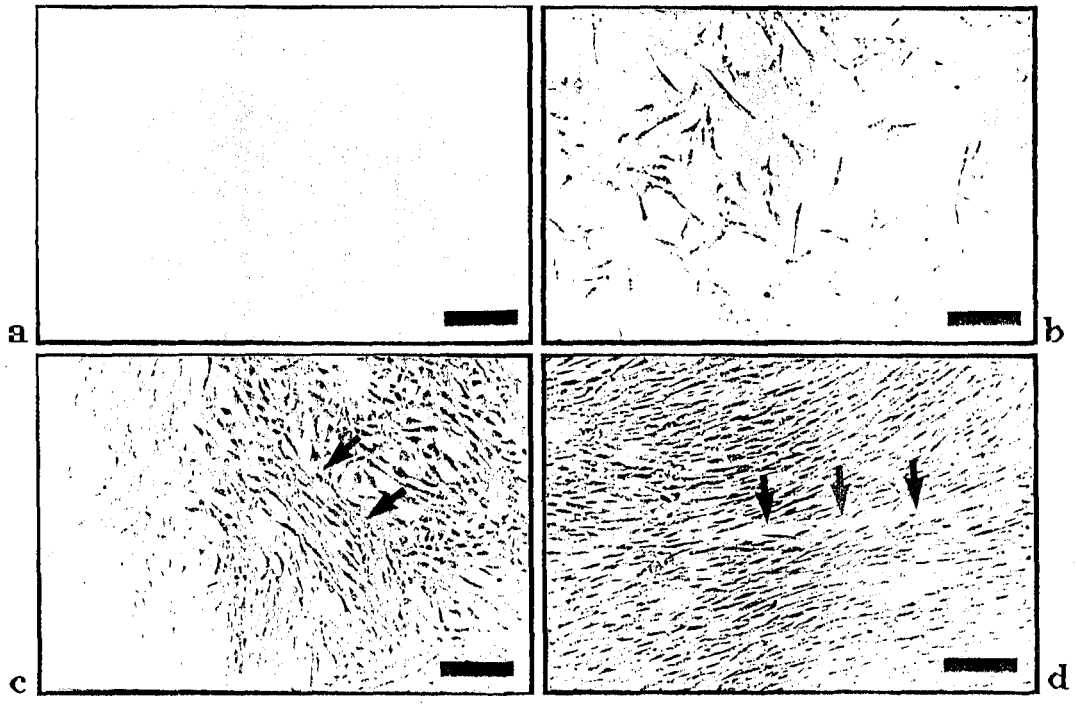

FIG.-4 : Culture of CO25 cells in the fusion medium (DMEM + 10% horse serum), (a) soon after plating out, (b) after 24 hours, (c) 3 days, arrows, ovoid cells became parallel to each other, and (d) 2 weeks, arrows, a formed myotube by fusion of cells; Bars= 100 µm

In contrast, cells grown in horse serum containing dexamethasone continued rapid proliferation (Graph-1) even after they reached confluence (at about 5 days cf. Table-1, and Fig. 5). The shape of the

cells was polygonal, and they had long thin processes, also most of them were localized by sticking together (Fig. 5b). Their shape became thinner, and also they grew on the top of each other (Fig. 5c). Transformed cells formed foci after 3 days. The cells which were in the foci had a more rounded shape (Fig. 5d), but the cells under the foci which adhered to the flask were seen as long thin cells (Fig. 5d). This is typical of transformed cells where overgrowth, associated with foci formation occurs (Fig. 5d).

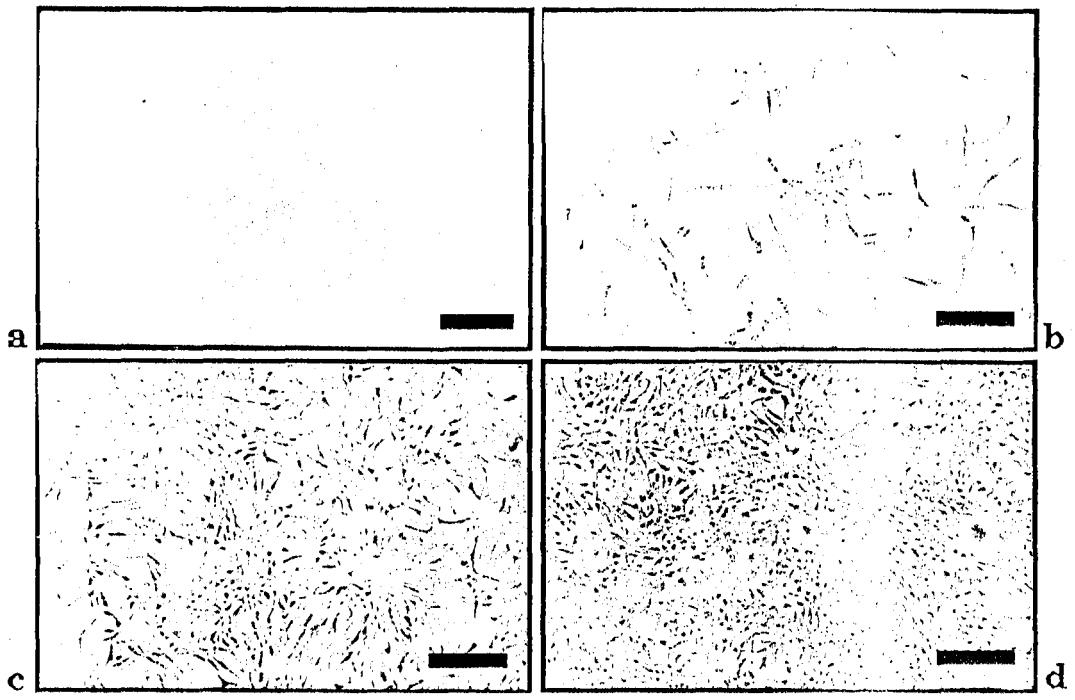

FIG.-5 : Culture of CO25 cells in the differentiation medium (DMEM + 10% horse serum + 1µM dexamethasone), (a) soon after plating out, (b) after 24 hours, (c) 3 days, and (d) 2 weeks; Bars= 100 µm

2.3.2. CHANGES IN CELL MORPHOLOGY DURING DIFFERENTIATION

During myogenesis, three main morphological stages of differentiation could be identified in CO25 cells; elongating myoblasts, fusing to form myotubes, and maturating to myofibrils.

2.3.2.1. ELONGATION

Undifferentiated CO25 myoblasts exhibited a flattened stellate shape in DMEM containing 10% foetal calf serum (Fig. 6a).

After two days when the cells reached 70-80% confluence, the growth medium was replaced by fusion medium. As a consequence withdrawal from the cell cycle occurred and the cells underwent elongation and differentiation. A consideration of Fig. 6b shows that, after two days in the fusion medium, many of the cells became considerably elongated and they were in the process of aligning one with the next. The polygonal shape of the undifferentiated cells was lost. Such cells had a rather round cell body, and the long thin terminal processes were drawn out at either end. There was no particular area where elongation of the cells started, but there must be some influence which aligns the cells as they lengthen (Fig. 6b). First, their shape became ovoid but without any significant processes.

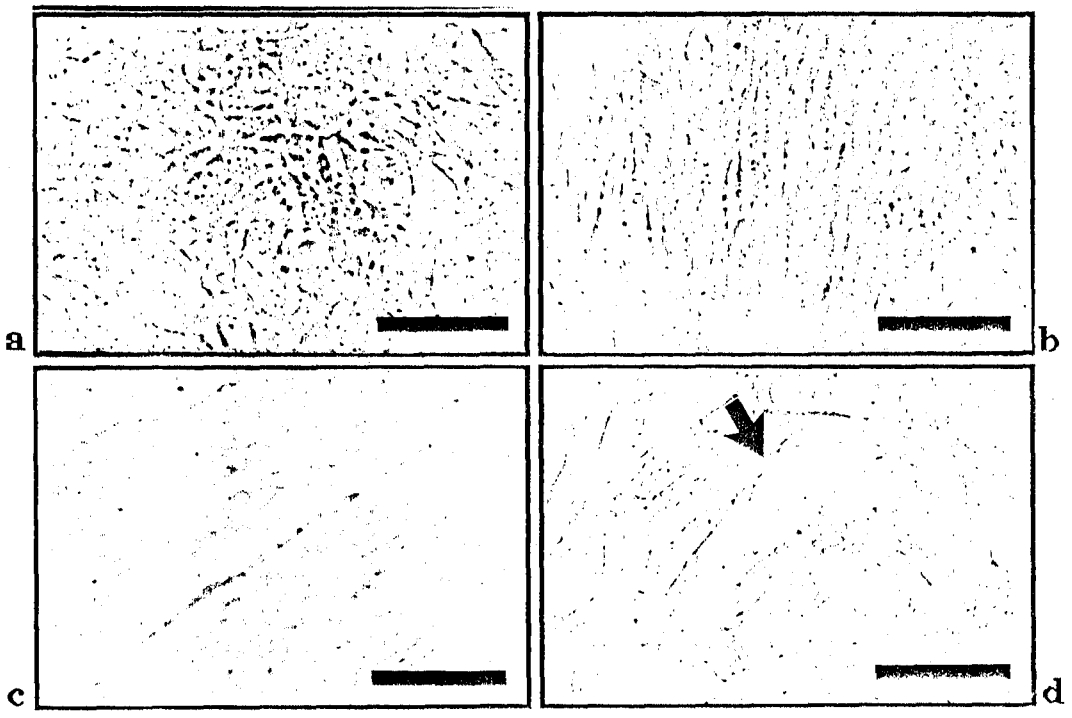

FIG.-6 : The cells were grown (a) in the growth medium for two days, (b, c, d) in the fusion medium for 2 days showing elongation, arrow shows the processes of elongating myoblasts stretched over the other cells; Bars - 50 μm .

Usually phase-bright edges to the cells were observed in the elongation phase. In this stage of differentiation the cells became raised above the surface of the culture (Fig. 6c). Then long thin processes formed as tails from the two opposite termini of the ovoid cell bodies.

So spindle shaped cells appeared in the culture (Fig. 6d). The processes of elongating myoblasts strecthed over the other cells (Arrow Fig. 6d).

2.3.2.2. FUSION

2 days after transfer to fusion medium, the cells made contact with each other and began to fuse (Figs. 7a, b, c). During the fusion stage of differentiation which was a very short period of about half an hour, the cells became much more elongated and had long thin processes. These elongated cells with long processes were frequently parallel to each other (Fig. 7a, b, c). During this stage, the processes of elongated cells were seen to touch together and fuse at the ends (arrows Fig. 7a, b, c). The other cells were beneath the touching cells (cf. Fig. 7c, d). After the fusion stage, the processes of the cells became thicker (arrows show on Fig. 7d).

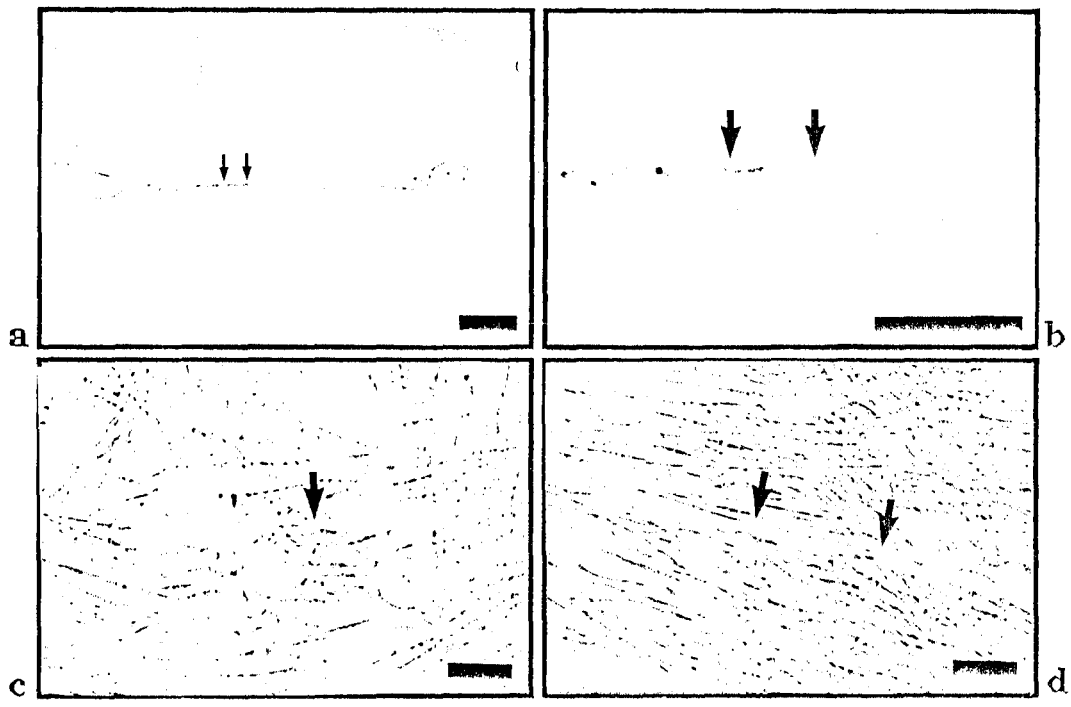

FIG.-7 : CO25 myoblasts during fusion in the fusion medium after 2 days; region of fusion (a) low power, (b) high power, (c) field showing cells in various stages of elongation and two newly fused cells above, arrows, touching of the thin processes of elongated cells, (d) field showing a later stage with more fused cells, arrows show that the processes became thicker after fusion; Bars= 20 µm.

2.3.2.3. FORMATION OF MYOTUBES

During fusion, the forming myotubes appeared as phase bright as unfused cells (Fig. 7c, d). After fusion, the phase bright edges of the cells gradually disappeared (Fig. 8a, b, c, d). The fusion region in these cells became thicker, thus the cells became shorter or seemed to be shorter than before (Arrows Fig. 8a, b). Normally by 4 days in the fusion medium, the cells ceased proliferation and colonies of cells contained the dense networks of long multinucleated fibres. This process did not occur simultaneously in all cells in the same culture. More and more myoblasts gradually fused into myotubes which became progressively larger (Fig. 8b, c). During myotube formation and maturation, lateral fusion of the cells was observed (thin arrow show on Fig. 8c). Progressively thicker myotubes were formed, but there was no uniform thickness for them (Fig. 8c, d).

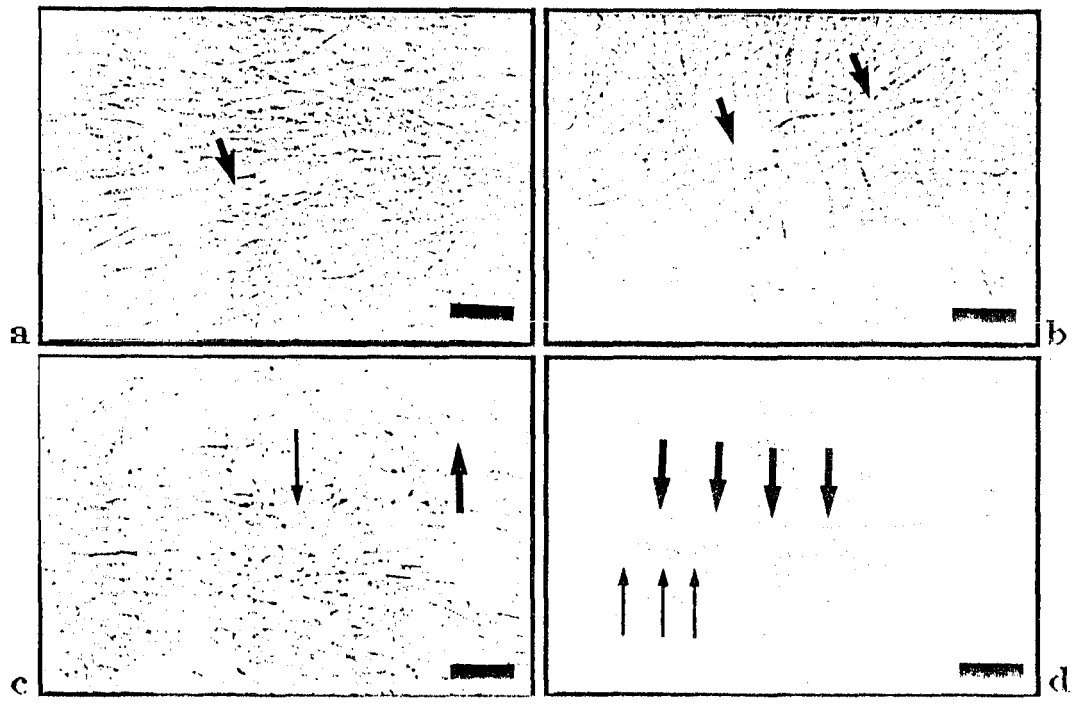

FIG.-8 : CO25 myoblasts during formation of myotubes and then myofibrils in fusion medium; (a) fusion progress after 4 days, (b) early stages of myotubes, arrows, showing the fusion region of the cells became thicker, (c) late stage myotube after 5 days, thin arrow, lateral fusion, thick arrow, clumping of nuclei in a new formed myotube, (d) maturation of myotubes to myofibril after 2 weeks, thin arrows, spaces between nuclei in a myofibril, thick arrows, striated pattern of a myofibril; Bars= 20 µm.

The clumping of nuclei were seen in the some of the new formed myotubes (thick arrow shows on Fig. 8c). In the older myotubes some spaces were observed between nuclei (thin arrows show on Fig. 8d). In the mature differentiated cells, the maximum diameters were very variable (Fig. 8d). Within these myofibrils only linear arrays of nuclei were visible, but they were localized usually in the middle of the myotube (Fig. 8d). The striation pattern was more visible at the borders of the myofibrils (thick arrows show on Fig. 8d).

2.3.3. CHANGES IN MORPHOLOGY DURING TRANSFORMATION

As described previously, CO25 cells had a polygonal shape in foetal calf serum and formed a monolayer in this medium with only a few cells overlapping by occasional thin processes(fig. 3d, 6a). After one or two days of culture in the presence of 1μM dexamethasone, the shape of some of the cells was triangular (Fig. 9a). The cells became smaller than before and the cell bodies rounded up. Many thin long processes were also visible (Fig. 9a). Transformed cells usually form multilayered sheets and spherical aggregates and CO25 cells followed this rule to form foci. After two days, the cells began to overgrow each other, forming multilayers and their average size became further reduced (Figs. 9a).

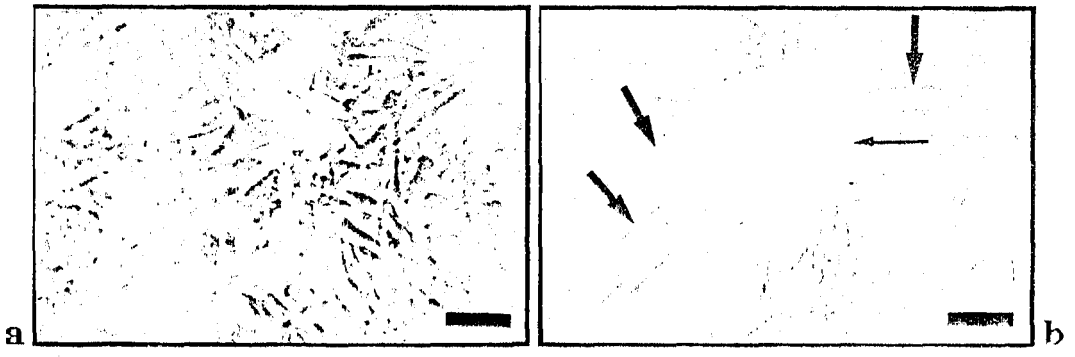

FIG.-9 : Effects of dexamethasone in fusion medium on morphology of CO25 cells after (a) 2 days, and (b) 4 days, thin arrow, rounded cells in a foci, thick arrows, long thin processes of the cells under the foci; Bars= 20 μm.

By four days, the foci were much larger (Fig. 9b). In this stage, there were two different morphologies of the transformed cells in the culture: cells in a rounded shape which were in the foci (thin arrow

shows on Fig. 9b), and some cells with long thin processes which were under the foci (thick arrows show on Fig. 9b).

2.3.3.1. REVERSIBILITY OF MORPHOLOGY AFTER TRANSFORMATION

The action of various oncogenic agents, such as chemical carcinogen, on cells in culture leads to the appearance of cells with relatively stable alterations in morphology. These genetically stable alterations in cell morphology are usually designated morphological transformations. In the presence of dexamethasone, suppression of differentiation occurred rapidly. Dexamethasone was withdrawn from the fusion medium to observe what change in the behaviour of the cells might occur.

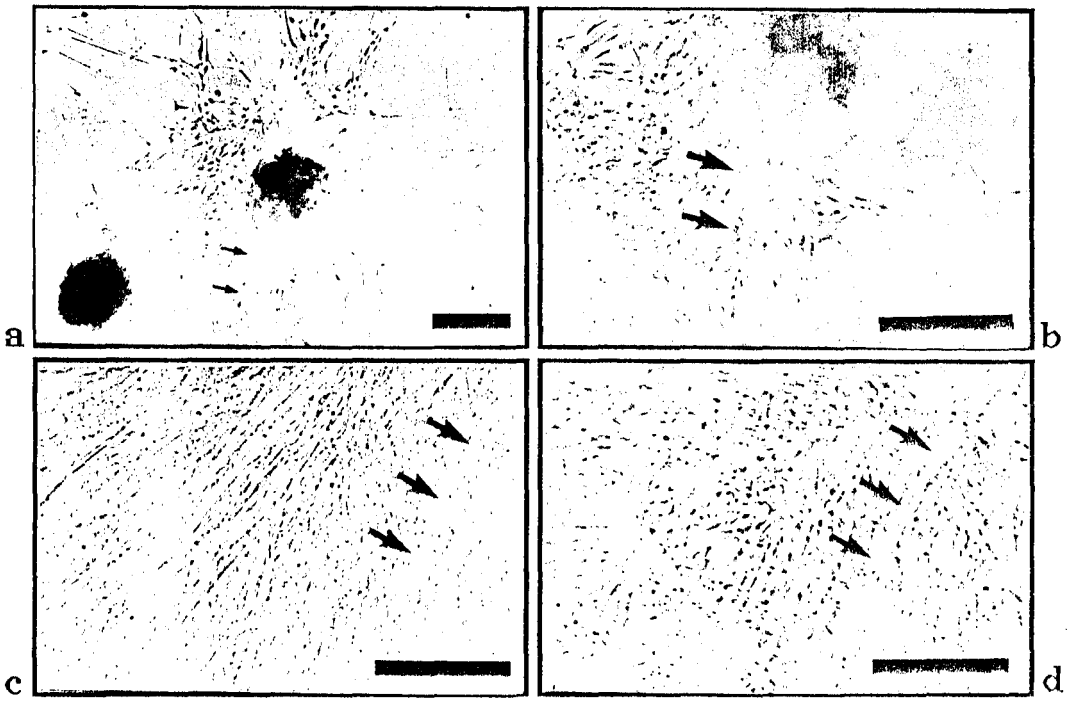

FIG.-10 : Effects of the removal of dexamethasone on CO25 cells where foci were formed after 3 days in fusion medium followed by 4 days in fusion medium lacking dexamethasone. (a) low power, (b) high power, arrows, showing a myotube, (c) after 4 days CO25 myoblasts formed to myotubes in the fusion medium, arrows show myotube, (d) after addition of dexamethasone in the fusion medium, the myotubes after 1 day, arrows show deformed myotube; Bars= 100 μm .

The medium was changed to the fusion medium without dexamethasone after the formation of foci by transformed cells. As a

consequence myotubes began to form within 3 days (arrows show on Fig. 10a, b). The foci of what resembled transformed cells and myotubes co-existed as the cells switched gradually to the pathway of myotube differentiation (Fig. 10 a, b).

After the myoblast cells became 70-80% confluent in the growth medium, it was replaced by the fusion medium, and after 4 days in the fusion medium, the myoblast cells formed myotubes (Fig. 10c). After four days forming myotubes in the culture, 1μM dexamethasone was added to the fusion medium to examine the effects of dexamethasone on the myotubes and also on the other myoblast cells. After 2 weeks, multilayer growth was observed in the cultures which had been exposed to dexamethasone (Fig. 10d). The myoblasts changed to a more rounded, and smaller shape than before addition of dexamethasone (Fig. 10d). The myotubes were seen to be deformed by the effects of dexamethasone (arrow shows on Fig. 10d).

2.3.4. OBSERVATIONS BY S.E.M.

2.3.4.1. S.E.M. OBSERVATIONS OF THE SURFACE OF CO25 CELLS DURING MYOBLAST DIFFERENTIATION

In the growth medium, undifferentiated CO25 myoblast cells had plasma membrane surfaces which had numerous microvilli on them (Fig. 11a, b).

During elongation, when cells were observed using the S.E.M., they had some small thick microvilli on their surfaces, but otherwise their surfaces were comparatively smooth after two days in the fusion medium (Fig. 11c, d). The elongated cells had longitudinal pleats on their processes (thin arrows in Fig. 11c, d), and also these pleats extended onto the cell body (thin arrows in Fig. 11c, d). These spindle shaped cells were seen to have some very small lateral processes present close to the basal surfaces (thick arrows in Fig. 11c, d).

The fusion followed on from and accompanied elongation. Differentiating myoblasts started to fuse forming multinucleated myotubes in tissue culture after three days. Cylindrical or conical cell processes were present which had a length much greater than their width (Figs. 12a). As fusion proceeded, the cells became attached to the syncytium by lateral fusion (Fig. 12a,b).

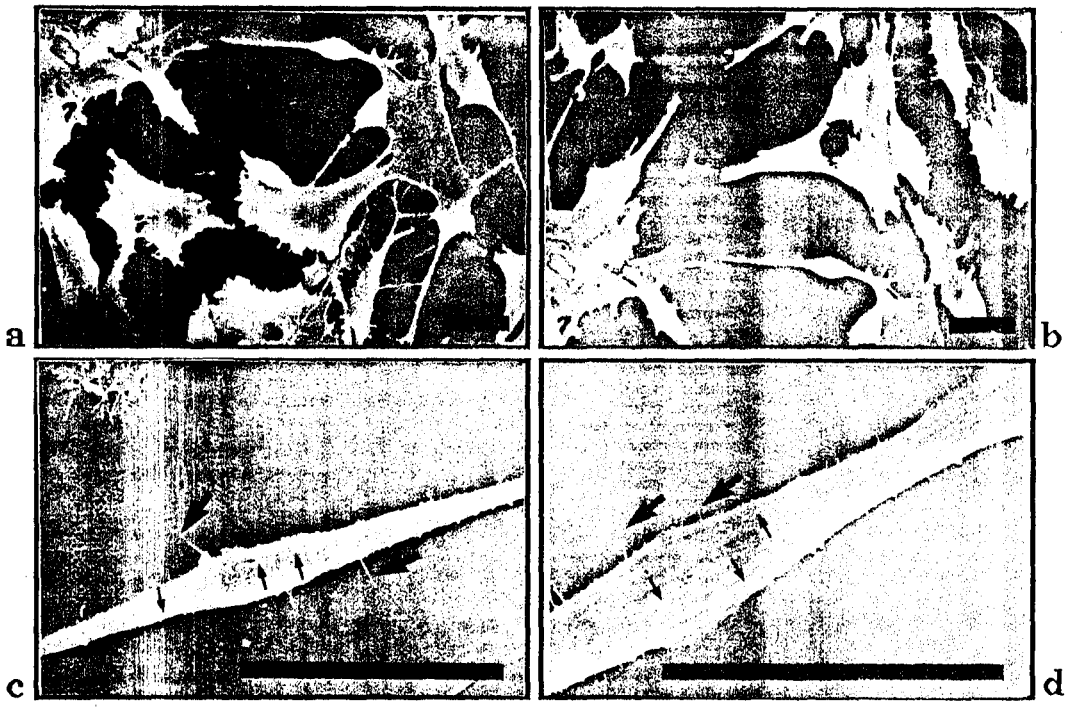

FIG.-11 : S.E.M. of CO25 cells after 2 days (a, b) in the growth medium, (c, d) in fusion medium, thin arrows, longitudinal pleats, thick arrows, lateral processes; Bars= 20 µm.

The elongated cells were initially distinct from the irregularly fused cells (arrows show on Fig. 12a), but gradually disappeared as all the cells fused. They were attached to the surfaces of marginal processes, but not to the upper surfaces of the cells (Fig. 12a,b).

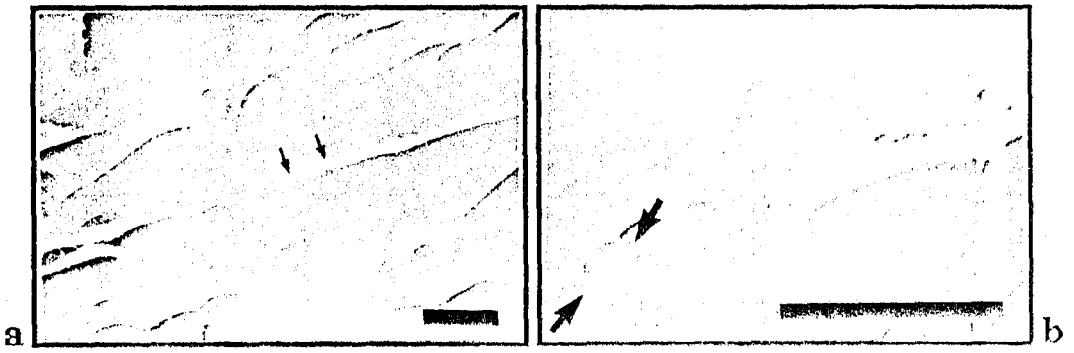

FIG.-12 : S.E.M. of fusing CO25 cells in fusion medium after 2 days (a) low power, (b) high power, arrows, syncytium of the processes of the cells by lateral fusion; Bars = 20 µm.

SEM observations showed that when the free processes of a myoblast cell met a similar processes of another cell during elongation, stable cell-cell attachments occurred such that fusion then followed (Fig. 12a, b).

During fusion, the long thin processes of the fused cells became shorter, and finally became rather thicker (Fig. 13a).The bodies of the fused cells changed to more cylindrical shape (Fig. 13a, b). In the S.E.M., after fusion had began, the myotube surface was seen to be fairly smooth but there were a few microvilli, and long pleat-like microvilli on the surfaces all the way along (arrows in Fig. 13c), and this remained as fusion proceded. After four days, the myotubes increased in their average width. The surfaces of the cells were still seen to be fairly smooth, with no microvilli, but cytoplasmic structures resembling ribbing were present at right angles to the long axis of the cells, and parallel to each other, all along the surfaces of the myotubes (arrows in Fig. 13d).

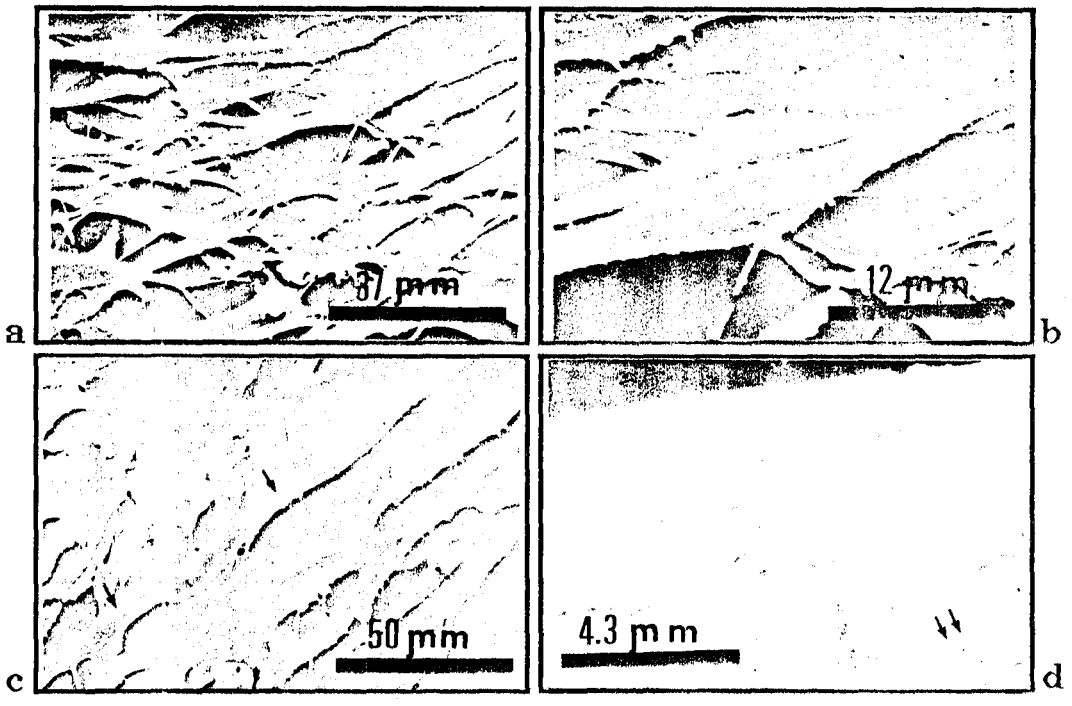

FIG.-13 : CO25 cells during formation and maturation of myotubes in fusion medium (a) early stage of myotube formation after 3 days (b) high power, (c) myotube after 5 days, arrows show a few microvilli on the myotube, (d) myofibril after 2 weeks, arrows, cytoplasmic structures resembling ribbing on the surface of the myofibril

2.3.4.2. S.E.M. OBSERVATIONS DURING TRANSFORMATION

After cells were grown in the growth medium or fusion medium, (1μM) dexamethasone was added to the each medium to examine the effects of dexamethasone on the cells.

In the growth medium, the cells were usually triangular or polygonal in shape (Fig. 14a). The surfaces of the cells were seen to be quite smooth, but the cells had many thin, small microvilli and blebs on their surfaces (Fig. 14b).

After addition of dexamethasone to the growth medium, the shapes of the cells changed to a more rounded form (Fig. 14c). Conspicuous membrane ruffles were visible around the edges of the cells (Fig. 14c) and all the surfaces of the cells were seen to be irregular (Fig. 14d).

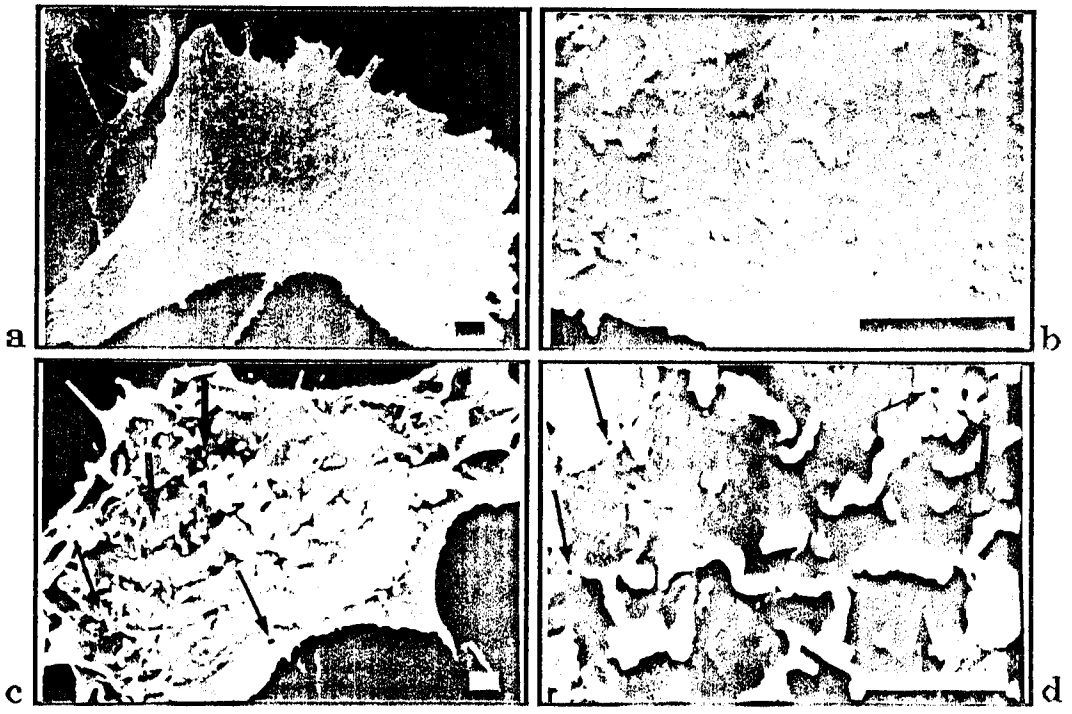

FIG.-14 : Effects of dexamethasone on CO25 cells observed by S.E.M. after 2 days; (a and b) Control cells in growth medium not exposed to dexamethasone (a) low power, (b) high power, (c and d)cells in the growth medium with dexamethasone (c) low power, (d) high power, thin arrows, holes on the cell surface, thick arrows, bleb-like microvilli; Bars= 2 μm.

However, they were much more convoluted than cells grown in the absence of dexamethasone, and there were some holes on the surfaces of

some of the cells (thin arrow in Fig. 14c, d). Also, after addition of dexamethasone to the fusion medium, most of microvilli assumed a conspicuous wave-like shape (Fig. 14d), but some small bleb-like microvilli were also observed (thick arrows in Fig. 14d).

In the fusion medium, the cells were spindle shaped with long processes at both ends (Fig. 15a). Also, short lateral processes were ussually seen (arrows in Fig. 15a). The elongated cells had some short microvilli, and also some longitudinal pleats visible on their surfaces, which ran along the long axes of the cells (Fig. 15b).

After addition of dexamethasone to the fusion medium, the cells became shorter than before, and the shapes of the cells were changed to a quite triangular form (Fig. 15c). These cells lost the long thin processes (Fig. 15c). Some ruffles were seen on their edges (arrow in Fig. 15c). The surfaces of the cells were quite smooth, and linear microvilli appeared on them. Also a few small bleb-like microvilli were observed (arrows in Fig. 15d).

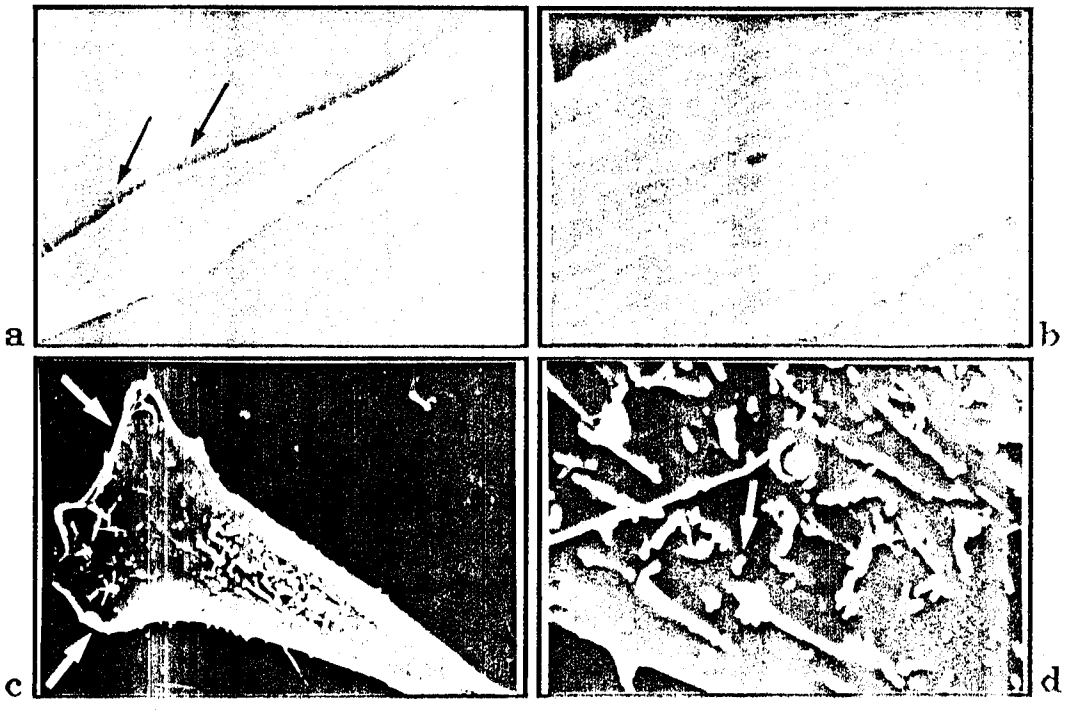

FIG.-15 : After 2 days the effects of dexamethasone on differentiating CO25 cells were observed by S.E.M.. (a, b) control cells in fusion medium not exposed to dexamethasone, arrows, lateral processes, (c, d) cells grown in fusion medium for 2 days, then dexamethasone was added and the cells were grown for further 2 days, arrows on (c), ruffles on the edges of the cell, arrows on (d), bleb-like microvilli; Bars= 20μm.

A further experiment was carried out to see what the effects of dexamethasone were on growing cells in the fusion medium from the beginning. The cells were grown in the growth medium until they became confluent, then the medium was changed to fusion medium with 1 μM dexamethasone. After three days, the cells were observed to be rounded in shape, and a few foci were present after 3 days (Figs. 16a). After 1 week, the transformed cells formed complete foci by dividing on top of each other (Fig. 16b). The cells which were in the foci were observed to be rounded in shape and 5-10 μm in diameter. However, some cells which were under the foci were observed long thin cells (arrows in Fig. 16a, c). The surfaces of the spherical cells were rarely found to be smooth but were usually covered with blebs or small microvilli (Fig. 16d).

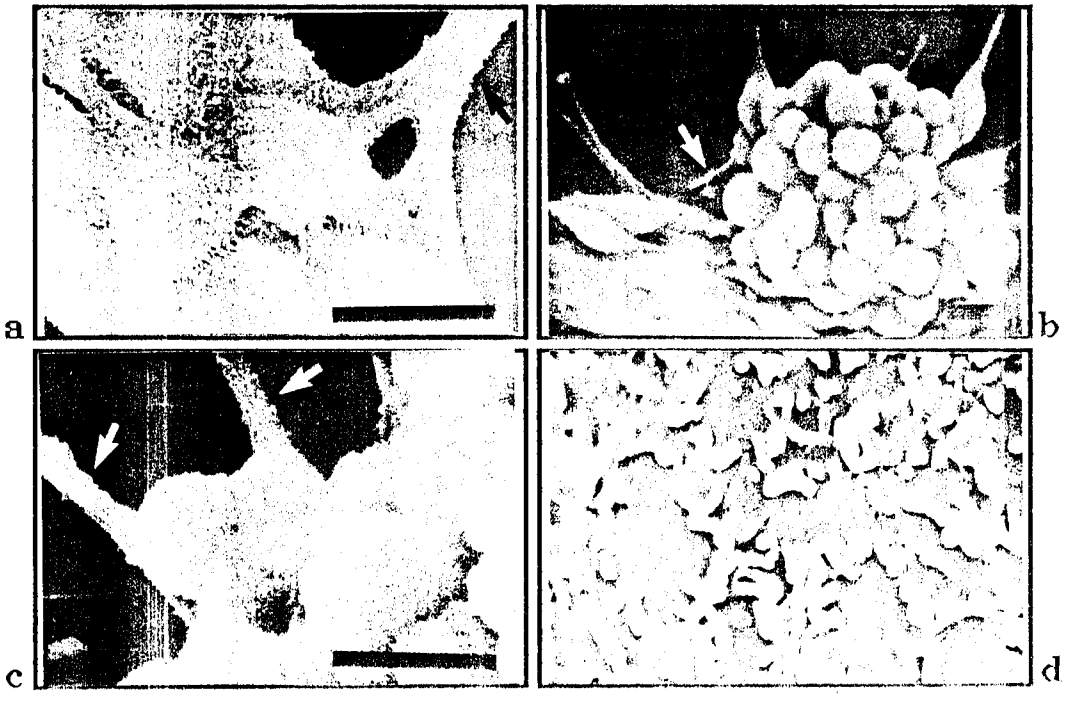

FIG.-16 : S.E.M. micrographs showing details of the effects of dexamethasone on CO25 cells in fusion medium; (a) after 3 days, (b, c, d) after 1 week, arrows show long thin processes of the cells under the foci; Bars= 20 μm.

reported that low pH in endosomes activates a fusogenetic protein (fusogen) in the viral envelope which catalyzes the fusion of the viral and endosomal membranes. Thus during differentiation, the pH level of elongated myoblasts could change to a lower pH activating one or more myoblast fusogenic proteins at the myoblast surface. This could occur by endocytosis. Although there is no direct evidence for such a mechanism triggering myoblast fussion, Kalderon and Gilula (1979) observed the presence of vesicles near the apical and lateral plasmamembranes of myoblasts at fusion sites.

During differentiation, only the membranes of elongated myoblasts seem to have a capacity for fusion. Elongated CO25 cells were seen to fuse with other elongated myoblasts or with myotubes, but not with undifferentiated myoblasts. This capability of the cells could come from an alteration of membrane receptors by a genetic switch or a direct effect of the environment for a short period during the fusion. Experimentally, substances such as polyethylene glycol (between muscle cells and fibroblasts or keratinocytes, or hepatocytes) (Pavlath *et al.*, 1989) and subtilisin (between erytrocytes) (Ahkong *et al.*, 1978) have been found to induce fusion. During fusion, elongated cells may produce either enzymes or other molecules to stimulate fusion.

It is known that lectins, are present on the cell surfaces and are thought to be involved in cell-cell recognition (Lis and Sharon, 1986). Also bindin protein, thought to be responsible for the species-specific adhesion of the sperm to the egg, was found to be a receptor on the cell surface (Lis and Sharon, 1986). CO25 myoblast cells may have specific lectin- or bindin-like proteins on their surfaces which confer specificity to elongated myoblasts during fusion. Sawyer and Akenson (1983) have found that the relative amount of a 200-250 kDa surface protein increased during L6 myoblast fusion. The function of this interesting protein remains to be determined.

Elongated CO25 cells were observed to be always parallel to each other and also to other myotubes during the fusion stage. Membrane fusion did not take place in all areas but initially was only restricted to areas at the ends of the myoblast processes. Nathason (1986) reported that fusion was related to position of the fusion myoblasts and the myotubes. Thus, the position of the cells or specific region of the cells (the ends of the processes) are likely to be critical for myoblast fusion. It was observed in this study that membrane fusion of CO25 myoblasts seemed to be irreversible. Knudsen and Horwitz (1977) have reported

rounded. Transformed CO25 cells may well secrete plasminogen activator or some similar molecule to loosen cell-matrix attachments. This change could in turn release an intracellular signal for enchanged cell division frequencies.

One of the most conspicuous features induced by transformation was the appearance of many conspicuous microvilli. This was in sharp contrast to the comparative loss of microvilli as fusion and differentiation proceeded. A similar formation of extensive microvilli has also been seen in a variety of transformed cells including fibroblasts transformed by the expression H-*ras* (Hagag *et al.*, 1990; Linstead *et al.*, 1988). A major question is why does the induction of a transformed phenotype generate many microvilli and the induction of differentiation result in a very significant loss of microvilli ? One theory, due to Pasternak *et al.* (1979), is that microvilli store plasmamembrane required at cytokinesis. The amount of plasma membrane of P815Y cells (mastocytoma) has been measured by Pasternak *et al.* (1979), who reported that it exactly doubles between the start of a new cell cycle (early G1) and the onset of cytokinesis (late G2). Also, morphological assessment by scanning electron microscopy showed that there was an approximately 2 or 3 times (Pasternak *et al.*, 1979) reduction in the number of microvilli after cytokinesis. Thus, the increased amount of microvilli on the surface of the transformed cells may be at least partly due to enhanced new membrane synthesis for daughter cells.

A second possible hypothesis is that the increase in microvilli is associated with increased membrane ruffling and micropinocytosis. Bar-Sagi and Feramisco (1986) reported that transformation of fibroblasts by the induction of H-*ras* was followed by a major increase in membrane ruffling and associated fluid phase pinocytosis. Furthermore Dowrick and Warn (1991) have demonstrated a causal relationship between ruffling and pinocytosis as a consequence of the addition of scatter factor to MDCK cells. In this study a number of small holes or pits were found on the apical surface of the transformed cells. Because they were seen only on transformed cells it was not thought that they were artefacts of preparation, rather pinocytotic vesicles. Thus CO25 cells may be responding to transformation by enhanced ruffling and pinocytosis.

A role of *ras* has been reported not only in control of cell proliferation and malignant transformation but also in the control of differentiation processes (Olson *et al.*, 1987). It has been reported that

ras oncogene protein promoted the morphological differentiation of phenochromocytoma cell (PC12) (Bar-Sagi and Framisco, 1985; Muroya *et al.*, 1992). In contrast *ras* oncogenes appeared to interfere with the differentiation of mammary epithelial cells (Andres *et al.*, 1988), and also the differentiation of human lymphoblasts (Seremetis *et al.*, 1989). Thus *ras* can to both promote or inhibit differentiation. In this study transformation of CO25 cells was seen to block their differentiation, in the fusion medium with dexamethasone. Gossett *et al.* (1988) also found that the induction of N-*ras* causing transformation also prevented the up-regulation of muscle specific gene products in myoblasts. Thus, transformed CO25 cells may continuously divide without undergoing differentiation in spite of the fusion medium. Or, N-*ras* protein could have an effect by blocking the expression of muscle-specific genes in CO25 cells and hence inhibiting differentiation.

CHAPTER 3

CHANGES IN MICROTUBULE ORGANIZATION DURING MYOBLAST DIFFERENTIATION

by cooling the solution back to 0 °C (Parysek *et al.*, 1984). Polymerisation requires a nucleoside triphosphate (GTP) (Carlier, 1989) and magnesium, and the polymer is sensitive to calcium ions (Borisy et al, 1975; Olmsted and Borisy, 1975). GTP and GDP bound to a specific binding site on β–tubulin at its N-terminus can exchange with nucleotide in the medium. (Linse and Mandelkow, 1988). GTP is hydrolysed here to GDP during polymerisation. α–tubulin contains a non-exchangeable GTP binding site from which GTP cannot be removed except by denaturation (Maccioni et al, 1986). Microtubule assembly is sensitive to ionic strength. High concentrations of potassium or sodium ions inhibit microtubule assembly (Kirschner, 1978). High concentrations of magnesium or glutamate induce aberrant forms of polymer (Dustin, 1984). Additionally there must be a sufficient concentration of tubulin (the critical concentration). The critical concentration is reduced by the presence of a number of factors which reduce the dissociation constant, including MAPs (Murphy et al,1977), glycerol (Yarbrough and Fishback, 1985), DMSO (Robinson and Engelborghs, 1982), and taxol (Hauser, 1986).

Several groups of drugs can bind to tubulin and affect its polymerisation *in vitro* and *in vivo* . Tubulin was originally identified as the soluble protein, found in nearly all eukaryotic cells, that tightly bound the antimitotic drug colchicine. Colchicine, isolated from the plants, *Colchicum antumnale* or *Colchicum speciosum*, inhibits the polymerisation of tubulin *in vitro* and causes rapid disassembly of most types of cellular microtubules *in vivo* (Bergen and Borisy, 1983). One drug molecule binds to each dimer. Stoichiometric binding of dimers are enough to block assembly at a microtubule end. Several other drugs, such as colcemid, benomyl, podophyllotoxin, or nocodazole bind to the same site of the tubulin molecule as colchicine, and have a similar effect in disassembling microtubules. However the effects of nocodazole are reversible.

Vinblastine, isolated from *Vinca speciosum* (periwinkle) and vincristine (isolated from *Vinca rosea*) form another group of drugs inhibiting microtubule polymerisation that also act by blocking the polymerisation of tubulin stoichiometrically. Vinblastine disassembles microtubules into helically coiled protofilaments (Amos et al, 1984).

Another drug is taxol. Taxol is derived from *Taxus brevifoia*. Its effect on the microtubules is in many respects opposite to those of other microtubule-binding drugs. Low concentrations of taxol (5-20 mM) can

stabilize microtubules (Rowinsky et al, 1990). Taxol not only affects the polymerisation of microtubules, but also causes a redistribution of the microtubules into short, distinct bundles not nucleated from the centrosome. The mechanism of bundle formation is not yet understood, but it is an energy requiring process (Manfredi *et. al.*, 1982).

3.1.1.2. GENETICS OF MICROTUBULE SYSTEMS

We now know, as had long been predicted, that tubulins are encoded by multigene families which direct the synthesis of peptides which are both highly conserved and show some variations in sequence (Raff, 1984).

The data from some lower eukaryotic species have demonstrated that single gene products are sufficient for the construction of all the essential microtubule arrays (Neff *et al.*, 1983). However most species have more than one genes for each type of tubulin monomer: For example *Chlamydomonas* (the green alge) has two genes for α–tubulin and two for β–tubulin (Brunke *et al.*, 1982), whereas *Drosophila* has four genes for α–tubulin and four for β–tubulin (Sanchez *et al.*, 1980). Results from higher species clearly suggest that multiple gene sequences are required (Sullivan *et al.*, 1984),

The following levels of variation exist for the expression of the different genes:

1. Selection of which multiple genes to be expressed
2. Coordination of the synthesis of α– and β–tubulins
3. Control of the level of tubulin expression during the cell cycle and during development and differentiation
4. Control of post-translational modification and attachment of MAPs with consequent regulation of microtubule stability.

Free β-tubulin regulates tubulin synthesis via a negative feedback loop. It binds to any nascent β–tubulin polypeptides on ribosomes, blocking further elongation and causing degradation of the mRNA. The synthesis of α–tubulin may be controlled in a related manner (Cleveland, 1989).

Weil *et al.* (1986) identified the gene mipA as a suppressor of a conditional lethal β tubulin mutation. The gene sequence was found to be related to both α and β-tubulin, leading Oakley and Oakley (1989) identify a new member of the tubulin family, which is named γ–tubulin. By immunogold electron microscopy, γ-tubulin appears to be a component of the centrosome (Stearns *et al*, 1991; Zheng *et al.*, 1991).

3.1.1.3. POST-TRANSLATIONAL MODIFICATIONS OF TUBULIN

The complexity of tubulin is further increased by various post-translational modifications. There are three well characterized forms of post-translational modification. Firstly, β–tubulin can be phosphorylated. And the phosphate was found to be positioned on a serine residue near the carboxyterminus (Gard and Kirschner, 1985). Mammalian brain β-tubulin was shown to be phosphorylated by Eipper (1974). The carboxy terminus is strongly acidic, with the β–subunit being slightly more acidic than the α–subunit, β-tubulin is also richer in glutamic acid in its sequence composition (Lu and Elzinga, 1978; Field *et al.*, 1984; Sullivan, 1988).

Secondly acetylation occurs on a lysine encoded by a codon at position 40 in animal and protistan α-tubulins (L'Hernault and Rosenbaum, 1985). Thirdly a tyrosine residue at the C-terminus of α–tubulin can be removed by a specific carboxypeptidase and replaced by a tubulin tyrosine ligase (TTL) (Review, Barra *et al.*, 1988). The modification involves the addition of tyrosine to the carboxy terminus of α–tubulin, catalysed by α-tubulinyl tyrosine ligase with the concomitant hydrolysis of ATP (Schroeder *et al.*, 1985). A specific tubulinyl tyrosine carboxypeptidase (TTC) has also been partially purified, which removes this terminal tyrosine to yield α–tubulin terminating in glutamic acid residue (Kumar and Flovin, 1981). Both of these modifications occur primarily on assembled microtubules and is reversed on unpolymerized α-tubulin (detyrosination, Kumar and Flovin, 1981; acetylation, Piperno *et al.*, 1987).

Subsequent sequence data have demonstrated that the terminal tyrosine of α-tubulin is encoded (Ponstingl et al, 1981), up to 15% of the total tubulin has been found to be detyrosinated (Ponstingl et al, 1982). Tyrosinated and detyrosinated tubulins polymerise equally *in vitro* (Wehland et al, 1983; Gundersen et al, 1984), and this is not suprising given that tyrosinated tubulin differs from detyrosinated tubulin by only a single amino acid residue in over 400. A search for, modulation of tubulin function by tyrosination has so for not given any conclusive results. So far a correlation in the C-terminal tyrosine content (or tubulin tyrosine ligase activity) has been made with changes in cell shape, and differentiation state (Gundersen et al, 1984; Bulinski and Gundersen, 1991).

Gundersen *et al.* (1984) raised polyclonal and monoclonal antibodies that specifically recognized tyrosinated α–tubulin (Tyr-) and detyrosinated α–tubulin (Glu-). They examined the distribution of Tyr- and Glu-rich microtubules in several tissue culture cell types, in dividing and non-dividing cells, and in specific cellular structures containing microtubules (Gundersen and Bulinski, 1986). Their findings suggest that microtubules that are rapidly turning over tend to have a high Tyr-tubulin content whereas those more stable to microtubule depolymerization predominantly contain glu-tubulin (Barra *et al.*, 1988; Schulze *et al.*, 1987). Acetylated α–tubulin is also present in significant amounts on microtubules that, under depolymerizing conditions are more stable than the majority of cytoplasmic microtubules (Piperno *et al.*, 1987). Microtubules *in vitro* exist in growing (polymerizing) and shrinking (depolymerizing) populations that interconvert frequently. This behaviour is termed dynamic instability (Micthinson and Kirschner, 1984). Schulze and Kirschner, 1986, 1987) observed (by injecting cells with biotin-labelled tubulin) that rapid incorporation occurs by elongation of existing microtubules. Prescott *et al.*, (1992) also found fast turning over microtubules using *Physarum* tubulin. A second sub-population of significantly slower turning over microtubules was discovered by similar methods (Schulze and Kirschner, 1987), and can remain stable for several hours. These slow turning over microtubules usually but not always corresponded to microtubules which have undergone post translational modifications (Schulze *et al.*, 1987; Kreis, 1987).

3.1.1.4. MICROTUBULE ASSOCIATED PROTEINS

Proteins that co-polymerize with tubulin through several cycles of assembly and disassembly that may promote microtubule assembly, and bind with fairly constant stoichiometries are described as microtubule associated proteins (MAPs).

LIST OF MAPs :

Protein name:	Molecular weight:	References:
Dyneins		
Axonemal	415-480 kD	(Gibbons, 1988)
Cytoplasmic	> 400 "	(Gibbons, 1988)
Kinesin	65-440 "	(Sawin and Mitchson, 1990; Schliwa,

			1989)
Dynemin	75-100	"	(Shpetner and Vallee, 1989)
Vesikin	292	"	(Preston et al, 1990)
Axolinin	255	"	(Preston et al, 1990)
Brain spectrin	220-240	"	(Preston et al, 1990)
Synapsin	76-78	"	(Kim et al, 1979)
MAPs 1,2,3,4, and 5	70-240	"	(Olmsted, 1986; Lewis et al, 1988)
Tau	35-40	"	(Goedert et al, 1989)
STOPs	60-80	"	(Margolis and Rauch, 1981)
Buttonin	75	"	(Preston et al, 1990)
Aster-forming protein	51	"	(Preston et al, 1990)

3.1.1.5. FUNCTIONS OF MICROTUBULES

Microtubules are involved in the determination of cell shape, the position of organelles (such as the nucleus, Golgi apparatus and endoplasmic reticulum), and the two-way traffic pattern of vesicles and organelles through the cytoplasm. One of the most important functions of microtubules is to provide tracks for transporting substances in the cell body. Microtubules form the spindle at mitosis and meiosis. As described above they also provide the force for the beating of cilia and flagella.

The main, functions of microtubule can be summarised as follows (representative references only are given):

1-) Supporting cell shape (Dustin, 1978; Schliwa, 1986)

2-) Intracellular motility

A– Organelles

* In animal cells, endosomes and lysosomes (Schroer *et al*, 1988)
* In plant cells, pigment granules (Lloyd and Seagull, 1985)

B– Axonal transport

* Small and large vesicles (Hollenbeck, 1989)
* Mitochondria (Hollenbeck, 1989)

C- Chromosome separation

* During mitosis, individual chromosomes (Mitchison *et al*,1986)

3.1.2. THE CENTRIOLE

Most of cells have a pair of centrioles which are generally located close to the nucleus (Review, Wheatley, 1982). Centrioles are on average about 0.4-0.7 μm long and 0.2-0.3 μm wide (Albrecht-Buehler, 1990). Each centriole is a nearly cylindrical organelle composed of a set of nine

parallel triple-fibres radially arranged about a central space which shows some sub–structure in the T.E.M. (Amos and Amos, 1991). Each triplet is tilted inward toward the central axis at an angle of about 45^{o} to the circumference (Albrecht-Buehler, 1990). Glu-tubulin antibodies provide an excellent marker for centrioles. The centriole may be able to perform several defferent types of function: Centrioles have been found to be absent in several animal cell types, e.g. a *Drosophila* embryonic cell line (Debec, 1982), and more significantly early stage mammalian embryos (Schatten *et. al.* , 1985; Schatten *et. al.*, 1986). Higher plant cells (Clayton *et. al.*, 1985), and fungi such as the slime mould *Dictyostellium* (Darnell *et. al.*, 1990) all lack centrioles. Thus they are not an obligatory feature of microtubule nucleating centres for all cells and their real function is unknown at the present time. However they are essential for the formation of the basal bodies of cilia and flagella (Anderson and Brenner, 1971).

3.1.3. CILIA AND FLAGELLA

These tiny, hair-like structures are about 0.25 μm in diameter. They are constructed from microtubules and are found in most animal species and some lower plants (Reviews, Wheatley, 1982; Bershadsky and Vasiliev, 1988; Preston *et al.*, 1990; Amos and Amos, 1991). Flagella are usually much longer than cilia. However the molecular basis for their structure and movement is considered to be the same. In both cilia and flagella the core structure is the *axoneme* . This consists of a bundle of microtubules arranged in a characteristic fashion with nine outer doublets and a central pair (9+2). The "9+2" structure seems to have been selected during evolution as an optimum for all groups. The lengths of axonemes are usually about 10 μm and can be as long as 200 μm. The outer doublet microtubules are made up of pairs of one complete 13 protofilament microtubule (the A–tubule), and an incomplete 10 protofilament microtubule (the B–tubule). The free edge of the B–microtubule makes a junction with the A–tubule to form a doublet, and they lie symmetrically around two central intact singlet microtubules (c.f. Amos and Amos, 1991). The central pair of fibres has been found to originate in a small, convex axilar granule or axosome (Dowben, 1971). The fibrils extend continuously along the length of the flagellum without twisting or spiralling. Usually the fibres of the peripheral ring of fibres are longer than the central pair.

The diameter of cilia is usually around 20 μm. A single cilium is surrounded by a membrane which is the cell membrane, although it is often referred to as the ciliary membrane (Afzelius, 1959). There are many other motile organelles consisting of bundles of stable microtubules found in numerous invertebrate species. The number of microtubules forming part of such structures has been variously reported as between 6 and 3500 (Bloodgood and Miller, 1974). The usual form in the animal kingdom is the "9+2" arrangement. In eukaryotes flagella differ from cilia only in length, beat, and number per cell. Bends are generated along the length of the flagellum by restricted sliding of the nine outer doublets. In contrast the prokaryote flagellum is made of polymerised flagellin, which is a 40 kDa subunit protein and is rotated by a basal body.

The diameter of the flagellum is around 0.14 μm. Flagella as short as 1μm in length have been described by Moestrup (1982). The other extreme is the flagellum of the spermatozoon of *Notonecta* which is about 10 μm long (Pantel and De-Sinety, 1906).

3.1.3.1. VARIANT AXONEMES

A–) Axonemes composed of varying numbers of outer doublets and lacking the central pair of microtubules. Motile 3+0, 5+0, 6+0 and 12+0 axonemes have been described as well as non motile 9+0, 12+0 and 14+0 patterns ;

B–) Axonemes composed of the normal number of outer doublet microtubules but varying numbers of central pair microtubules. This is the 9+n pattern where " n " is " 0" (eel, diatoms), " 1" (mosquitoes, scorpions), " 3" (spiders) or " 7" (caddis flies);

C)-Axonemes which contain an extra ring of microtubules surrounding the usual 9+2 arrays to give the so-called 9+9+2 patterns (mutants of *Chlamydomonas*);

D-) Axonemes which contain fewer than a outer doublet microtubules such as 8+1, or 7+2 cilia.
(Prensier *et al*, 1980; Wheatley, 1982; Preston *et al*,1990)

3.1.3.2. TYPES OF CILIA

A) Compound cilia: Cilia which are grouped in a bundle and beat in unison, as if fused, are known as compound cilia. Ctenophore swimming–plates are the largest compound cilia, consisting of as many as 100.000 cilia (Afzelius, 1961)

B) Macrocilia: Electron microscopy has shown the macrocilium to consist of about 3500 axonemes, which are all joined by the same type of lamella as has been found in swimming–plate cilia, but which in this case occurs in several planes around each axoneme. Horridge (1965) first described a macrocilium on the lips of the ctenophore *Beroe*.

3.1.3.3. TYPES OF FLAGELLA

A) Protozoan flagella: Flagella from protoza may have the usual appearance or carry additional components including scales, hairs, or other structures (Moestrup, 1982).

B) Flimmer-flagella: In many protozoa and some multicellular plants the flagellum bears one or two rows of hair-like appendages called flimmers or mastigonemes.

C) Flagella with a 9+1 pattern: Turbellaria (Silveira and Porter, 1964), and *trematodes* (Shapiro *et al*, 1961) have a 9+1 pattern in the flagella.

D) Flagella with a 9+0 pattern: *Myzostomum* has a mobile flagellum without central filaments (Afzelius, 1963).

E) Flagella with a 9+7 or 9+9 pattern: The sperm of several species of treehoppers (*Hemiptera*) have such a pattern and have been studied by Phillips (1966).

F) Sperm tails: In many animal and plant species the sperm tail conforms to the description of 9 + 9 +2. The sperm tails of mammals, birds and snakes have 9 dense fibrils, one immediately outside each of the peripheral doublets.

G) The Sciara–type flagellum: In the flagellum of *Sciara coprophila* the axial filament complex consists of approximately 70 double outer filaments (Phillips, 1966)

3.1.3.4. OTHER TYPES OF CILIA–LIKE STRUCTURES

Sensory hairs: These structures detect stimuli which may be mechanical, chemical, electrical, or visual. Usually their 9+2 filament structure has been correlated with a directional sensitivity of the sensory cell. For example: mechanoreceptors in the inner ear.

3.1.3.5. CILIA FORMATION

A centriole is a permanent feature of the ciliary axoneme, where it is called a basal body. The centrioles that form the basal bodies perform a specialized function in the cell leading to cilium or flagella production.

In a variety of cell types, centrioles take part in the formation of cilia and flagella to form one or two basal bodies (Sorokin, 1962). This process is called ciliogenesis.

A good description of ciliogenesis is found in Novikoff and Holtzman (1970). Large numbers of basal bodies appear and after migration to the surfaces of the cells, lead to cilia formation in the cells of the respiratory and reproductive tracts of mammals.

3.1.4. THE BASAL BODY

3.1.4.1. STRUCTURE OF THE BASAL BODIES

The base of the cilium has received many designations: basal body, basal granule, basal corpuscle, kinetosome, blepharoplast, etc. This structure takes a cylindrical form which is present at the base of each cilium or flagellum. The ultrastructure of basal bodies consist a ring of nine fibres without any central fibres (9+0). The wall of the basal body is made up of nine triplets (rather than doublets) of fibrils similar to centrioles joined by inter-fibrillar linkages. The fibrils are about 24 nm in diameter (Dowben, 1971). The basal bodies control in some as yet unknown way the assembly of ciliary and flagellar subunits such that the 9+0 structure of the basal body gives rise to the 9+2 structure of cilia and flagella.

Recent work has shown that basal bodies contain a small DNA molecule, like chloroplasts and mitochondria, that codes for many basal body proteins (Preston *et al.*, 1990).

3.1.4.2. BASAL BODY FORMATION

In many cells, centrioles appear to duplicate by the growth of a new procentriole near the old centriole, which subsequently splits away from the parent. The procentriole contains the 9+0 pattern but is shorter (50-100 nm) than the old centriole until it matures (Dirksen and Crocker, 1965).. Usually, this occurs in cells where centriole duplication is part of cell division, as well as in some cells where many basal bodies form.

A ring of tubules appears first then further tubules add on in quick succession. In some species, a cartwheel structure appears before the cylinder of triplet tubules (Gould, 1975). In some cell types forming basal bodies, several procentrioles appear more or less simultaneously (Wheatley, 1982). First, a small probasal body is formed which then elongates to form the mature structure (Johnson and Porter, 1968).

3.1.5. PRIMARY CILIA

There are several reports about ciliogenesis in a variety of cell types but up to now there are few published reports about the primary cilium. This is particularly true of situations where a primary cilium in present but is not associated with ciliogenesis. Up to now most authors have confined themselves to a description of changes in the primary cilium during various phases of the cell cycle. In recent times only a few workers have been interested in the primary cilium and most reports about it are now very old. Therefore rather little is known about many aspects of the primary cilium, in particular its function(s) when not associated with ciliogenesis.

Bernhard and De Harwen (1960) first described an incomplete cilium (9+0 arrangement) in fibroblasts and smooth muscle cells from neonatal chicken and mammalian tissues in culture. Gallagher (1980) studied corneal endothelial cells by transmission electron microscopy (TEM), and reported that primary cilia are formed of nine transitional fibres, four striated satellite arms and several rootlets.

There have not been many reports about the number of primary cilia in cell types carrying it. Sorokin (1968) reported that the cells usually produced one and rarely two primary cilia. He found that most of the structure of the primary cilium remained inside the cell body of pulmonary cells from the lungs of foetal rats.

The biological function(s) of primary cilia within such cell types are largely unknown as yet. According to Barnes (1961), one may suspect them of having a sensory function in mammary carcinoma endocrine cells. A similar conclusion has been reached for 3T3 cells by Albrecht-Buehler and Bushnell (1980). An alternative suggestion due to Tucker and Pardee (1979) was that primary cilia may be involved in control of the cell cycle. Albrecht-Buehler and Bushnell (1980) observed using TEM that microtubules seemed to originate from primary cilia in quiescent 3T3 cells. All these studies have been done on cultured cells where variable ultrastructural morphologies are common. Prescott *et al*, (1991) looked at the microtubule organization of cells within the lens epithelium, which can be detached as a monolayer. They found each lens epithelial cell to contain a single apical primary cilium and reported that the focus of the microtubule array was at the cell apex close to a centrosome present at the base of the primary cilium. Some microtubules, those rich in detyrosinated and acetylated α–tubulin, seemed to be associated with the primary cilium rather than the

centrosome. This organization suggests a possible role of the primary cilium in microtubule nucleation.

3.1.5.1. PRIMARY CILIUM FORMATION

Sorokin (1962) first proposed that the centrioles are involved in primary cilium formation in fibroblasts and smooth muscle cells. According to Sorokin's data, the primary cilia form after a vesicle grows around the distal end of one of the centrioles, and the shaft of the cilium then elongates into the vesicle. A distinction between primary and functional cilia was drawn by Sorokin (1968) ,who observed that 9+0 primary cilia developed from centrioles at an earlier time than the 9+2 sort appeared. Only the latter type formed the ciliated border. There is a similar report about the origin of the primary cilium in a fibroblastic cell population *in vitro* by Wheatley in 1969. Rash *et al* (1969) made the further observation that the primary cilia were absent during mitosis in fibroblasts.

High cell density or low serum can induce the formation of primary cilia (Tucker and Pardee,1979). When they examined 3T3 cells, which had been stopped in the G1 phase of mitosis in low serum, or where cell division had been inhibited by high cell density, primary cilia formed. Further confirmation that the primary cilium forms in the absence of cell division came from Mori *et al* (1979) who reported that 9+0 cilia occur in rat liver cell cultures only after the cells reached confluence and not before.

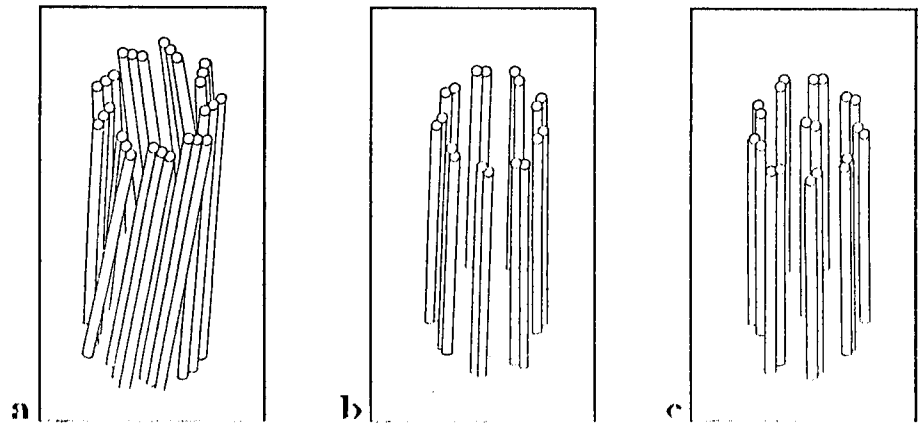

DIAGRAM-1 : Simplified schematic diagrams of the microtubule organization of (a) centriole, (b) primary cilium, and (c) cilium or flagella.

3.2. MATERIALS AND METHODS

3.2.1. CELL CULTURE

3.2.1.1. CELL TYPE

As described in section 2.2.1.1

3.2.1.2. PREPARATION OF CULTURE MEDIUM

As described in section 2.2.1.2

3.2.1.3. CELL CULTURE

As described in section 2.2.1.3.

3.2.1.4. TRYPSIN SOLUTION

As described in section 2.2.1.4.

3.2.1.5. PREPARATION OF PLASTIC DISCS

As described in section 2.2.1.5.

3.2.2. BUFFERS

3.2.2.1. MES BUFFER

2-(N-Morpholino)-ethane sulphonic acid (MES) buffer consisted of 0.1 M MES, 2 mM EGTA, 1 mM $MgSO_4$, at pH 6.9.

3.2.2.2. PBS

As described in section 2.2.2.1.

3.2.2.3. PEM BUFFER

PEM buffer consisted of 100 mM Piperazine-N,N'-bis(2-ethanesulfonic acid) (PIPES), 1 mM Ethylene glycol-bis (β–aminoethyl ether) N,N,N',N'-tetraacetic acid (EGTA), 1 mM $MgCl_2$, at ph 6.9.

3.2.2.4. PERMEABILISATION BUFFERS

3.2.2.4.1. PERMEABILISATION BUFFER-1

Permeabilisation buffer-1 consisted of 50 mM PIPES, 50 mM KCl, 0.5 mM $MgCl_2$, 1 mM EGTA, 0.1 mM EDTA (Disodium ethylene diamine tetraacetate.$2H_2O$) , 1 mM 2-Mercaptoethanol, at pH 6.8, 1% Triton X100 (Sigma), 4% Polyethyleneglycol (40 K; Sigma).

3.2.2.4.2. MOPS PERMEABILISATION BUFFER

Morpholinopropane Sulphonic Acid (MOPS) permeabilisation

buffer consisted of 80 mM MOPS, 5 mM EGTA, 1 mM $MgCl_2$, at pH 7.4, 0.05% Nonidet (NP40; Sigma), 20% Glycerol.

3.2.3. FIXATIVES AND FIXATION

3.2.3.1. PARAFORMALDEHYDE

Paraformaldehyde was dissolved in PBS (4% w/v) at 60 °C with the aid of 1M NaOH added dropwise until the solution cleared. After the solution had cooled the pH was adjusted to 7.4. Cells grown on glass coverslips or in flasks were fixed with 4% paraformaldehyde at room temperature for 15 minutes. After fixing the cells were extracted with acetone (-20 °C) for 30 seconds, and then washed in 3 changes of PBS/BSA.

3.2.3.2. 90% METHANOL

Cells grown on coverslips or in flasks were fixed with 90% methanol in MES buffer at -20 °C for 5 minutes. After fixing the cells were extracted with acetone (-20 °C) for 30 seconds, and then washed in 3 changes of PBS/BSA.

3.2.4. STAINING FOR FLUORESCENCE MICROSCOPY

3.2.4.1. DOUBLE IMMUNOSTAINING FOR GLU- AND TYR-TUBULIN

Cells were fixed with 90% methanol/10% MES buffer (described in section 3.2.3.2). The staining protocol was done sequentially as follows; rabbit serum (Dako), 1:10; ID-5 tissue culture supernatant (Wehland and Weber, 1987; from Dr. Wehland,J.), undiluted, TRITC rabbit anti-mouse, 1:50; YL1/2 (Kilmartin *et al*, 1982; Serα–Lab), 1:200; FITC rabbit anti-rat, 1:100. The cells were exposed to all antibodies at 37 °C in a humid chamber for 1 hour.After final washing preparats were mounted in Citifluor (Citifluor Ltd., London). The cells were examined using epifluorescence microscopy (as described in section 3.2.5.1.).

3.2.5. MICROSCOPY

3.2.5.1 EPI-FLUORESCENCE MICROSCOPY

Stained cells were mounted in Citifluor (Citifluor Ltd., London), and examined using a Zeiss Standard R microscope equipped with epifluorescence optics.

3.2.5.2. ELECTRON MICROSCOPY

3.2.5.2.1. TRANSMISSION ELECTRON MICROSCOPY

Cells were grown in plastic petri dishes (30 mm diameter, Sterilin). The cells were washed for 5 minutes with PBS + 0.2% BSA, and fixed in 2.5% glutaraldehyde as described in section 2.2.3.1.. They were then washed again with PBS for 30 minutes and postfixed with 1% osmium tetroxide in PBS for 30 minutes at room temperature. They were washed with distilled water for 30 minutes, dehydrated with a series of increasing concentrations of ethanol for 30 minutes each (20%, 40%, 60%, 2X100%). They were progressively embedded in resin (London Resin White) in ethanol at an increasing concentrations for 1 hour for each (20%, 50%, 75%, 2X100%), and polymerized in 100% resin at 60°C for 24 hours in plastic dishes or flasks. Sections were cut from the blocks of a thickness 70-90 μm with glass knives using an ultra microtome (LKB Nova ultramicrotome) and collected on gelatin-coated copper grids.

Sections were examined at 80 kV in a JEOL 100 CX electron microscope. Photographs were taken as described in section 3.2.8..

3.2.5.2.2. SCANNING ELECTRON MICROSCOPY

As described in section 2.2.4.2..

3.2.6. LENSES AND FILTERS

3.2.6.1. LENSES AND FILTERS FOR EPI-FLUORESCENT MICROSCOPY:

FOR FITC (Fluorescein Isothiocyanate):

LENSES:

Zeiss 16/0.50 Plan Neofluar (oil/water)
" 40/1.00 Planapochromat (oil)
" 63/1.40 Planapochromat (oil)
" 100/1.25 Achromat (oil)

FILTERS:

Exciter filter:	BP 485/20
Dichromatic beam splitter:	FT 510
Barrier filter:	BP 520/560

FOR TRITC (Tetramethylrhodamine Isothiocyanate):

LENSES:

Zeiss 16/0.50 Plan Neofluoar(oil/water)
" 40/1.00 Planapochromat (oil)

" 63/1.40 Planapochromat (oil)
" 100/1.25 Achromat (oil)

FILTERS:

Exciter filter:	BP 546/12
Dichromatic beam splitter:	FT 580
Barrier filter:	LP 590

3.2.7. DRUG TREATMENT

3.2.7.1. NOCODAZOLE

Nocodazole (Mw=301.3; Aldrich) solid was dissolved in DMSO and then diluted to give a final concentration of 24 µg/ml nocodazole using PBS. A control consisted of DMSO diluted to the same final concentration as used in the nocodazole containing solutions (final concentration of DMSO= 0.125%). For each concentration, coverslips were fixed with 90% methanol (described in section 3.2.3.2.) after 1, 2, and 3 hours of cell culture in the presence of nocodazole. The cells were double stained (described in section 3.2.4.), and examined as described in section 3.2.5..

3.2.7.2. TAXOL

Taxol was dissolved in DMSO and then diluted to give a final solution of 12 µM taxol using PBS. It was applied to the cells for 12 or 24 hours, which were incubated at 37 °C in 10% carbon dioxide as described previously.

Taxol was added to undifferentiated cells after 1-2 days in growth medium, and to myotubes after two weeks in fusion medium. After appropriate incubation periods the cells were washed once in phosphate buffered saline + 0.02% bovine serum albumin and then fixed (described in section 3.2.3.2.) and double stained (described in section 3.2.4.).

3.2.8. PHOTOMICROSCOPY

3.2.8.1. CAMERAS

Photographs were taken using an Olympus OM2N camera for fluorescence and phase contrast microscopy, and a Mamia 50A roll film holder for transmission electron microscopy.

3.2.8.2. FILMS

Ilford cut film (6.5X9.0 cm) was used for TEM, Kodak T-Max 400 for fluorescence microscopy.

3.2.8.3. PHOTOGRAPHIC SOLUTIONS

For T-Max 400 developer

1A– Developer solution; 20% T-Max, 80% distilled water. Wash with developer solution for 10 minutes at room temperature, shake every 20 seconds for 20 seconds.

1B– Stopper solution; 19.5% Hypam, 2.4% Rapid Hardener, 78.1% distilled water. Wash with stopper solution for 5 minutes at room temperature, shake every 20 seconds for 20 seconds.

For APX 25 developer

2A– Developer solutions; 10% Aculux, 90% distilled water. Wash with developer solution for 7 minutes at room temperature, shake every 20 seconds for 20 seconds.

2B– Stopper solution; 20% Hypam, 2% Hardener, 78% distilled water. Wash with developer solution for 5 minutes at room temperature, shake every 20 seconds for 20 seconds.

After processing, all films were washed with warm water for 30 minutes. 3 drops of Anti-static were added to last rinse.

3.2.8.4. PHOTOGRAPHIC PAPER

Ilford MG photographic paper was used.

3.3. RESULTS

3.3.1. CHANGES IN THE ORGANIZATION OF MICROTUBULES AND CENTRIOLES DURING DIFFERENTIATION

3.3.1.1. CHANGES IN THE DISTRIBUTION AND LOCATION OF MICROTUBULES DURING ELONGATION OF CO25 MYOBLAST CELLS

Fluorescently labelled YL1/2 and ID-5 antibodies were used to study the distribution of cytoplasmic microtubules in CO25 cells during differentiation. The YL1/2 antibody stained the tyrosinated α-tubulin present along the microtubule network, and the ID-5 antibody stained glu-α-tubulin. In general few glu-rich microtubules were found and ID5 proved to be an excellent marker for the centrioles in CO25 cells.

In this study, it was found that most of CO25 cells contained 1-4 centrioles, but the number of centrioles in the cells was very variable. The numbers of centrioles present could be up to 35. In this chapter, some cells which had larger numbers of centrioles, were chosen to show clearly how they were moved, and new structures formed during differentiation.

In general in the growth medium all the microtubules stained strongly with YL 1/2 and appeared to be mainly nucleated from around the nuclei, radiating out to the cell periphery (Fig. 17a, c). Thus the traditional central MTOC does not seem to exist in these cells rather there is nucleation from several or many centrosomes. After staining with ID-5 antibody, very few microtubules stained strongly and in general they were only stained as dots along their length (thin arrow shows on Fig. 17b, d). The only structures which stained strongly with ID5 were the centrioles, or rarely primary cilia,(arrows show on Fig. 17d) which were identified by their size and position around the nuclei.

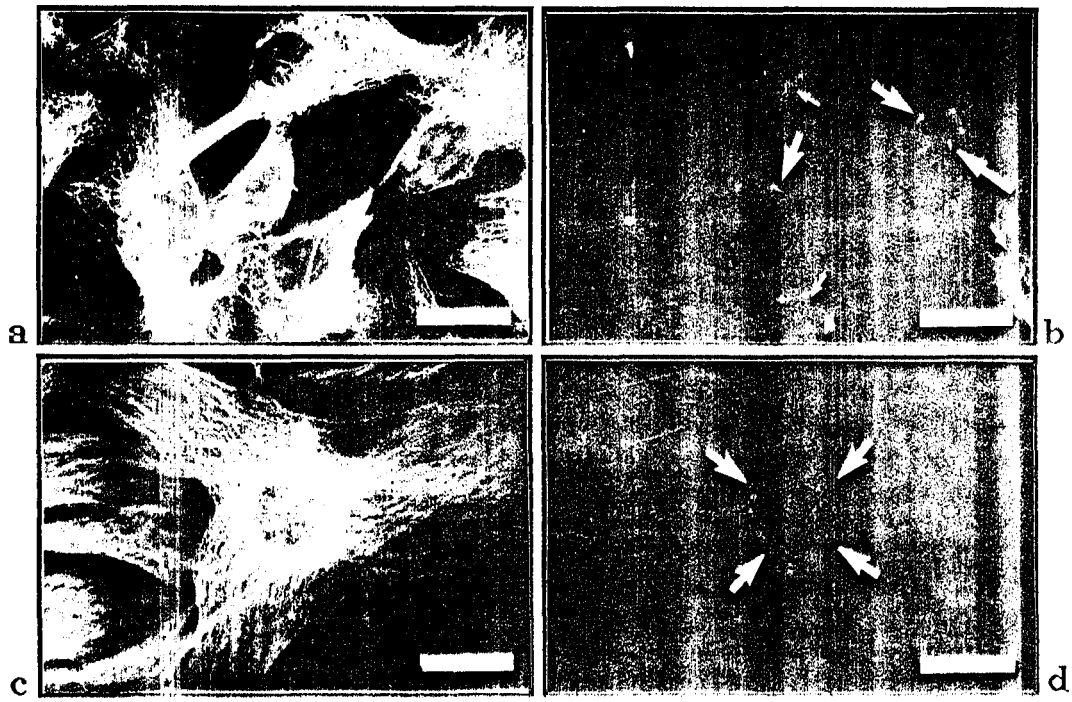

FIG-17 : Organization of microtubules in control CO25 cells in growth medium; (a, c) YL1/2 staining (b, d) ID-5 staining; (b) thick arrows: primary cilia, thin arrow: dot-like staining along microtubules, (d) arrows, centrioles localized around a nucleus; Bars= 20 µm.

Sometimes cells showed a horn-like primary cilia rather than a number of centrioles (Fig. 17b). In the growth medium, most cells had centrioles. Primary cilia were found only rarely. The number of cells containing centrioles or primary cilia were counted in a total of 400 cells as shown in Table-1.

	Number of cells with one or more primary cilia	Number of cells with centrioles	Number of cells with nothing obvious
Number of cells	24	347	29
Percentage	6	86.75	7.25

TABLE-1 : Frequency of centrioles and primary cilia after one day in the growth medium. 400 cells were counted in 4 different preparations.

Approximately 87 % of cells contained centrioles. Primary cilia were 6 % of the population and nothing was obvious in 7% of the cells (see page 63, Graph.- 2-A).

After replacing the growth medium with fusion medium, the cells were examined carefully for stages corresponding approximately to every 6 hours. Within the first 6 hours, tyr- rich microtubules were found to fan out seemingly from around the nuclei. All the microtubules run towards the periphery of the cells (Fig. 18a). Some bundles of glu-rich microtubules were seen in the edges of the cells (arrows show on Fig. 18b). 6 hours after transfer to the fusion medium, the centrioles were found to begin movement towards each other on the top of the nucleus to form one or more groups (Fig. 18b).

12 hours after replacing with fusion medium, in many cells a polarized shape with microtubules frequently running along the long axis of the cell began to be obvious (compare Fig. 19c with 19 a). Tyr-rich microtubules were observed to have formed long thin bundles, which nucleated from around the nucleus, and radiated out to basically two sides of the periphery of the cell (Fig. 18c, 19c). Some microtubules were now seen to originate from the top of the nuclei (arrow shows on Fig. 18c, 19c). When cells were stained by ID-5, they were still poor for glu-rich microtubules. Group of centrioles were now observed to be congregated on the top of nuclei (Fig. 19b, d). A number of microtubules were nucleated from them but the numbers obviously associated with the centrioles were small (Fig. 19a, c). In general it

seemed that many microtubules were nucleated from around the outer edges of the nuclear envelopes (Fig. 19a, c).

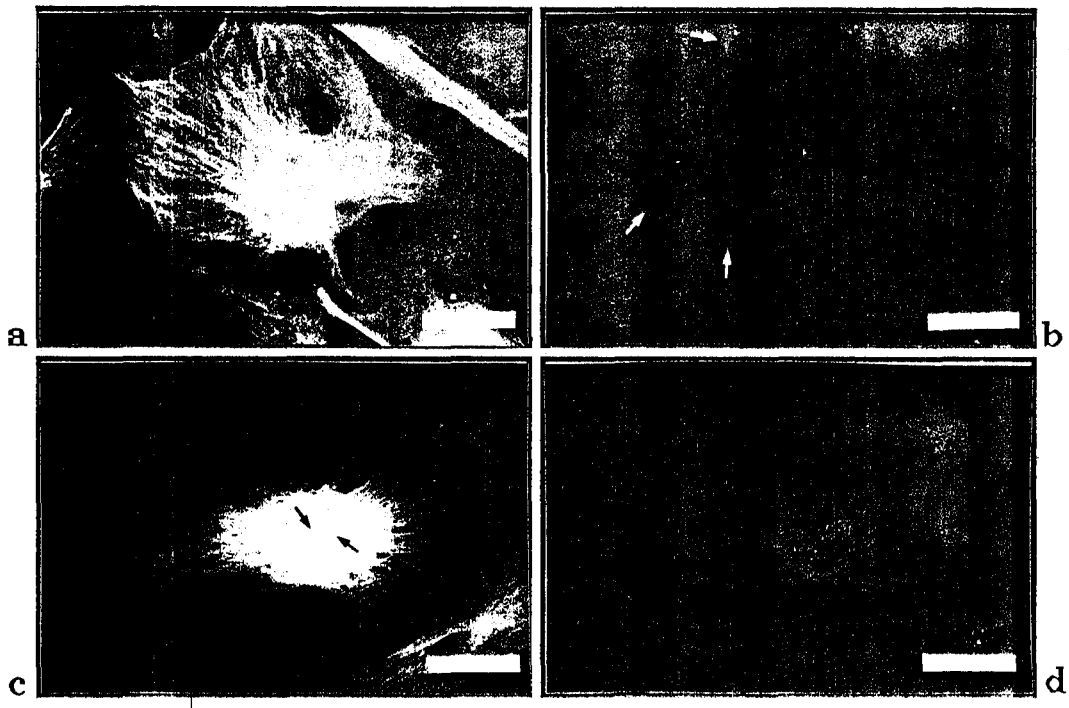

FIG-18: Distribution of microtubules in the fusion medium during differentiation of CO25 cells; (a, c) YL1/2 staining, (b, d) ID-5 staining, (b) arrows, glu-rich microtubules at the edge of a cell, (c) arrow shows some microtubules originating from the top of a nucleus; Cells in fusion medium after 6 hours (c) YL1/1 (d) ID-5, and after 12 hours; Bars= 20 μm.

After 16 hours, there were no significant changes in the distribution of the tyr- rich microtubules in the cell bodies and the amount of glu- tubulin present, but more compact groups of centrioles were present over the nuclei (Fig. 19 b). After 24 hours, Fig. 19d shows that a group of centrioles had aggregated on the top of nuclei (arrows show on Fig. 19d).

After 30 hours in the fusion medium, Figs. 20a-d show that it was possible to find different stages of the differentiation of CO25 cells. The rate of aggregation of centrioles during differentiation was found to be quite variable. In some cells dense clumps of almost fused centrioles were seen (arrows show on Fig. 20b, d) whereas in other cells the process of aggregation proceeded much more slowly (Fig. 20d).

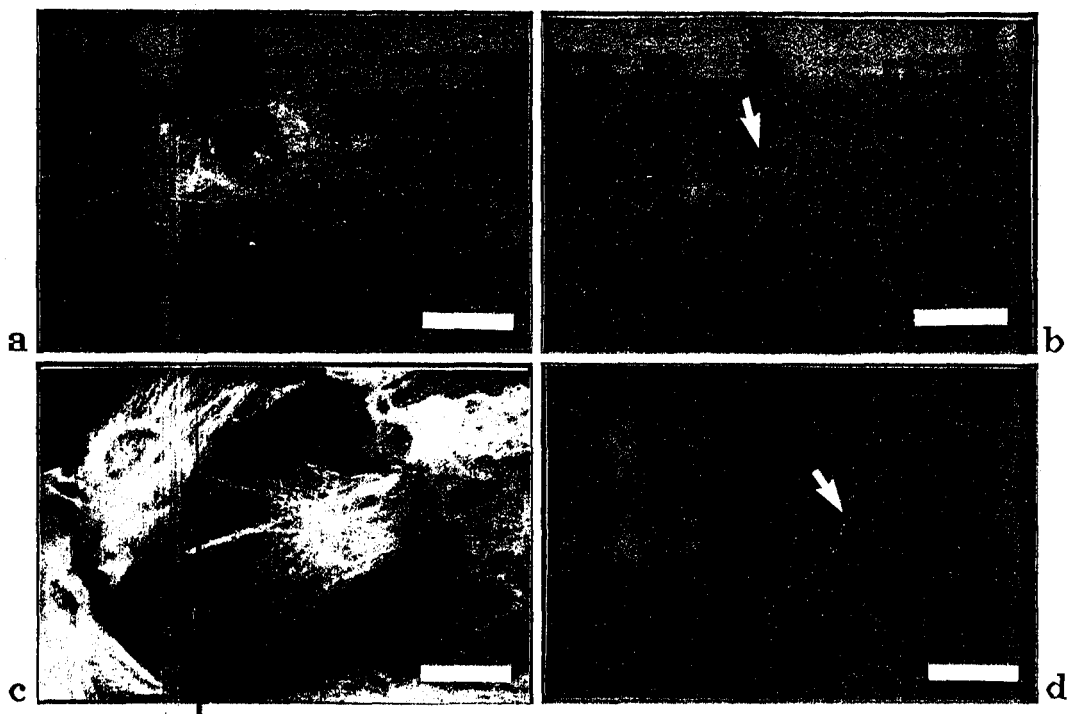

FIG-19 : Organization of microtubules in CO25 cells in the fusion medium (a, c) YL1/2 staining; (b, d) ID-5 staining. (a, b) after 16 hours, (c, d) after 24 hours, (d) arrow, a group of centrioles; Bars= 20 µm.

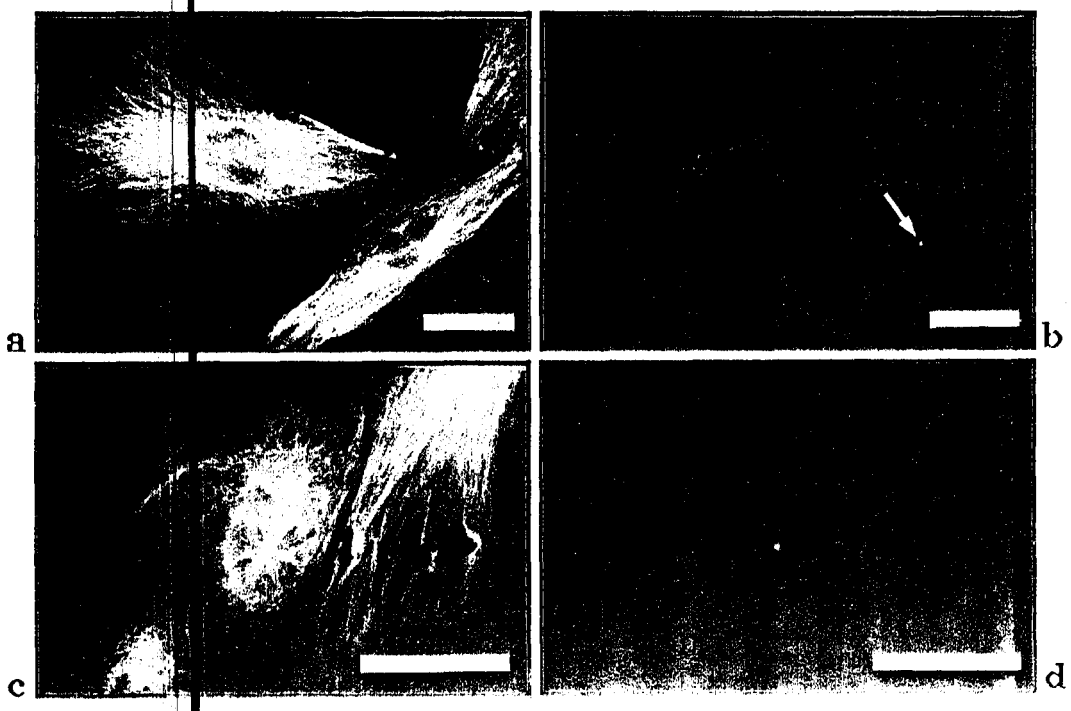

FIG-20 : CO25 myoblast cells after 30 hours in the fusion medium using (a, c) YL1/2 antibody, and (b, d) ID-5 antibody, (b) arrow shows a clumps of centrioles; Bars= 20 µm.

3.3.1.2. FORMATION OF PRIMARY CILIA

During the formation of the primary cila, there was not a significant difference in the distribution of microtubules. However microtubules were frequently seen in bundles running along the long axis of the cells. Some of the bundles were associated with the fusing centrioles whilst others seemed to originate from around the nuclei (Fig. 21a). Glu-tubulin rich microtubules were only rarely seen in cells at stage (Fig. 21f).

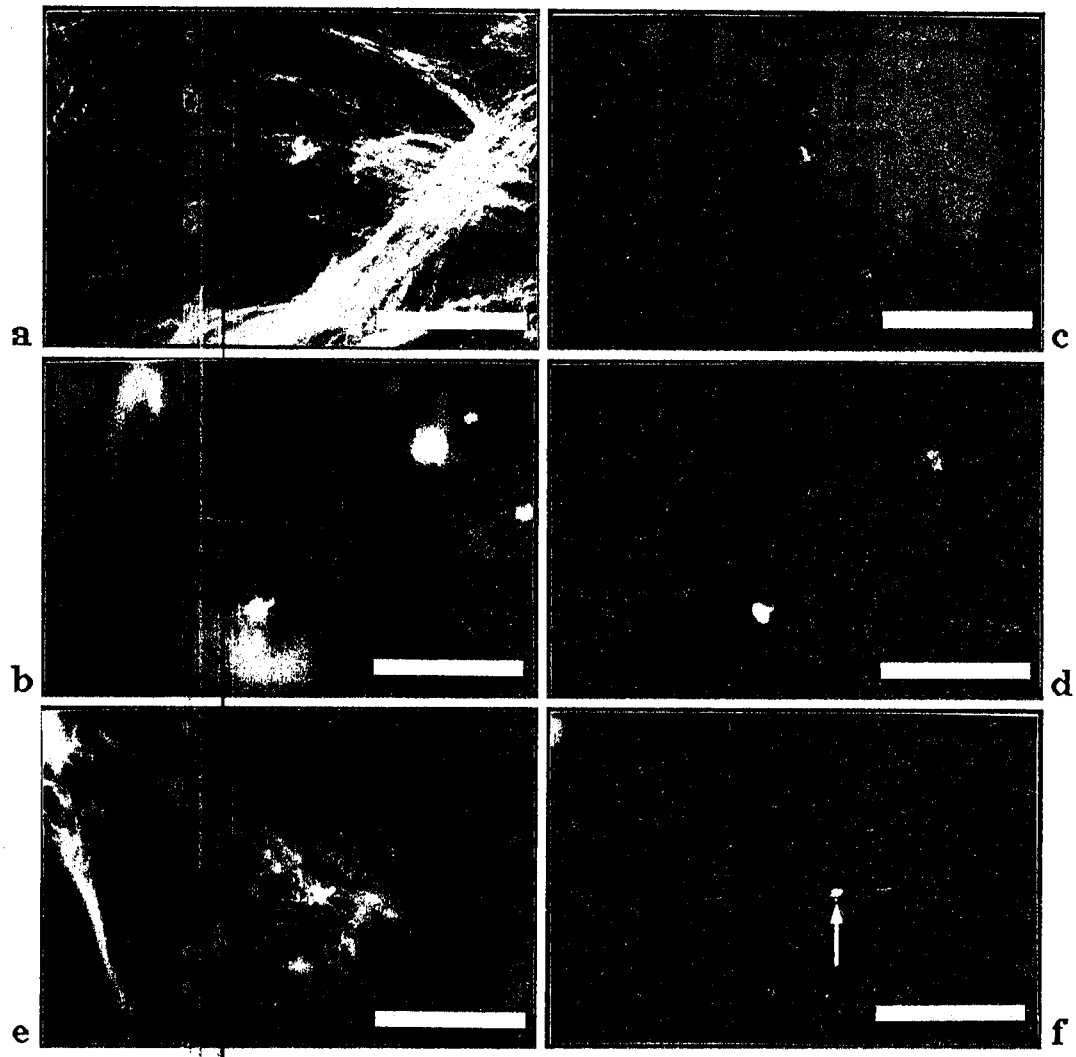

FIG-21 : Double immunofluorescence labelling of CO25 myoblast cells in the fusion medium using (a, c, e) YL1/2 antibody, and (b, d, f) ID-5 antibody; (a, b) after 50 hours, (c, d) after 60 hours, and (e, f) after 61 hours, (f) arrow shows an isolated centriole during the formation of primary cilium; Bars= 20 µm.

ID-5 staining showed that, around 60 hours it first became evident that primary cilia were growing out from the fused centriole aggregation (Fig. 21b, d, f). The forming primary cilia had seemingly rather larger bases than the fully formed ones (Fig. 21d). The cells still showed very few glu-rich microtubules indeed. Sometimes there were some bright dots near the bases of the primary cilia, which were most probobly either individual unfused centrioles or two or three of them which have fused together but not with the main mass (thin arrow shows on Fig. 21f). At later times these isolated centrioles were lost.

The centrioles became progressively aggregated in most cells with increasing time in the fusion medium to forming progressively more primary cilia (Figs. 22a, b). But in some cells the centrioles were still moving together at the same time as aggregation had already occurred in other cells (arrow shows at top right of Fig. 22b). The aggregated centrioles were always localized over the tops of the nuclei (Fig. 22b, d).

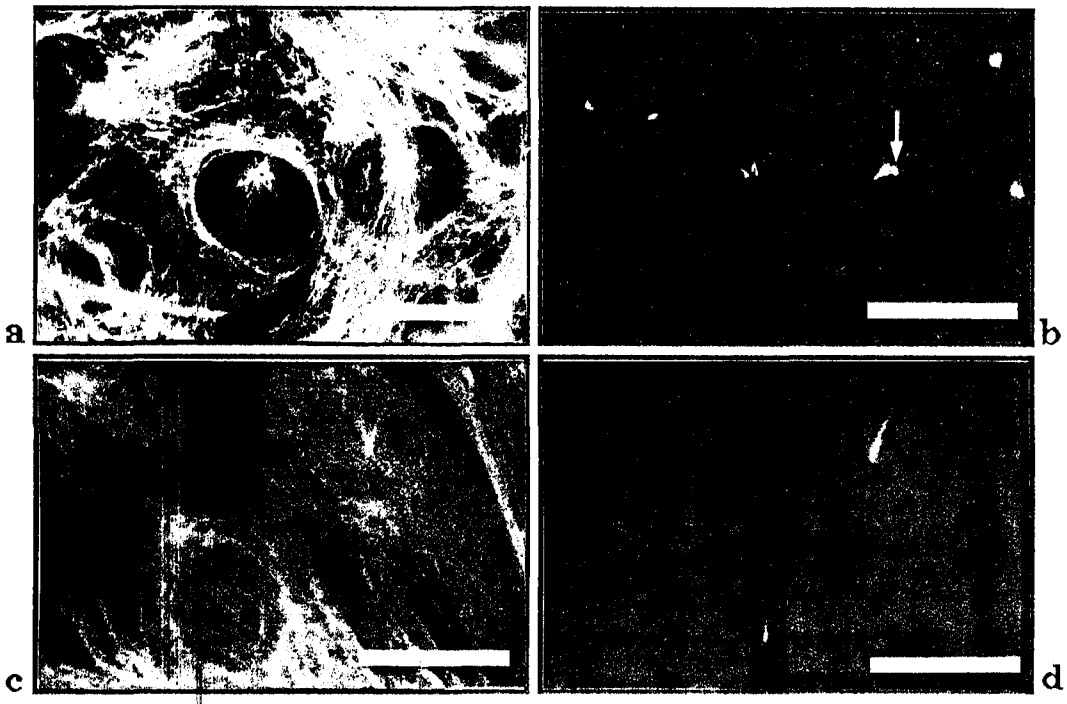

FIG-22 : Double immunofluorescence labelling of CO25 myoblast cells in the fusion medium using (a, c) YL1/2 staining, and (b, d) ID-5 staining, (b) arrow shows aggregated centrioles; (a, b) after 63 hours, and (c, d) after 66 hours; Bars= 20 μm.

Usually the differentiating myoblast cells had one primary cilium, but rarely two or three (e.g. Fig. 22b). The primary cilia were strongly

stained by anti Glu-tubulin and also they usually showed some weak staining with the anti Tyr-tubulin stain (Fig. 22c). Some microtubules always radiated out from the bases of the primary cilia but the numbers of microtubules associated with the primary cilia were very variable (Fig. 22a, c). Many microtubules seemed to originate around the nuclei but no discrete foci were evident apart from those microtubules associated with the primary cilium. The primary cilia always had a wider base (Figs. 22b, d), and the bottom of the shaft was thicker than the upper part (Figs. 22b, d). A count of 400 cells showed that 79% of the cells contained primary cilia, 17% of them still contained centrioles, and 4% nothing obvious in the culture after culture for one week (Table-2; see page 63, Graph- 2-B).

	Number of cells with one or more primary cilia	Number of cells with centrioles	Number of cells with nothing obvious
Number of cells	315	68	17
Percentage	78.75	17	4.25

TABLE-2 : Frequency of centrioles and primary cilia after one week in the fusion medium. 400 cells were counted for a total of 4 different preparations.

3.3.1.3. ULTRASTRUCTURE OF PRIMARY CILIA AS SEEN WITH THE TRANSMISSION ELECTRON MICROSCOPE

Transmission electron microscopy (TEM) was used to investigate the ultrastructure of the primary cilium. The primary cilia were localized very close to the nuclei of the cells in all examples observed. Investigation of both vertical (Fig. 23c), and transverse (Fig. 23a, b, d, and e) sections of primary cilia indicated that the shafts of primary cilia were surrounded by a vacuole (letter "V" shows on Fig. 23b, and Fig. 23c). There were nine doublets tubular fibrils forming a ring around the periphery of the primary cilium, but there was no central pair as would be seen in functional cilia (Fig. 23b). Thus the typical 9+0 structure of a centriole was observed and not the 9+2 structure of a cilia. TEM images showed that at the base of the primary cilium, there were sometimes tubular structures frequently perpendicular to the long axis of the cilia,

These might be unfused centrioles or alternatively microtubular rootlets (Fig. 23e).

Scanning electron microscope (SEM) images showed that the surfaces of the elongated cells were quite smooth and there was no hint of cilia protruding out of the cells (Figs. 12a, b in chapter 2).

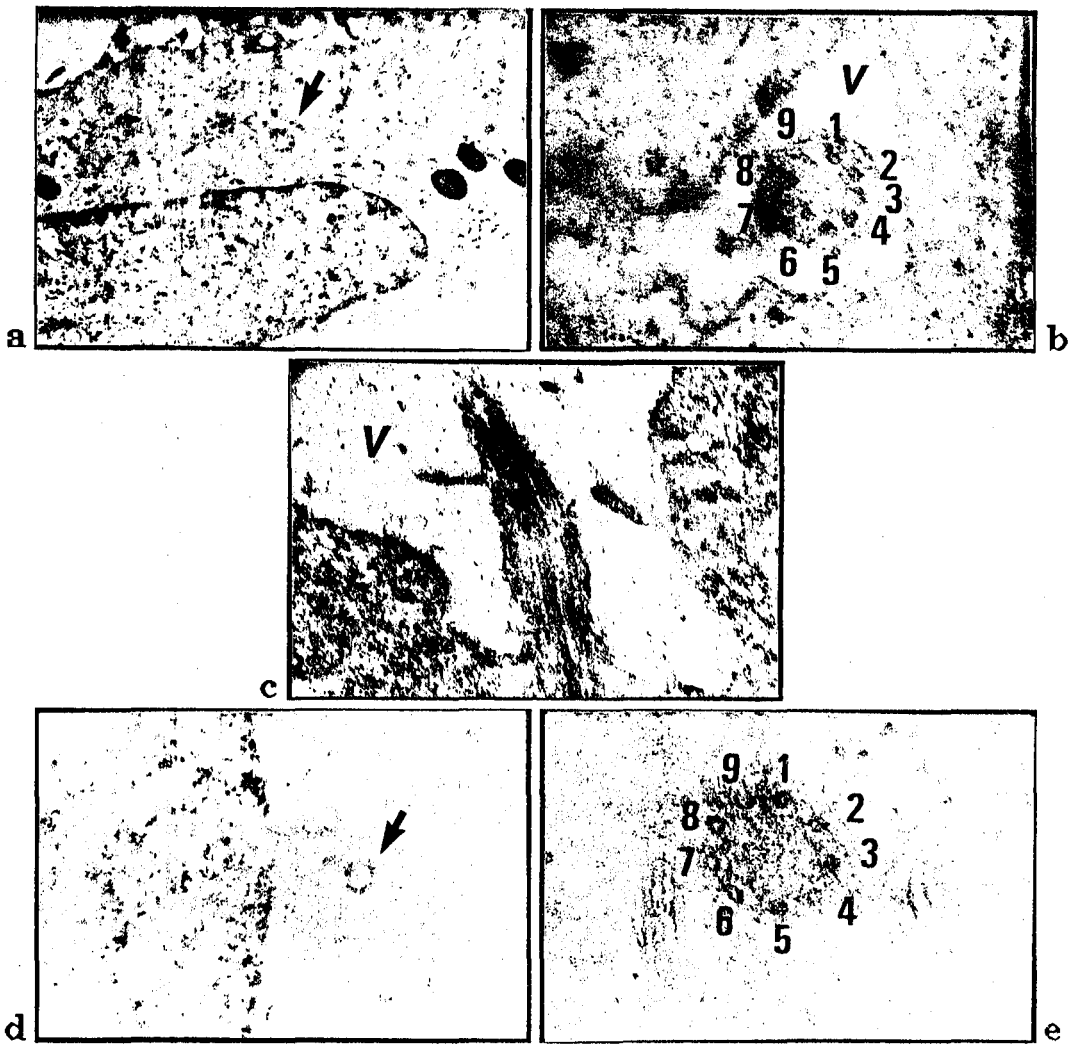

FIG-23 : Primary cilia in CO25 myoblast cells as seen with T.E.M.; tranverse sections of the upper region (a, d) X10.000, (b, e) X50.000, (c) oblique section of the apical region, X66.000. "V" shows the vacuole which surrounds the shaft of each cilium.

3.3.1.4. DISTRIBUTION OF MICROTUBULES DURING FORMATION OF MYOTUBES

After 70 hours but before cell fusion occured, all the tyr-rich microtubules were observed to run along the long axis of the elongated myoblasts (Fig. 24a, b, and c). During the fusion stage, most of the tyr-

rich microtubules seemed to originate from around the nuclei, but some microtubules originated from primary cilia localized on top of the nuclei (Fig. 24a). As shown on Fig. 24a and b most of the cells had a primary cilium on the top of the nuclei. Interestingly, shortly before fusion occurred bundles of glu-rich microtubules were observed for the first time (Fig. 24b). Some of these were associated with the processes forming the ends of the elongated cells. The glu-microtubules were increased in the elongated cell body (Fig. 24b). Fig 24d shows distribution of tyr-rich microtubules in a fusing cells. All microtubules were running parallel along the long axis up to fusing processes.

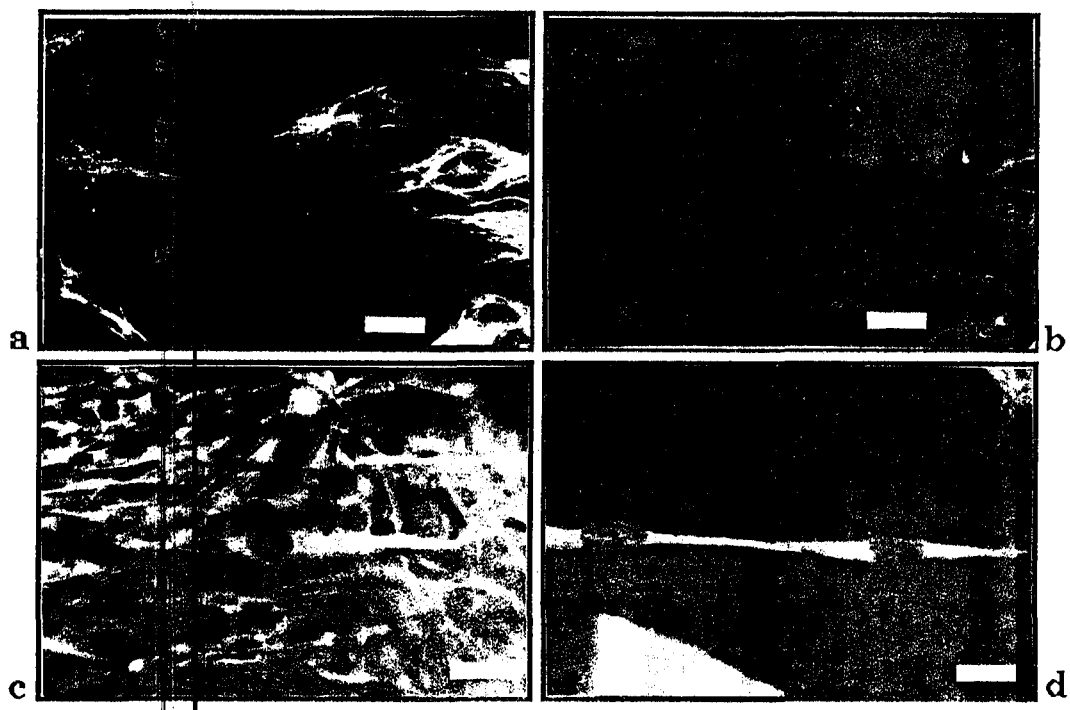

FIG-24 : Organization of microtubules in elongated CO25 cells in the fusion medium (a) microtubules by YL1/2 staining (b) microtubules stained by ID5 after 70 hours, (c) after 78 hours by YL1/2 , (d) by ID-5 staining; Bars= 20 μm.

After fusion (80-100 hours in the fusion medium) staining of CO25 cells with YL1/2 antibody indicated clearly that all the microtubules now run along the long axis of the myotubes (Fig. 25). The longitudinal distribution of the microtubules along the myotubes was seen to be parallel to each other, and filled the whole myotube except the nuclei (Fig. 25c, d). No microtubule foci, indicative of MTOCs, were visible. In the myotubes, only a rather weak glu-staining along the

microtubules was now observed (Fig. 25b), and the level of glu-tubulin staining rapidly decreased after fusion during myogenesis. Soon after fusion the myotube nuclei were still associated with primary cilia (thin arrow shows on Fig. 25b).

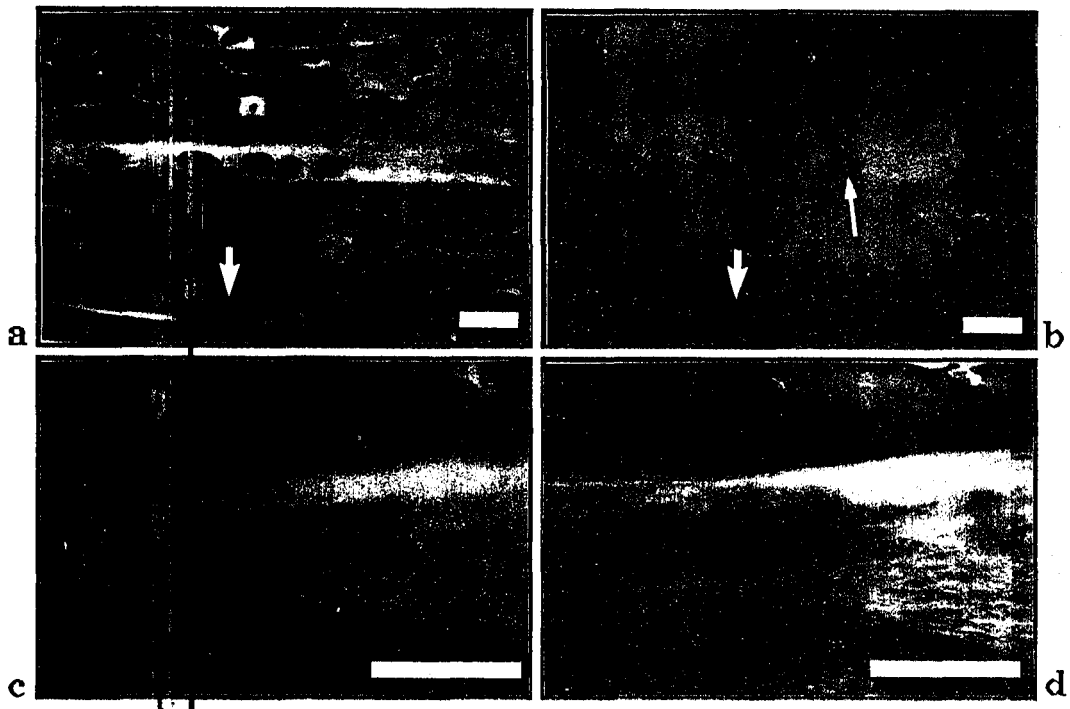

FIG-25 : Distribution of microtubules in myotubes in fusion medium after 80 hours of culture. Double immunostaining (a) YL1/2, (b) ID-5, (a, b) thick arrow show an elongated myoblast, thin arrow shows a primary cilium in the myotube. (c and d) YL1/2 staining; after 90 hours (c) top level, (d) middle level; Bar= 20 µm.

3.3.1.5. FATE OF THE PRIMARY CILIA

At an early stage after myotube formation, investigation showed that groups of centrioles were visible again localized near or top of the nuclei in a similar position where the primary cilia were previously observed (Fig. 26b). These changes occurred quickly and no intermediates were seen. The most likely source of the centrioles would seem to be disassembly of the primary cilia the bases of which may break up into centrioles. Alternatively a single centriole is release from the base of the cilium which rapidly duplicates. The kinds of structures observed are rather variable. In Fig 26b what appears to be a group of somewhat degraded primary cilia are visible associated with several nuclei, and this may represent the first stage in the process of primary

cilium breakdown. Fig. 26d shows a very tight cluster of centrioles. "Older" myotubes (e.g. Fig. 27b) frequently had more scattered groups of centrioles suggesting that they are released as a group from the remains of a primary cilium. However single centrioles were also frequently seen in such myotubes (Fig. 26b).

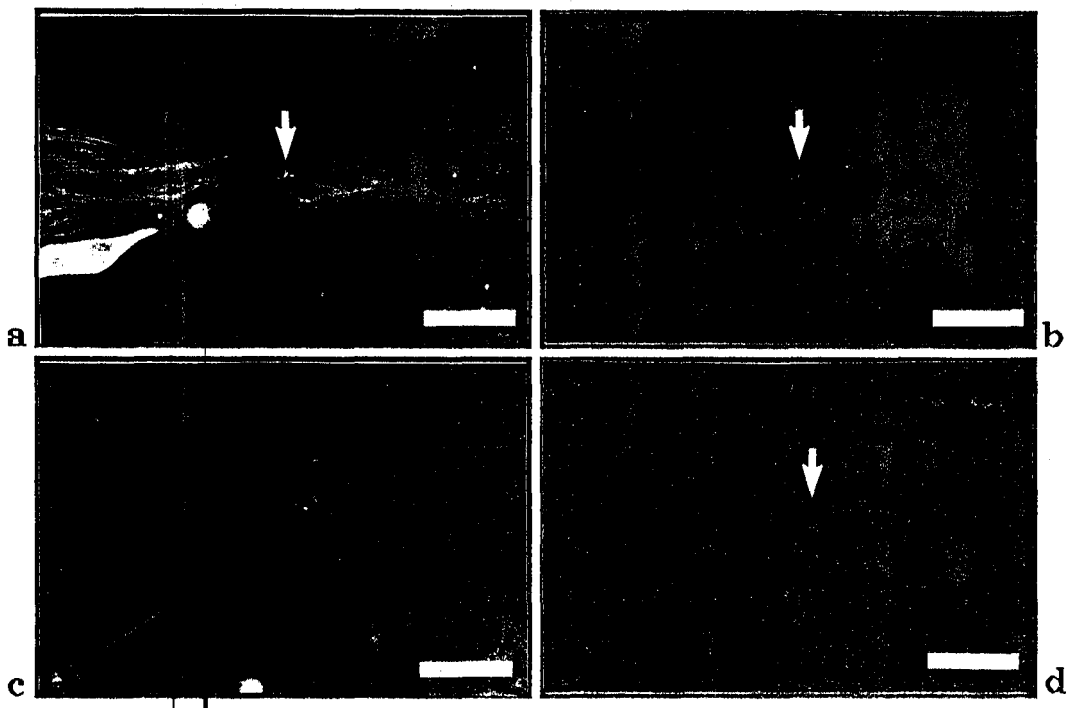

FIG-26 : Double immunofluorescence labelled CO25 myotubes after 96 hours in the fusion medium using (a, c) YL1/2 antibody, and (b, d) ID-5 antibody, (a, b) arrows show a group of centrioles or degraded primary cilia, (d) arrow indicates a group of cilia; Bars= 20 μm.

Usually all of them were localized very close to a nucleus in the myotubes (Fig. 27b). After approximately 2 weeks in the fusion medium, single centrioles were observed standing on a line along the long axis, and each associated with a nucleus (thin arrows show on Fig. 27b). After terminal differentiation of the myotubes, actin staining with rh-phalloidin showed a periodic distribution of actin along the myofibrils (Fig. 27f). The distribution of the bundles of tyr-rich microtubules was parallel to the newly formed myofibril actin bundles, and ran along the long axis (Fig. 27e). By the time mature myofibrils have formed the amount of glu-tubulin present along the microtubules has been reduced to very low amounts and only the centrioles stain strongly with ID5.

The pattern of staining corresponds to that seen prior to myoblast elongation, and all the glu-rich microtubules disappear.

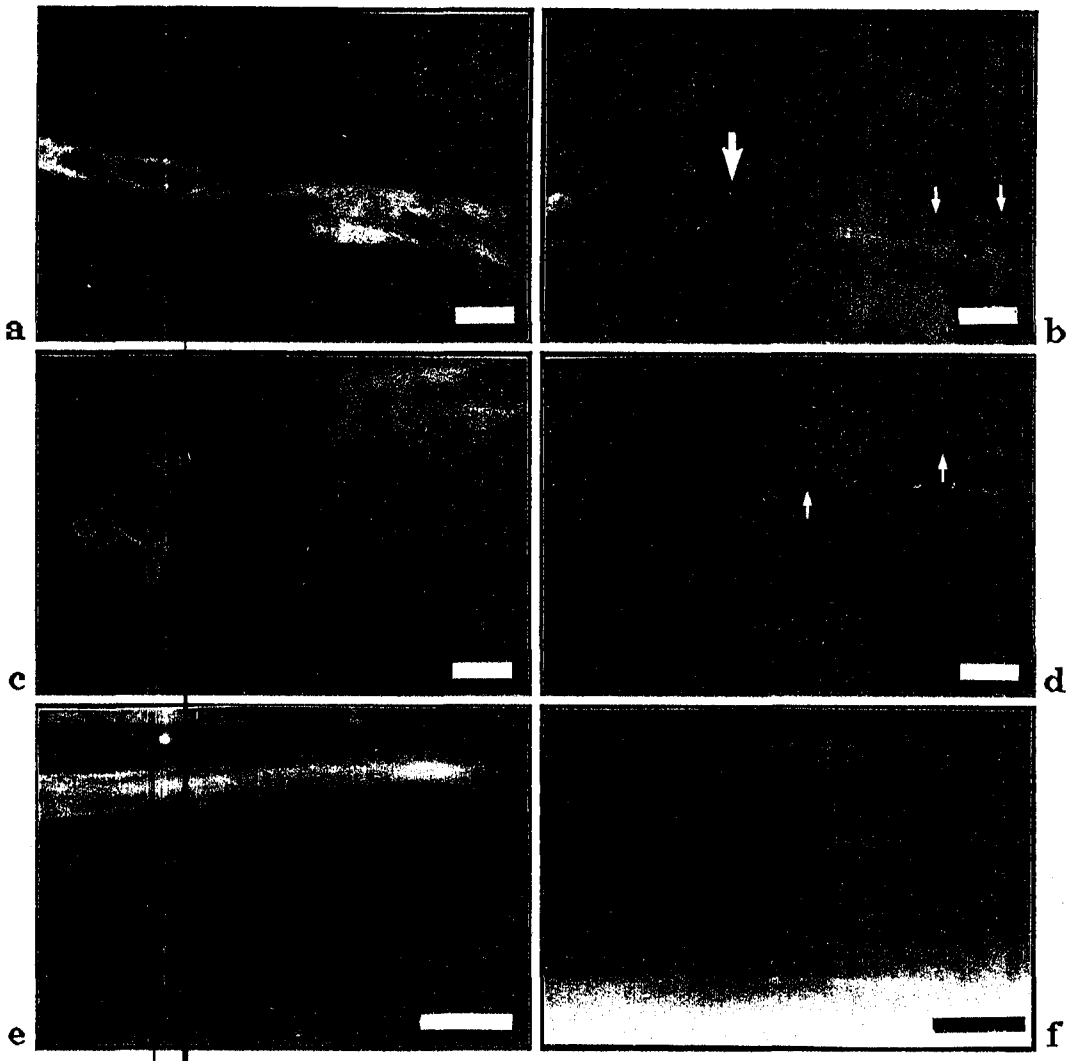

FIG-27 : Double immunofluorescence labeling of CO25 myotubes in the fusion medium using (a, c, e) YL1/2 antibody, and (c, d) ID-5 antibody, (f) Rhodamin-phalloidin; (a, b)after 105 hours, and (c, d, e, f) after 300 hours, (b) thin arrows show single isolated centrioles, thick arrow shows a group of centrioles; Bars= 20 µm.

After 2 weeks in the fusion medium a count of 400 cells showed that approximately 14% of them contained primary cilia, approximately 80% contained centrioles, and nothing obvious was present 6 % of the cells (Table-3 see page 63, Graph.- 2-C).

These percentages were significantly, different from the figures found after one week in the fusion medium, and were much more similar

to the precentage of centrioles present in undifferentiated myoblasts (Graph-2A; 2C). Graph-2 shows the dramatic increase in the number of primary cilia which occurs during cell elongation prior to fusion and their rapid disappearance as myotubes form.

	Number of cells with one or more primary cilia	Number of cells with centrioles	Number of cells with nothing obvious
Number of cells	58	318	24
Percentage	14.5	79.5	6

TABLE-3 : Frequency of centrioles and primary cilia after 2 weeks in the fusion medium. 400 cells were counted for 4 different preparations.

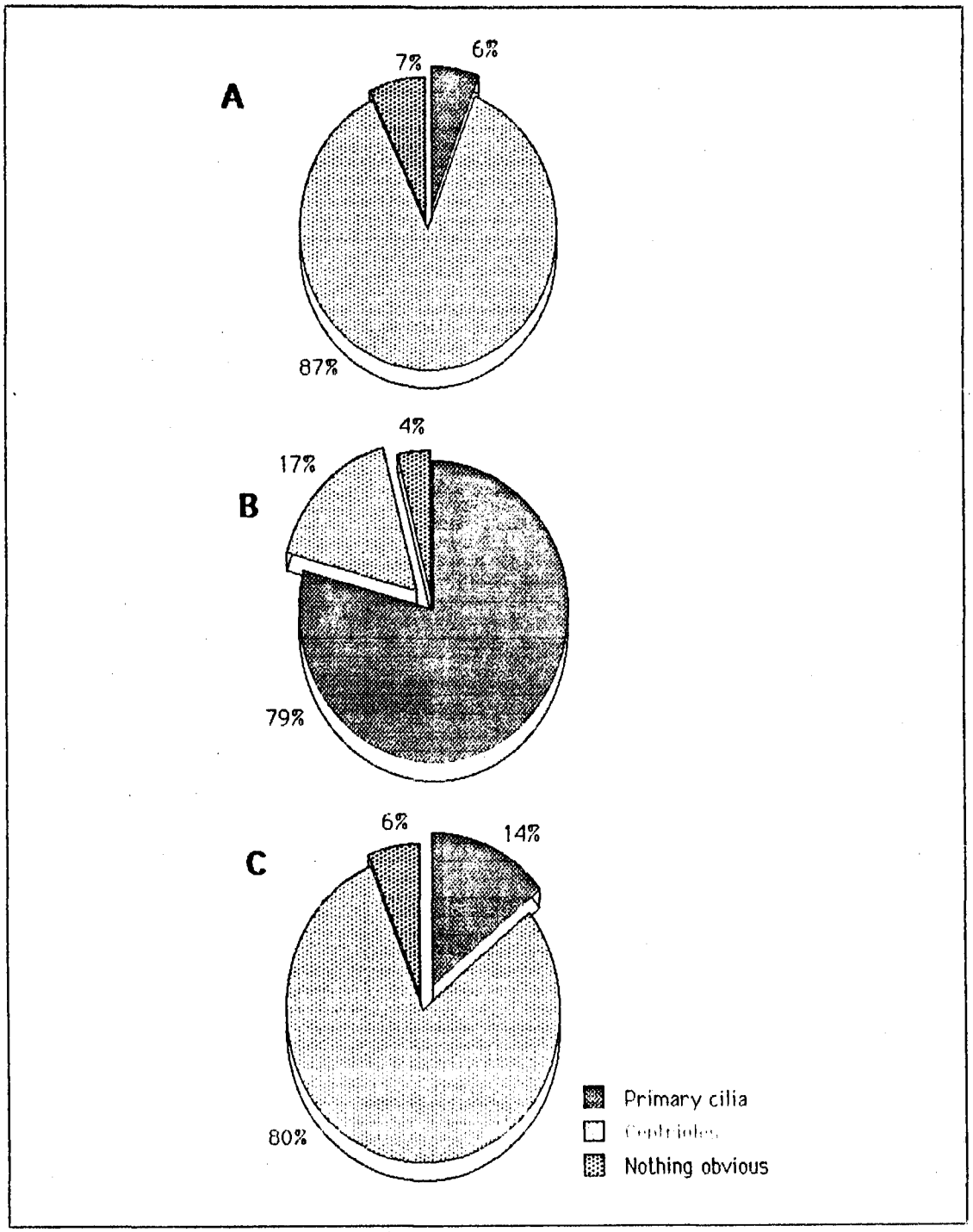

GRAPH-2 : Proportion of CO25 cells showing primary cilia or centrioles centres,400 cells counted for each sample; (A) after 2 days in the growth medium, (B) after a week in the fusion medium, (C) after 2 weeks in the fusion medium. Data from Tables-1, 2, and 3 were used to prepare pie diagrams 2A, 2B, and 2C.

3.3.2. DISTRIBUTION OF MICROTUBULES IN DRUG TREATED CO25 CELLS

3.3.2.1. MICROTUBULE REGROWTH AFTER NOCODAZOLE TREATMENT

In this experiment, myoblasts and myotubes were first treated with nocodazole (as described in section 3.2.7.1.) then the nocodazole containing medium was washed away to relieve cells from the effects of nocodazole, and the microtubules were allowed to regrow for varying periods of time.

The cells were treated with 24 µg/ml nocodazole for 1 hour and then stained and examined with the fluorescence microscope. The effect of using 24 µg/ml nocodazole for 1 hour on the cells was to depolymerize all the microtubule network (Fig. 28a). As shown in Fig. 28 ID-5 staining showed that only the centrioles remained visible in the myoblasts (arrow shows on Fig. 28b). After 4 minutes removal of nocodazole from medium, tyr-microtubules started to regrow as starlike structures, and to elongate from the tops of the nuclei (arrow shows on Fig. 28c, and 29a).

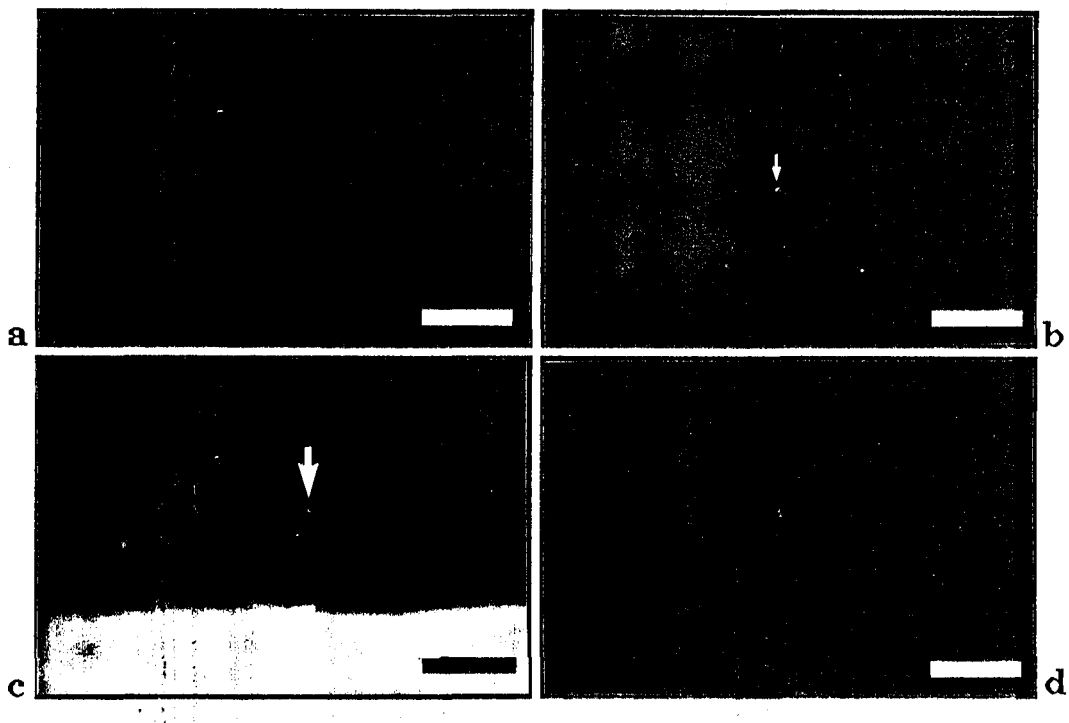

FIG-28 : Microtubule patterns in myoblasts (a, b) after (24 µg/ml) nocodazole (1 hour) treatment, and (b, c) after 4 minutes removal nocodazole; (a, c) Yl1/2 staining, (b, d) ID-5 staining, (b) arrow shows centriole, (c) arrow shows microtubule regrowth; Bars= 20 µm.

The results showed that microtubules elongated from one or more MTOCs in myoblasts after nocodazole treatment (arrow shows on Fig. 29a). At this time of regrowth some microtubules appeared to be completely free in the cytoplasm and not associated with any centrosomes (Fig. 29c, e). ID-5 associated showed only brightly stained centrioles (Fig. 29b, d, f) as would be expected.

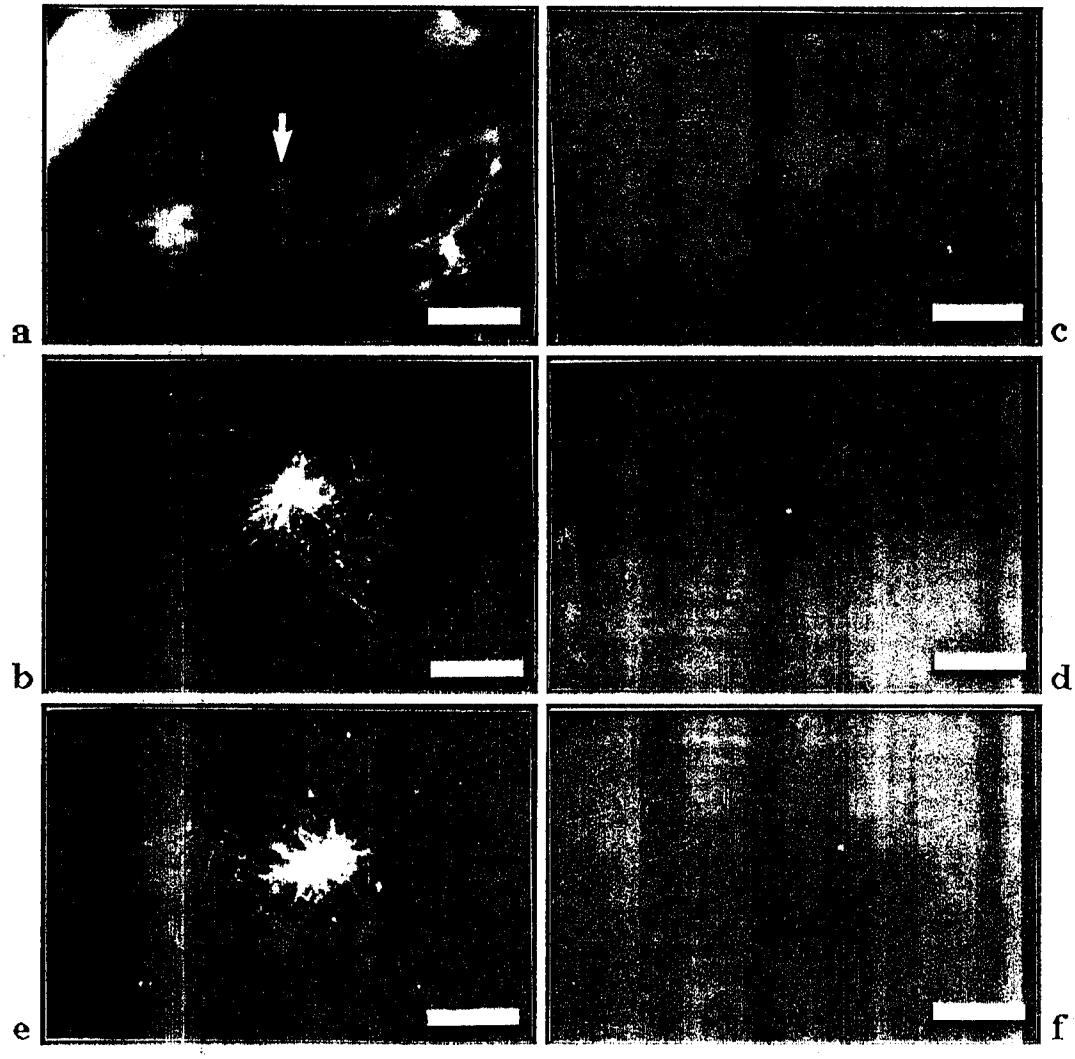

FIG-29 : Microtubule pattern in myoblasts after 4 minutes removal from nocodazole; (a, c, e) YL1/2 staining, (b, d, f) ID-5 staining, (a) arrow shows regrowth of microtubules; Bars= 20 µm.

By 15 minutes considerable microtubule regrowth had occurred, although it was frequently hard to be certain how for the network had

regrowth because of the remaining depolymerized tubulin (Fig. 30a), but only centrioles were visible using ID-5 staining (Fig. 30b).

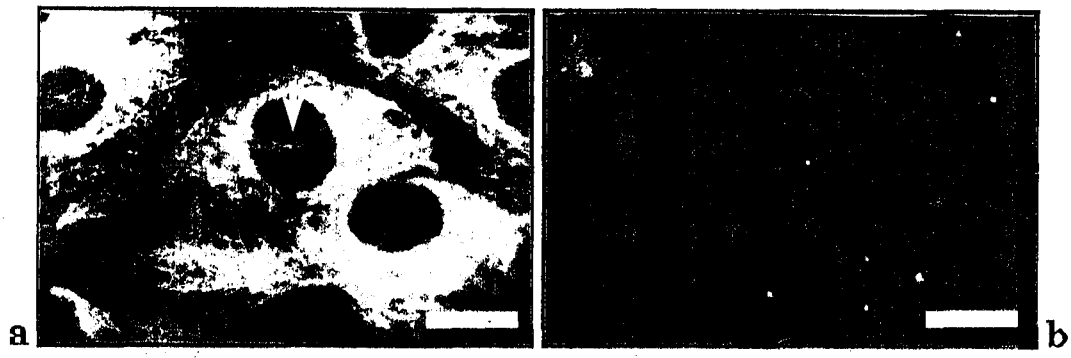

FIG-30 : Microtubule pattern in myoblasts after 15 minutes removal from nocodazole; (a) YL1/2 staining, arrow shows regrowth of microtubules, (b) ID-5 staining; Bars= 20 µm.

After staining myotubes which had been treated with 24 µg/ml nocodazole for 1 hour, all the microtubules had disappeared (Fig. 31a), only centrioles were seen along the long axis (arrows show on Fig. 31b), glu-rich microtubules were not present either in the myotubes.

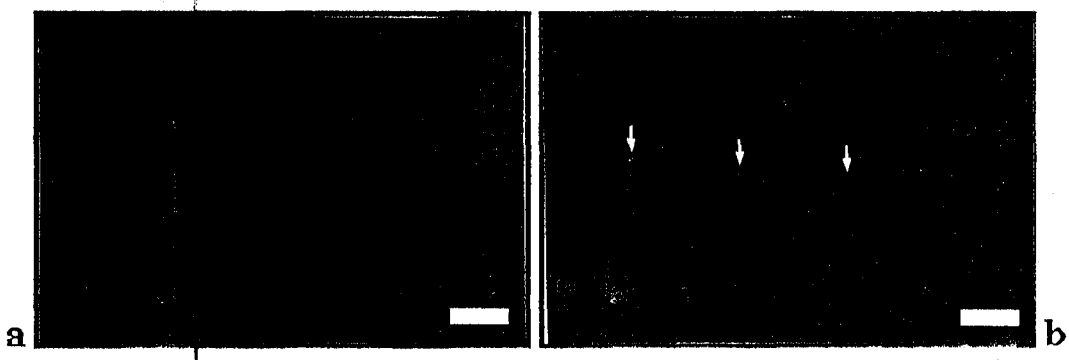

FIG-31 : A myotube after 1 hour treatment with 24 µg/ml nocodazole (a) YL1/2 staining, (b) ID-5 staining, arrows show centrioles; Bars= 20 µm.

After removing nocodazole from the medium, regrowth of the microtubules was very rapid in the myotubes. By 5 minutes it was found that a basket-like distribution of microtubules had started to regrow mainly from around the nuclei (arrows show on Fig. 32a). After 10 minutes, the myotubes were filled with microtubules (Fig. 32c). Most microtubules were seen to be distributed parallel to the long axis of the myotubes (Fig. 32c). But, as best seen at high magnification, some

microtubules initially regrew obliquely in the myotubes (arrows show on Fig. 32a), ID-5 staining showed that there was no visible glu-rich microtubules in the cytoplasm, only single, isolated centrioles along the myotubes (arrows show on Fig. 32b, d).

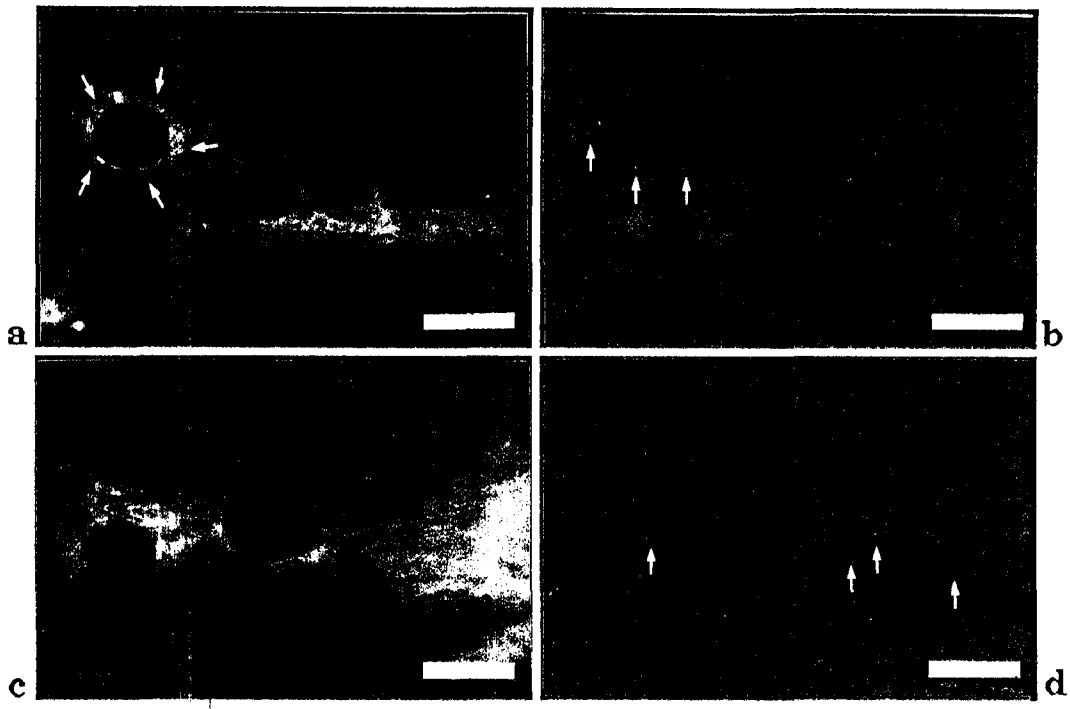

FIG-32 : Myotubes treated with (24 µg/ml) nocodazole for 1 hour; (a, c) distribution of tyr-rich microtubules by YL1/2 staining, (b, d) distribution of glu-rich microtubules by ID-5 staining, (a, b) 5 minutes after removal from nocodazole, (c, d) 10 minutes after removal from nocodazole, (a) arrows show a basket-like microtubule regrowth, (b, d) arrows show centrioles; Bars= 20 µm.

3.3.2.2. MICROTUBULE DISTRIBUTION AFTER TAXOL TREATMENT

After treating myoblasts and myotubes with 12 µM taxol for 12 hours (as described in section 3.2.7.2.) the cells were double stained with YL1/2 and ID-5 antibodies to examine the effects of taxol on the distribution of microtubules.

After incubation with taxol, the effects were quite spectacular on the microtubule networks, showing obvious structural changes in all myoblast cells. The distribution of tyr- and glu-rich microtubules were found always to be identical in taxol treated myoblast cells. However the bundles of tyr-rich microtubules were stained somewhat more strongly

than the staining of glu-rich microtubules (Fig. 33a-d). It was mostly observed that quite large bundles of microtubules formed throughout the cytoplasm in different orientations (Fig. 33a-d). These microtubules were much shorter than those found in normal control myoblasts. In general bundles of short parallel microtubules were found, but some individual microtubules running in different directions were observed (thin arrows show on Fig. 33a). The bundles showed no relationship with the nucleus or any other structure (Fig. 33a-d). Some centrioles could be seen in taxol treated cells (thick arrows show on Fig. 33b, d), although they were difficult to see and often masked by the strongly stained glu-microtubules.

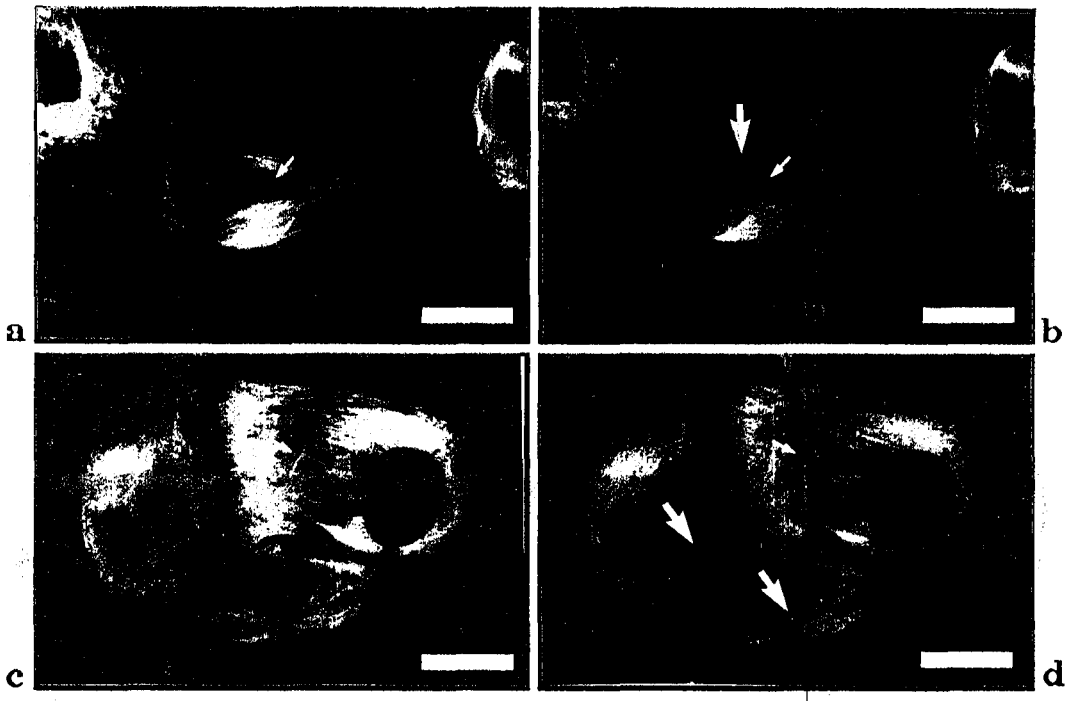

FIG-33 : Myoblasts treated with (12μM) taxol for 12 hours; (a, c) distribution of tyr-rich microtubules by YL1/2 staining, (b, d) distribution of glu-rich microtubules by ID-5 staining, thin arrows shows individual microtubules, thick arrows show centrioles; Bars= 20 μm.

After taxol treatment of myotubes, all the microtubules were similarly stained by YL 1/2 and ID5 showing that increased amounts of glu-tubulin were present (Fig. 34). In myotubes, most microtubules were observed to run parallel to each other in short bundles (Fig. 34). However short bundles of microtubules were seen which were not in

parallel (Fig. 34d). The bundles were not centred around the nuclei and not seem to have any relationship to the nuclei. Frequently the bundles were in some kind of register (Fig. 34). Centrioles could not be easly seen in taxol treated myotubes. Most of them were masked by the strongly stained bundles of glu-rich microtubules.

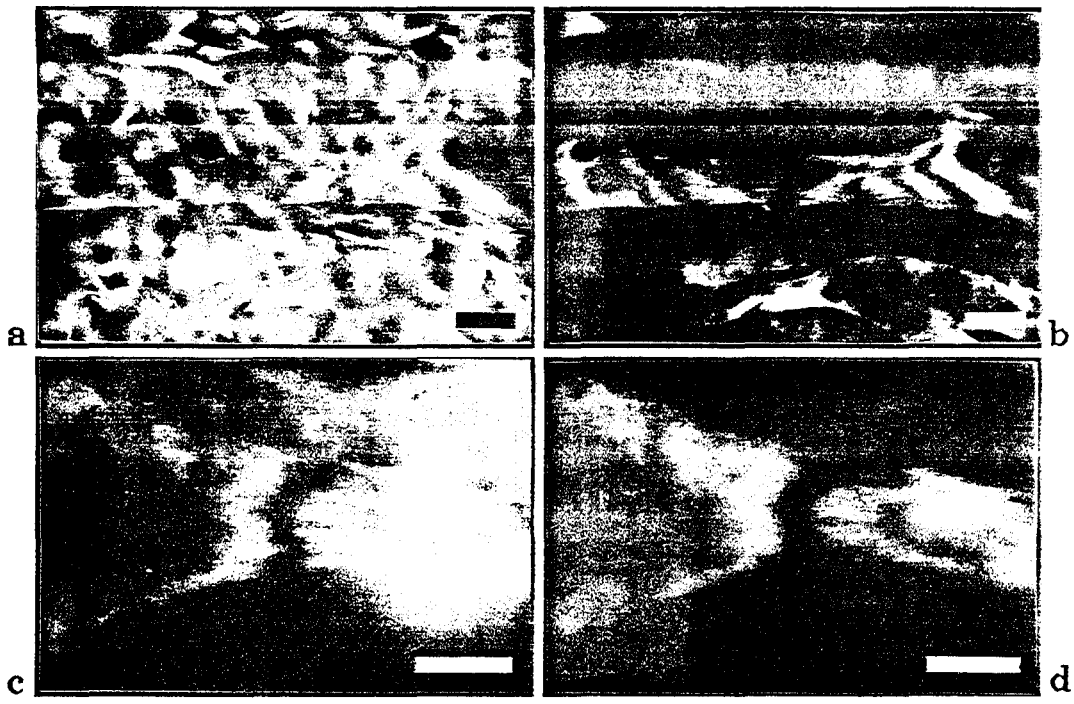

FIG-34 : Myotubes treated with (12mM) taxol for 12 hours; (a, c) distribution of tyr-rich microtubules by YL1/2 staining, (b, d) distribution of glu-rich microtubules by ID-5 staining; Bars= 20µm.

3.4. DISCUSSION

3.4.1. NUCLEATION OF MICROTUBULES

Two different microtubules nucleation centres were identified during CO25 myogenesis as the result of regrowth after drug induced depolymerization. In myoblasts it was observed that centrioles were markers of the primary nucleation centres of the microtubule network, Tassin *et al.* (1985a) also reported similar results using human myoblasts *in vitro* .

After formation of the myotubes, the nucleation centres of the microtubules seemed to be replaced by nucleation at the periphery of the nuclei. There was no relationship between microtubule regrowth and the position of the centrioles. These striking findings of a major change in

the microtubule nucleating centres upon myotube formation confirms the previous work of Tassin *et al.* (1985a). It has also been reported that microtubules were densely aggregated around the nuclei in mature skeletal muscle fibres (Kano *et al.*,1991; Cartwright and Goldstein, 1982), and in cardiac muscle cells (Rappaport and Samuel, 1988; Watkins *et al.*, 1987), suggesting a nuclear MTOC in these cell types as well. The microtubules were reported to be nucleated from some amorphous material around the nucleus in myotubes (Tassin *et al.*, 1985a). This is likely to correspond to the peri-centriolar material which has become redistributed. Microtubules which were not associated with any obvious nucleating structures have also been observed in erythrocytes (Murphy and Wallis, 1986), in melanophores (McNiven and Porter, 1988), in neurons (Baas *et al.*, 1989), and in epithelial cell extensions (Troutt and Burnside, 1988). Also in this work, some free regrown microtubules were found in myoblasts regrowing after nocodazoletreatment, and possibly also in myotubes. This result resembles the finding of Bre *et al.* (1987) that MDCK cells contain many microtubules apparently free in the cytoplasm and not associated with the centrosome or any other structure. In addition to Mogensen and Tucker (1987), Mogensen *et al.*, (1989) have hypothesied that microtubules grow from hemidesmosomes located at the apical cell surface in *Drosophila* in original disc cells. All these results demonstrate that there may not be only one particular microtubule nucleation centre, but it may take a variety of forms. The pericentrosomal material may be able to nucleate microtubules on a variety of structures within the cell, not associated with a centriole.

3.4.2. LOCATION OF TYR-TUBULIN

In this work, the distribution of tyr-tubulin on microtubules was similar to that observed in many other types of proliferating cells (e.g. Gundersen and Bulinski, 1986; Gundersen *et al.*, 1986; Wehland and Weber, 1987; Kreis, 1987). But, during the differentiation of CO25 myoblasts, the tyr-microtubules were found to redistribute parallel to the long axis in myotubes and myofibrils. Assembly of non-radial microtubule arrays during differentiation has also been reported by several authors including Holtzer *et al.* (1985), Tassin *et al.* (1985a), Antin *et al* (1986) observed longitudinally orientated microtubules in myotubes *in vitro*. Daniels and Sandra (1990) also reported that early stage myotubes demonstrated nuclei aligned in parallel rows with

all the elements of the cytoskeleton (also F-actin microfilaments) become aligned parallel to the long axis of the myotubes. How this is determined and regulated is not at all clear at present. This study further demonstrates that as the microtubules re-grow after drug induced disassembly they retain their previous orientation in general. Microtubules, which were initially somewhat out of register rapidly came to conform to the parallel distribution. Again what forces cause this are very unclear.

Serial focussing has shown that, microtubules run parallel along the long axis and to each other all along the myotubes. This location of tyr-rich microtubules was in contrast with Kano *et al.* 's results (1991). They reported that microtubules were found more abundantly in the periphery of rat and mouse muscle fibres, especially just beneath the sarcolemma as compared with deeper regions *in vivo*. It is known that skeletal muscle fibers contain numerous nuclei which are located at the fiber periphery *in vivo*, but the nuclei were not found at the periphery of the myofibres in this work. The difference in distribution of microtubules and nuclei may be due to the fact that Kano *et al.* (1991) were looking at tissues *in situ* whereas this study examined cells grown *in vitro*. The microtubules seem to be mostly nucleated from the periphery of the nuclei in the centres of the myotubes and myifibrils as seen in this work. Therefore the location of microtubules *in vitro* and *in vivo* may well be different. Whether this is an artefact of tissue culture or a failure to complete morphological differentiation is not known.

3.4.3. DISTRIBUTION OF GLU-TUBULIN

It was clearly observed in this work that an increase in the level of glu-tubulin occured during myogenic differentiation shortly before myoblast fusion. An increase in glu-tubulin has also been detected at a similar stage in microtubules of prefusion L6 myoblast cells by Gundersen *et al.* (1989). The increase in glu- tubulin content at the begining of the differentiation would seem to be most likely due either to a change in the balance between the detyrosination/tyrosination cycle or alternatively to the appearance of a sub-population of longer lived microtubules. In CO25 cells, numerous bundles of glu-rich microtubules were found in elongating myoblasts, especially in the tail-like processes. Prescott *et al.* (1989) also reported that the tails of several motile fibroblast cell lines contained conspicuous bundles of glu-rich

microtubules. Furthermore Prescott *et al.* (1992) found that the microtubules within the processes of highly motile PtK2 cells, treated with scatter factor, turned over more slowly than those elsewhere in the cells. Thus the more likely hypothesis is that a sub-population of glu-rich microtubules appears in the elongating myoblasts, particularly in the processes. These glu-rich microtubules may have some role in the elongation of the processes, either a structural function in maintaining them or more simply a role in the transport of mitochondria and other materials to the ends of the processes.

3.4.4. TRANSLOCATION OF CENTRIOLES

Usually translocation of centrioles takes place during mitosis. However, it has been found by Wang *et al.* (1979) that during the process of cell fusion and nuclear migration, centrioles were transported forming large aggregates in baby hamster kidney cells (BHK21-F) syncytia. This study shows that, during differentiation, the centrioles first started to translocate to the top of the nuclei to become aggregated before fusion. A clustering or aggregation of centrioles has been observed in myoblast cells by Connolly *et al.*(1985), but this occurred during and after fusion. In this study, aggregation of centrioles was seen to lead to the formation of a primary cilium a short period of time before cell fusion. After elongation, myoblasts which had aggregated centrioles or a primary cilium did not undergo a further mitosis. So, the centrioles may be aggregated to prevent the cell dividing or to push the cells into differentiation. Alternatively the aggregation of centrioles may simply reflect the exit from mitosis or that they are required to do so for primary cilium formation.

When aggregation of the centrioles occurred (associated with primary cilium formation), the microtubule nucleation centres became re-localized around the periphery of the nuclei in the myotubes. Therefore aggregation of the centrioles could serve to change the MTOCs by releasing the pericentriolar material.

3.4.5. FORMATION OF THE PRIMARY CILIUM

Primary cilia were clearly visible in a small proportion of mononucleated myoblast cells before fusion so there is not an obligatory relationship between the formation of primary cilia and myoblast differentiation. However there certainly appears to be some relationship between primary cilium formation and the elongation or fusion of the

myoblasts. This is based on the further finding that elongated myoblasts always contained one or more primary cilia. Previous reports observed that, the primary cilium was present during the G1 phase of the cell cycle in confluent cells (Tucker and Pardee, 1979; Albrecht-Buehler and Bushnell, 1980; Vorobjev and Chentsov, 1982; Jensen *et al.*, 1987), but no report has linked the appearence of primary cilia to a cell differentiation event. Zalin (1979) reported that myoblast cells fuse during the G1 phase. The role of the primary cilium in CO25 myoblast cells during differentiation might be simply to keep the myoblasts in G1 phase to allow fusion to occur. On this hypothesis primary cilium formation simply absorbs all the centrioles. An alternative hypothesis is that the primary cilium may have some function in elongation or fusion. One distinct possibility is that it is involved either in the nucleation or organization of the glu-rich microtubules characteristic of the elongating myoblasts.

In these cells the primary cilium seems to be formed from multiple centrioles by aggregation, and all the centrioles may contribute to growth of the primary cilium. However it is not clear whether just the bases of the primary cilia or all the shafts are formed from multiple centrioles. T.E.M. results show that primary cilia have nine outer tubules, and no central tubules. It is also known that centrioles have nine outer tubules without central tubules as well so this does not help in determining the contribution of the centrioles. Some primary cilia were significantly larger than others and the larger forming primary cilia were associated with many centrioles. Thus the number of centrioles may influence the size of the primary cilium formed.

All previous reports i.e. Sorokin (1968), Tucker and Pardee (1979), Albrecht-Buehler and Bushnell (1980), Tassin, et. al. (1985a), Prescott, et. al. (1991) reported or showed that there was just one primary cilium in the each cell body. I have occasionally found two, or even three primary cilia in CO25 myoblasts before fusion. So this system is the first where multiple primary cilia have been recorded within a single cell. However in situations where true cilia are being formed, numbers of basal bodies appear simultaneously (Novikoff and Holtzman, 1970)

CHAPTER 4

MPM-13 AS A PERI-CENTROSOMAL MARKER

4.1. INTRODUCTION TO MICROTUBULE ORGANISING CENTRES

Microtubule organizing centres (MTOCs) can have a variety of different appearances in cells. The most common and best described MTOC structure is the centrosome, which is described below in section 4.1.1.

In some cell types the basal body is a similar structure to the centrosome and acts to nucleate the microtubules which form the cilia and flagella (Novikoff and Holtzman, 1970). In addition other structures can act as MTOCs. One of these is the plasmamembrane. In *Drosophila* pupal wing epidermal cells microtubules run from the apical to the basal surfaces directly and centrosomes are lacking (c.f. Mogensen and Tucker, 1987). The minus ends of these microtubules are associated with hemidesmosomal anchorage points at the apical surfaces, which are proposed to act as nucleation centres (Mogensen *et al.* ,1989). This system may act as a model for other epithelial cell types both in Arthropods and Vertebrates. Other cell types which may well possess membrane nucleated microtubules include the inner ear supporting cells, neurones and lens cells (Mogensen *et al.*, 1989). MDCK cells, a canine kidney line, contain many microtubules which are not nucleated from the centrosome (Bre *et al.*, 1987). This may represent an epithelial line where microtubules were originally nucleated from the plasmamembrane but have lost the organization of the nucleating centres upon tissue culture *in vitro*. For this cell type electron microscopy has failed to distinguish which component of the cell nucleated the majority of the microtubules.

4.1.1. THE CENTROSOME

4.1.1.1. THE CENTROSOME

Centrosomes consist of one or a pair of centrioles (diplosomes) (described in section 4.1.1.2.) surrounded by an electron dense cloud of the pericentriolar material (PCM) (Reviews, Wheatley, 1982; Brinkley, 1985). In most but not all animal cells a single or pair of centrioles, surrounded by the pericentriolar material, constitutes the major microtubule organizing centre (MTOC) as demonstrated by re-growth of microtubules after drug induced depolymerization (DeBrabander *et al.*, 1980). Gould and Borisy (1977) reported that, on the basis of a TEM study, microtubules rarely originated from the centrioles, rather from the pericentriolar material. Some cell types, including some mammalian

cells types lack centrioles at critical times in their life cycle (c.f. Maro and Bornens, 1981; Hiraoka *et al.*, 1989), also higher plants have no obvious morphological structure associated with a MTOC function (Cande, 1990). Furthermore Karsenti *et al.* (1984) and more recently Maniotis and Schliwa (1991) have found that cytoplasts lacking centrioles can nucleate microtubules. Thus the concept that each cell must have one or more discrete MTOCs is not clearcut. Brinkley (1985) concluded that the centrosome is not a compact, centralized body stationed permanently in the centre of the cell but rather a structure that can assume different forms and locations in different cell types, and within a single cell type change position and shape during the cell's life. The centrosomal MTOC "cloud" may turn out to be a very labile entity and impart the ability to form microtubules to a variety of structures. Recently γ-tubulin, a new form of tubulin, has been found as a constituent of pericentriolar material (Zheng *et al.*, 1991; Stearns *et al.*, 1991) and there is now evidence that it has a role in microtubule nucleation (Joshi *et al.*, 1992).

4.1.1.2. PERICENTRIOLAR MATERIAL (PCM)

The pericentriolar material is a very poorly defined structure which would seem to have an extraordinary flexibility in its organization, location, and functions. The pericentriolar material has not yet been defined biochemically. However, several group have recently described preparations of centrosomes that retain their MTOC activity, given PCM's (Mitchison and Kirschner, 1984; Ohta *et al.*, 1988; Komesli *et al.*, 1989). Several investigators have used isolated spindles cells to identify proteins associated with the centrosome (Kuriyama and Borisy, 1985; Toriyama *et al.*, 1988). As an alternative to biochemical purification of the centrosomes, auto-immune serum has been used on several occasions to identify centrosomes, in particular the human scleroderma autoummune centrosomal antiserum 5051 (e.g. in plant cell, Clayton *et al.*, 1985; in mouse and sea urchin eggs, Schatten *et al.*, 1986). It has been reported that MTOC's contain:

PERI-CENTROSOMAL AREA:

- ATPase-dyncin (Anderson, 1977);
- Steroid hormones (Nenci and Marchetti, 1978);
- Tubulin (Paper and Brinkley, 1979);
- RNA (Rieder, 1979; Snyder, 1980)

OTHER PROTEINS:

- 17.4, 90, and 180 kDa proteins (Anderson and Floyd, 1980);
- 35 and 45 or 47 kDa proteins (Turksen *et al.*, 1982);
- 14 and 17 kDa proteins (Shyamala *et al.* , 1982);
- 14, 20, and 34 kDa proteins (Cox *et al.* , 1983);
- 15 and 33 kDa proteins (Ayer and Fritzler, 1984);
- 17 and 114 kDa proteins (Earnshaw *et al.*, 1984);
- a 195 kDa protein (Guldner *et al.*, 1984);
- a 70 kDa protein (Nishikai *et al.*, 1984);
-18 and 80 kDa proteins (Valdivia and Brinkley, 1984);
- a 185 kDa protein (Frash *et al.*, 1986);
- a 51 kDa protein (Toriyama *et al.*, 1988; Ohta *et al.*, 1988);
- 43 or 56 kDa protein (Rao *et al.*, 1989);
- a 180 kDa protein (Kuang *et al.*, 1989; Chevrier *et al.*, 1992);
- 62 and 64 kDa proteins (Dinsmore and Sloboda, 1989; Moudjou *et.al.*, 1991);
- a 74 kDa protein (Buendia *et al.*, 1990);
- 180 and 210 kDa proteins (Tousson *et al.*, 1991)
- 39, 85, 190, and 220 kDa proteins (Balczon and West, 1991)

Virtually nothing is known about how the centrosomal cloud is maintained around the centrioles and divided at mitosis. Karsenti and Maro (1986) have speculated that the pericentriolar material also contains information for seeding centrioles and maintaining their growth.

4.1.2. THE MPM-13 ANTIBODY

MPM-13 is a mouse monoclonal IgM antibody raised against mitotic HeLa cell extracts (Rao *et al.*, 1989). Rao and co-workers reported that this antibody was specific to centrosomal structures and recognized a perinuclear distribution in interphase cells and the spindle poles in mitotic spindles. Interestingly it stained a variety of cell types including HeLa cells, mouse 3T3 cells, hamster CHO cells to name only a few, and also the protozoan *Tetrahymena*. In all groups a major protein species of 43 kDa was identified. A variably staining band of MW 56.000 was also sometimes seen. To us the distribution seemed intriguing, partly because the distribution seemed to be much more peri-centrosomal rather than centrosomal. It was therefore decided to

compare the distribution of MPM-13 in myoblasts and myotubes, where previous study had determined that the distribution of MTOC activity changed markedly during the transition. A further consideration was the possibility that some microtubules might originate from a pericentrosomal rather a centrosomal MTOC.

4.1.3. THE GOLGI APPARATUS

The Golgi apparatus is a key organelle involved in intracellular membrane traffic, transport, and secretory functions that interacts closely with microtubules (Tartakoff,1982; Kreis, 1990). Many different proteins that must ultimately reside in such diverse cellular compartments as the surface membrane, secretion granules, and lysosomes are synthesized or initially found in the same compartment, the endoplasmic reticulum and then transported via the Golgi apparatus (Rothman, 1981; Tartakoff,1982). The structure of the Golgi apparatus appear to be simple units closely conserved in all eukaryotes: a stack of about a half-dozen or more flattened, membrane-bound cisternae (about 1 micrometer in diameter) from which many small vesicles (in the range of 5 to 10 nanometers in diameter) bud off from or fuse to (or both), especially at the rims (Whatley, 1975).

It is believed that the Golgi apparatus and the microtubules in many cell types may direct the transport of new membrane material from the Golgi apparatus to the edges of the cell (c.f. e.g. Allan and Kreis, 1986; Bergmann *et al.*, 1983). Also Singer and Kupfer (1986) indicated that both the Golgi apparatus and the MTOC change their location in a coordinated way during cell locomotion. In all animal cell types, the Golgi apparatus is closely associated with the centrosome or MTOC, even when the MTOCs are dispersed in the cytoplasm (c.f. Tassin *et al.*, 1985b; Thyberg and Moskalewski, 1985). Also, there is a functional inter-dependence between detyrosinated microtubules and the structural integrity and position of the Golgi apparatus (Skoufias *et al.*, 1990).

There are a number of reports which concern the identification of proteins of the Golgi apparatus. Several Golgi specific proteins have been described; monoclonal antibodies have been identified which recognize the Golgi's peripheral membrane proteins of 54 and 86 kDa in natural killer cells by Chicheportiche *et al.* (1984). Smith *et al.* (1984) have reported monoclonal antibodies which recognize 103-108 kDa proteins in the Golgi of rat pancreatic acinar cells. Chevrier *et al.* (1992) have characterized a 180 kDa polypeptide and a 58 kDa (Bloom

and Brashear, 1989) Golgi protein. Allan and Kreis (1986) described the M3A5 monoclonal antibody raised against microtubule-associated protein 2 (MAP2), also stained the Golgi apparatus in a variety of tissue culture cell types and using this antibody they identified a Golgi protein of about 110 kDa.

It has been reported that drugs which induce depolymerization of microtubules cause a re-distribution of the Golgi apparatus which normally has a perinuclear organization (Reaven and Reaven, 1980; Rogalski and Singer, 1984). This demonstrates the close interrelationship between the two structures.

4.2. MATERIALS AND METHODS

4.2.1. CELL CULTURE

4.2.1.1. CELL TYPE

As described in section 2.2.1.1

4.2.1.2. PREPARATION OF CULTURE MEDIUM

As described in section 2.2.1.2

4.2.1.3. CELL CULTURE

As described in section 2.2.1.3.

4.2.1.4. TRYPSIN SOLUTION

As described in section 2.2.1.4.

4.2.1.5. PREPARATION OF PLASTIC DISCS

As described in section 2.2.1.5.

4.2.2. BUFFERS

4.2.2.1.MES BUFFER

As described in section 3.2.2.1.

4.2.2.2. PBS

As described in section 2.2.2.1.

4.2.2.3. PEM BUFFER

As described in section 3.2.2.3.

Ltd., London). The cells were examined using epifluorescence microscopy (as described in section 3.2.5.1.).

4.2.4.2. DOUBLE IMMUNOSTAINING WITH MPM-13 AND M3A5

Cells were stained with the supposed anti-centrosomal MPM-13 antibody and counterstained with M3A5, used as a marker for the Golgi apparatus. The cells were fixed following with 90% methanol/10% MES buffer (as described in section 3.2.2.1.), and then stain the following protocol; rabbit serum, 1:10; M3A5 antibody (gift of Dr V. Allan), 1:20, TRITC rabbit anti-mouse, 1:50; MPM-13 antibody, 1:500, FITC rabbit anti-mouse, 1:100. The cells were exposed to all antibodies at 37 ^{o}C in a humid chamber for 1 hour. After final washing the preparations were mounted in Citifluor (Citifluor Ltd., London). The cells were examined using epifluorescence microscopy (as described in section 3.2.5.1.).

4.2.5. MICROSCOPY

4.2.5.1. EPI-FLUORESCENCE MICROSCOPY

As described in section 3.2.5.1.

4.2.5.2. LENSES AND FILTERS FOR EPI-FLUORESCENT MICROSCOPY:

As described in section 3.2.6.1.

4.2.6. DRUG TREATMENT

4.2.6.1. NOCODAZOLE

As described in section 3.2.7.1.

4.2.6.2. TAXOL

As described in section 3.2.7.2.

4.2.7. IMMUNOBLOTS

4.2.7.1. PROTEIN EXTRACTION

Cells were prepared by seeding into a flask (25 cm^2, 5 ml, Gibco) in growth medium. When the cells reached 80% confluence the medium was changed to fusion promoting medium for periods of time up to several weeks. The cell monolayers of one flask were used for each experiment, and they were lysed in 1 ml of lysis buffer (as described in section 4.2.2.5.1.) with incubation on ice for 20 minutes with

occasional rocking. The lysed cells were transfered to a 1.5 ml Eppendorf tube, vigorously vortexed for 10 seconds, and then centrifuged at 13 000 g for 10 minutes at 4 °C. The supernatant was kept for analysis. The amount of total protein present was determined using the method of Bradford (Bradford, 1976).

4.2.7.2. SDS-POLYACRYLAMIDE GEL

4.2.7.2.1. STACKING GEL

The stacking gel consisted of 1 M Tris (pH 6.8), 30% acrylamide-bisacrylamide mix, 10% SDS, 10% ammonium persulphate (APS), 0.2% N,N,N',N'-tetramethylene diamine (TEMED), H_2O.

4.2.7.2.2. RESOLVING GEL

The resolving gel consisted of 30% acrylamide mix, 1.5 M Tris (pH 8.8), 10% SDS, 10% APS, 0.4% TEMED, H_2O.

4.2.7.2.3. ELECTROPHORESIS AND BLOTTING

For each sample, 30 µg of protein in 20 µl volume was mixed with 5 µl of 4 X SDS sample buffer, denatured by boiling for 5 minutes and then resolved on a 10% SDS-polyacrylamide mini-gel. Some samples were not boiled to compare the effects. To one of the samples a cocktail of protein inhibitors was added including phenylmethylsulphonyl fluoride (PMSF), leupeptin, aprotinin and pepstatin A, all at 10 µg/ml, 10 µM benzamidine hydrochloride and 1 µg/ml phenanthroline. Electrophoresis was performed at 80 volts (stacking gel) and 100 volts (resolving gel) respectively, using a Trisglycine electrophoresis buffer. Proteins were transferred to a 0.45 µm nitrocellulose filter (NEN Research) in a LKB Multiphor II apparatus using the Tris-glycine buffer containing 20% methanol at a current of 10-15 volts for 1.5 hours and the blot was then air dried.

4.2.7.2.4. IMMUNOLABELLING

After rinsing in the rinse buffer the blot was blocked for 1 hour in rinse buffer containing 5% bovine serum albumin (BSA) and probed for 2 hours in the same buffer containing MPM-13 antibody at one of several concentrations, 1:1500, 1:2000, or 1:2500. The blots were washed four times for 5 minutes each in the rinse buffer, reblocked for 10 minutes in the blocking buffer and incubated with peroxidase conjugated rabbit anti-mouse IgG (HRP; Dako), 1:500, in the rinse

buffer containing 0.2% BSA for 1 hour, and then washed six times for 10 minutes each in the rinse buffer, and finally twice for 10 minutes each in the rinse buffer without Tween-20 (Sigma).

4.2.7.2.5. ENHANCED CHEMILUMINESCENCE

Detection of proteins was performed using an enhanced chemiluminescence technique (ECL), a new and sensitive method for protein detection on Western blots. The protocol used was that recommended by Amersham from which the reagents were obtained. After washing well in a dark room the blot was drained then incubated in a 1:1 mixture of enhanced chemiluminescence Western blotting detection reagents A and B for 1-2 minutes. The blot was drained again, placed on a glass plate in a High-Speed casette and covered with Saran-Wrap. All excess reagent, and air bubbles were squeezed out and the blot was exposed to Kodak X-ray film for 3-60 seconds. To determine the amount of total protein on the blot, at the end of the experiment, the blot was washed for a few times in the washing buffer, then stained with amido black stain (0.1% gr amido black, 45% ethanol, 10% glacial acetic acid in deionized water) for a 1-2 minutes. After destaining in a mixture of 25% ethanol and 8% glacial acetic acid in deionized water for 30 minutes, blot was air-dried and photographed.

4.2.8. PHOTOMICROSCOPY

4.2.8.1. CAMERAS

As described in section 3.2.8.1.

4.2.8.2. FILMS

As described in section 3.2.8.2.

4.2.8.3. PHOTOGRAPHIC SOLUTIONS

As described in section 3.2.8.3.

4.2.8.4. PHOTOGRAPHIC CARDS

As described in section 2.2.6.4.

4.3. RESULTS

4.3.1. IMMUNOSTAINING BY MPM-13

4.3.1.1. UNDIFFERENTIATED MYOBLASTS

The localization of MPM-13 was found to be rather variable: Granular or dot-like structures were seen showing a different pattern of localization in each cell. Their sizes and numbers were very variable in the cells. The cells were classified into three types according to the pattern of MPM-13 staining (Fig. 35: A1, A2, A3).

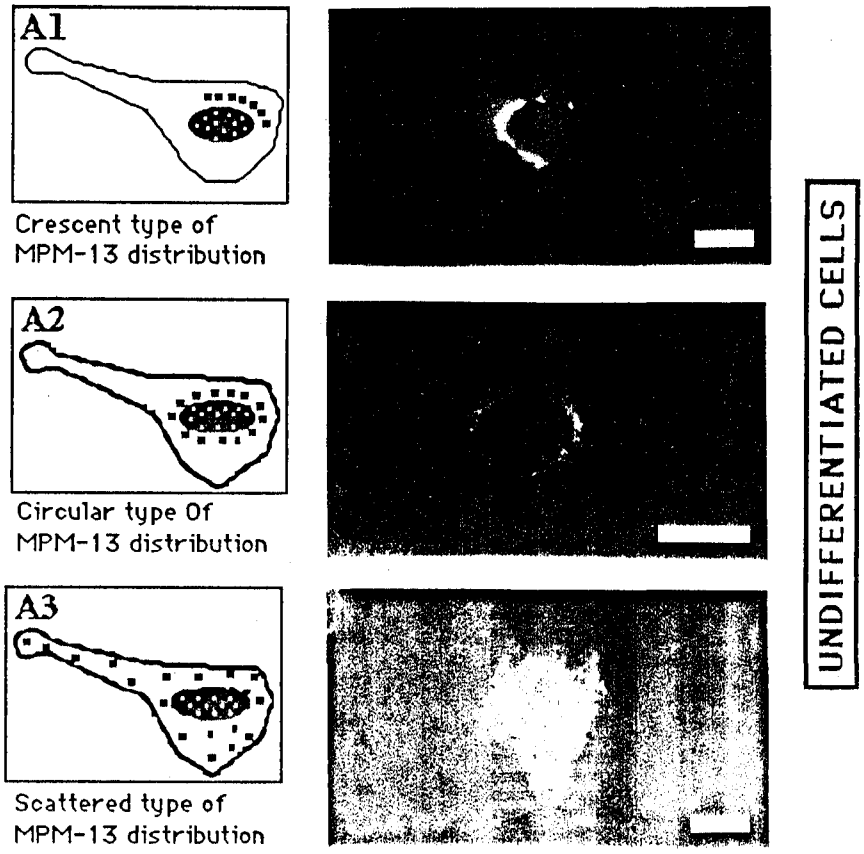

FIG-35 : Distribution of MPM-13 as shown by immunostaining of undifferentiated CO25 cells in growth medium after 1 day. A1, A2, and A3: schematic representation of distribution of MPM-13 proteins for each corresponding pictures; Bars= 20 µm.

A total of 400 cells were counted from 4 different preparations to find the frequency of each type. Data is given in Table-3 for counting the types of MPM-13 pattern seen in myoblast cells incubated in growth medium for 1 day.

The patterns of localization of MPM-13 staining in myoblasts was split into 3 types: (A1) crescent, (A2) circular or (A3) scattered.

The crescent type was found to be the most common type comprising 63% of the total (Graph-3) and was seen to stain as a group of granular structures on one side of the nuclei (Fig. 35). A circular distribution of MPM-13 staining was found in the 33% of the cell population (A2, Graph-3), MPM-13 in these cells showed as a pattern of fluorescence all around the nucleus. The pattern in which the granules were dispersed throughout the cell body (A3, Fig. 35) was found in a very small percentage of cells, about 4% (Graph-3).

	A1 Type cells	A2 Type cells	A3 Type cells
Number of cells	253	131	16
Average	63.25	32.75	4

TABLE-3 : Cell counts to localize each type of MPM-13 distribution. 4 separate preparations of CO25 cells in growth medium for 1 day were observed. A total of 400 cells were counted and the averages calculated.

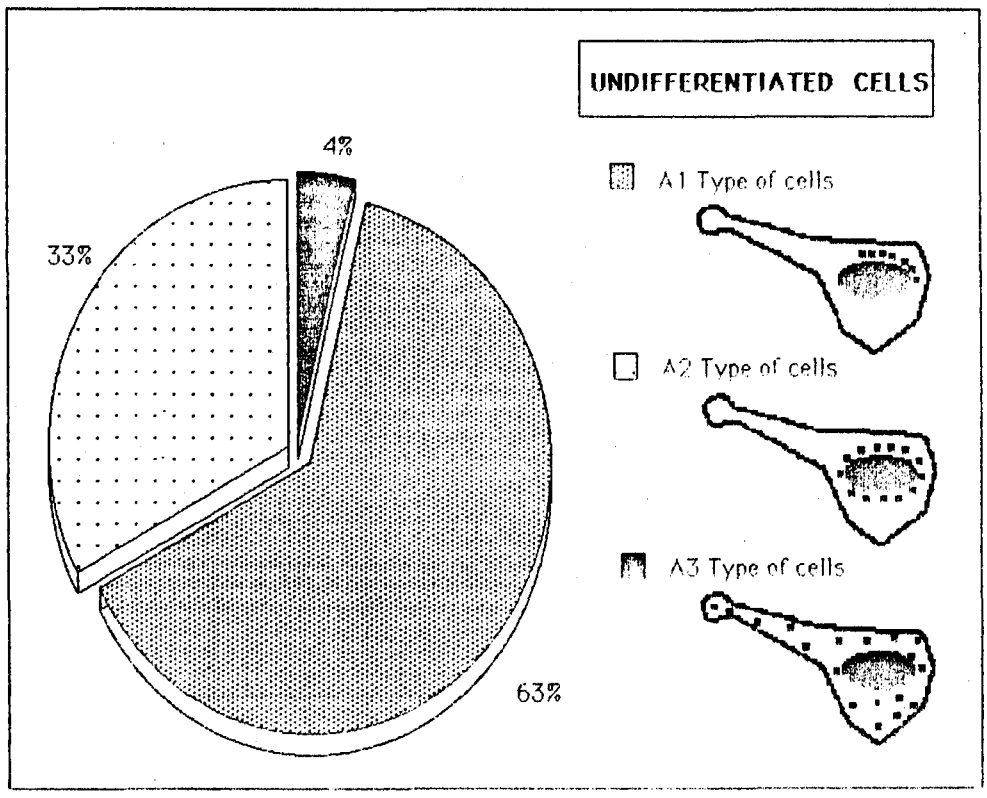

GRAPH-3 : Frequency of MPM-13 patterns in CO25 cells in growth medium after 1 day. 400 cells were counted for each sample.

4.3.1.2. CELLS UNDERGOING DIFFERENTIATION

After one week when all the myoblasts were elongated, and in the process of fusion, four types of MPM-13 distribution were found (Fig.36, Table-4 and see page 87, Graph-4). These are described as the B1, 2, 3, and 4 types of cells. The distribution of MPM-13 in the B1 type of the cells was dispersed (1%; Table-4; Fig. 36; see page 87, Graph-4). In the B2 type MPM-13 staining granules made a group which were close to one side of nucleus forming a crescent (37%; Table-4; Fig. 36; see page 87, Graph-4). In the B3 type of cells the distribution of MPM-13 was observed as two groups on either side of the nucleus forming twin crescents (45%; Table-4; Fig. 36; see page 87, Graph-4). In the B4 type MPM-13 granules were all around the nucleus (8%; Table-4; Fig. 36; see page 87, Graph-4).

Types B5 and B6 represent fused myotubes in the same cultures. In the B5 type of cells MPM-13 granules were distributed around the nuclear envelopes in a circular pattern in approximately 85% of the myotubes, cresents were never seen (Table-4). In addition, some staining was always observed in the more peripheral cytoplasm (Fig. 36-B6). In the B6 distribution of MPM-13, granules were dispersed throughout the myotubes (16% of the myotubes formed ; Table-4; Fig. 36; see page 87, Graph-4). It was evident that some change was in the process of taking place in the distribution of the granules. There was significantly more dispersion of the granules throughout the cytoplasm in the myotubes and all the granules were dispersed in about 16% of the myotubes. This compares with 4% for undifferentiated myoblasts (Table-3) and just over 1% in differentiating myoblasts (Table-4).

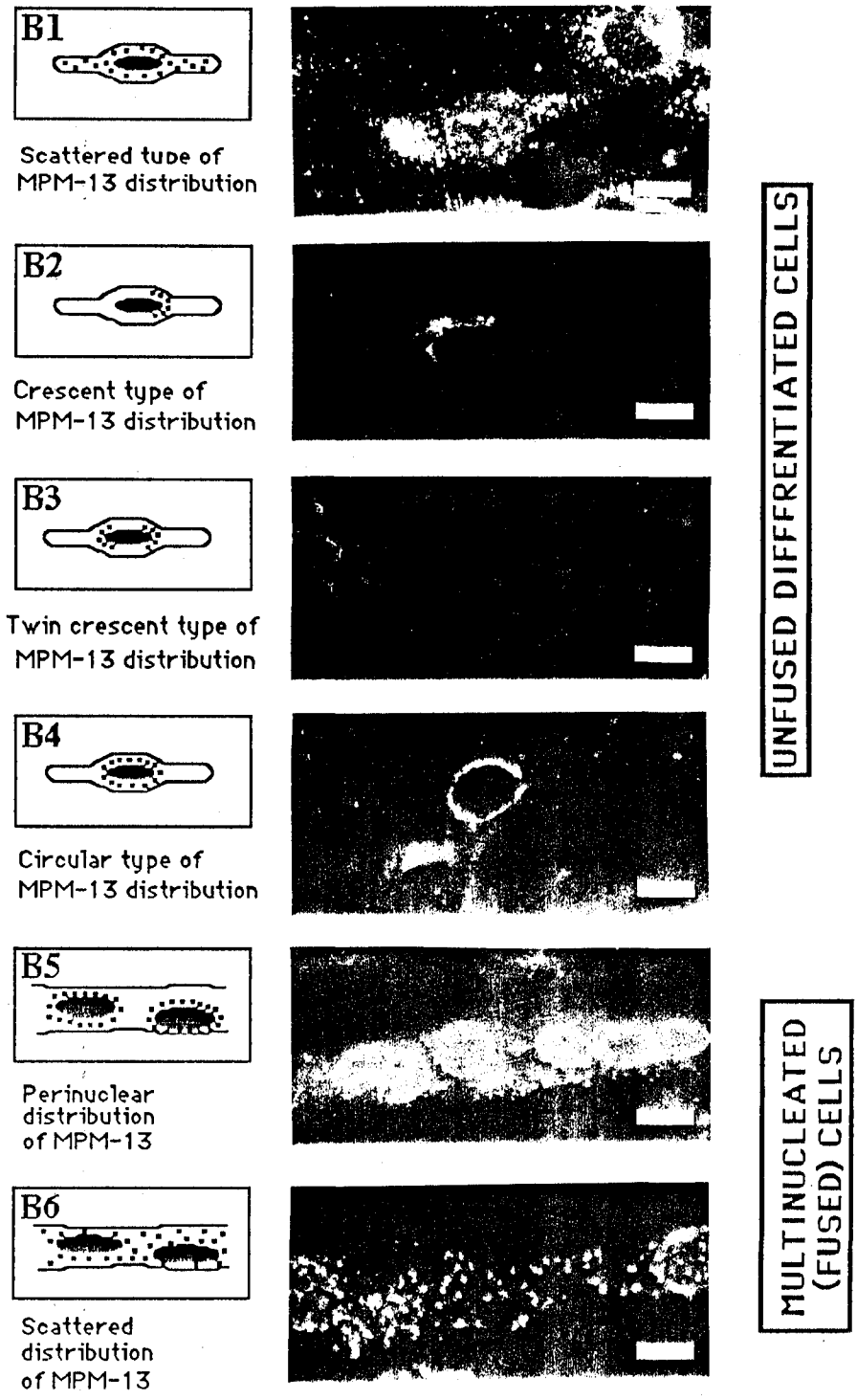

FIG-36 : Distribution of MPM-13 in differentiated CO25 cells in fusion medium after 1 or 2 weeks. Four hundred cells were counted at random. Bars= 20 μm.

	B1 Type of cells	B2 Type of cells	B3 Type of cells	B4 Type of cells	B5 Type of cells	B6 Type of cells
Number of cells	3	146	181	33	31	6
Average	0.75	36.5	45.25	8.25	7.75	1.5

TABLE-4 : CO25 cells in fusion medium after 1 week. 400 cells were counted for samples.

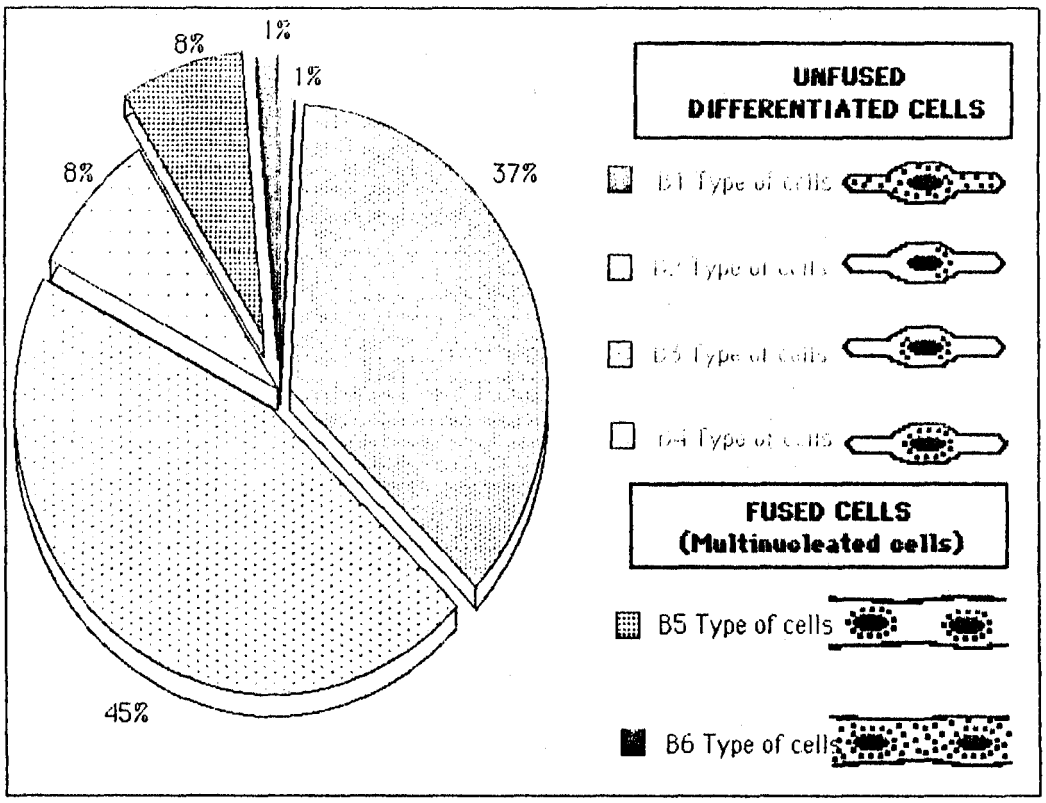

GRAPH-4 : Distribution of MPM-13 into the various patterns in differentiating CO25 cells in fusion medium after 1 week. 400 cells were counted for samples.

A similar count of the variety of patterns of MPM-13 distribution was performed after 2 weeks in the fusion medium (Fig. 36; Table-5). The kinds of pattern seen were similar to those observed after one week in fusion medium, but the frequencies had changed. The frequency of the B1 type of cell was 2% (Table-5; Fig. 36; see page 88, Graph-5), the B2 type was 25% (Table-5; Fig. 36; see page 88, Graph-5), B3 type was

29% (Table-5; Fig. 36; Graph-5), and the B4 type of cell was 11% (table-5; Fig. 36; Graph-5) for unfused elongating cells in fusion medium after 2 weeks. The frequency of the B5 type of cell was 13% (Table-5; Fig. 36; Graph-5), and for the B6 type it was 20% (Table-5; Fig. 36; Graph-5) for multinucleated fused cells in the same culture. Many more myotubes were observed in two week old cultures than in one week old cultures.

	B1 Type of cells	B2 Type of cells	B3 Type of cells	B4 Type of cells	B5 Type of cells	B6 Type of cells
Number of cells	7	100	117	44	53	79
Average	1.75	25	29.25	11	13.25	19.75

TABLE-5 : CO25 cells in fusion medium after 2 weeks. 400 cells were counted for samples.

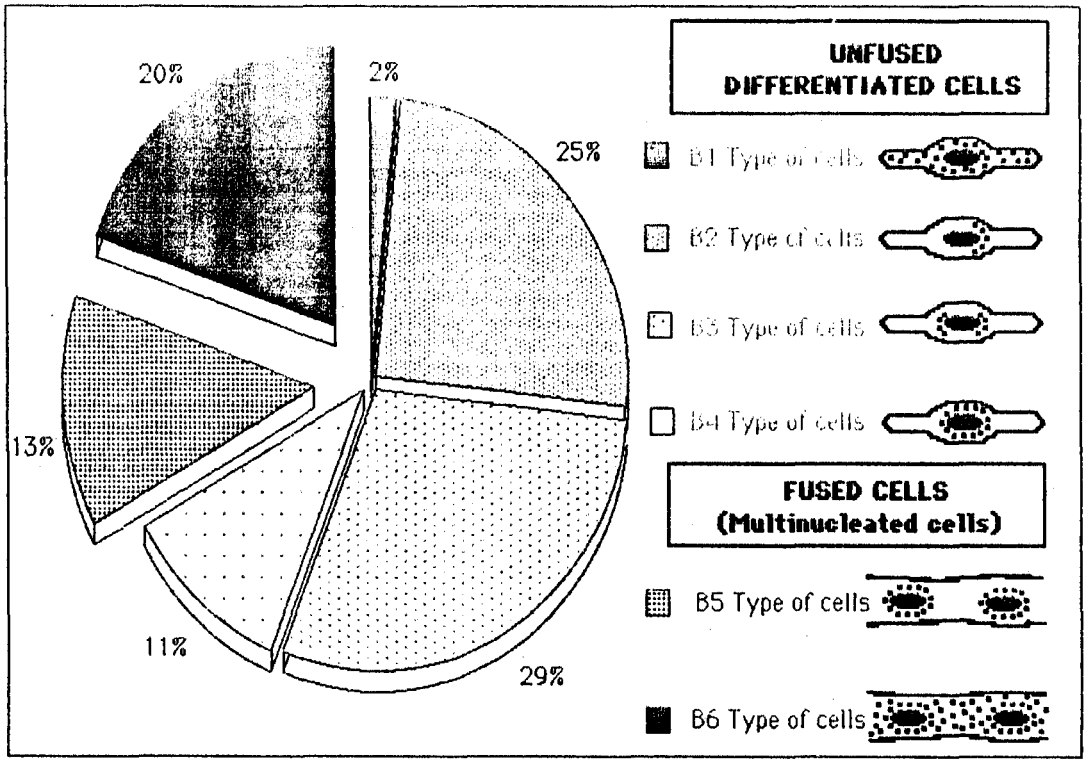

GRAPH-5 : Distribution of MPM-13 into the various patterns in differentiating CO25 cells in fusion medium after 2 weeks. 400 cells were counted for samples.

There was a significant increase in the numbers of myotubes found with the proportion increasing from 9% of the total to 33%.

Furthermore the majority of the myotubes showed dispersed granules in the cytoplasm (the B6 form) rather than a perinuclear distribution (B5 form). Thus as myotubes formed a shift was seen, firstly to a perinuclear distribution of granules and then to a dispersed cytoplasmic distribution.

4.3.2. PROTEINS IDENTIFIED BY MPM-13

The proteins binding to MPM-13 were analysed on Western blots using MPM-13 antibody. Total proteins were isolated from CO25 myoblast cells and 30 μg of protein from each sample was run on 10% (w/v)-SDS-polyacrylamide gels. To reduce the effects of proteases on the sample proteins, a mixture of protease inhibitors including PMSF, leupeptin and aprotinin (e.f. page 9) was added to the protein samples. To investigate whether complete reduction by boiling caused the appearance of lower molecular weight sub-units, into parallel wells were placed samples reduced by boiling for 5 minutes, or unreduced samples not boiled which were then run on gels.

To distinguish the specific binding of MPM-13 antibody from non-specific binding of the second antibody (a polyclonal rabbit antibody), triplicate gels were performed for each protein sample. One blot was incubated with only MPM-13 antibody (Fig.37a), the second blot with only secondary rabbit anti-mouse antibody (Fig.37b), and the third blot sequentially with first and second stage antibodies together (Fig.37c), and then all the blots were treated with the detection reagents of the ECL system (Fig.37a, b, c).

As shown the first and second blots did not show any binding and were entirely clean. The blot incubated with first and then second antibody showed both strong and weak bands due to MPM-13 antibody staining. To check whether these rather different results (compare with Rao *et al.*, 1989) were due to differences in preparation I ran samples boiled for 5 minutes and unboiled, but otherwise identical samples. But there were no differences between the reduced and unreduced samples (Fig. 37c). Total cellular protein was isolated from CO25 myoblast cell lines in the fusion medium after 5 days (as described in section 4.2.7.1.), and also in the growth medium after 2 days. For a comparison 3T3-15 fibroblast cells (a gift of R. Russell), and primary chick heart cells (a gift of D. Brown) were run at the same time (as described in section 4.2.7.2.5..).

Fig. 37c shows a typical blot and demonstrates that MPM-13 identified two rather strong bands, (kDa's of 49, 38), and at least eight weaker bands which were 56, 42, 40.5, 34, 31.5 30, 28,24.5kDa in molecular weight. In the reduced gels, the bands were somewhat weaker as compared with the bands for the unreduced samples but otherwise similar.

When proteins of undifferentiated and differentiated CO25 cells were compared, the major bands of differentiated CO25 cells (49 and 38 kDa) were seen to be stronger than the corresponding bands of the undifferentiated cells. Two weak protein bands seen in the lanes of the undifferentiated cells, both bigger than 49 kDa, were stronger than the equivalent protein bands of the differentiated cells. Also the undifferentiated cells protein had a band about 34 kDa, but this band was very weak in the differentiated cells lane. On the lanes for the CO25 cells in fusion medium were two weak bands of about 30 and 28 kDa, but they were stronger than the same bands present in the lanes for CO25 cells cultured in growth medium. Otherwise undifferentiating and differentiating myoblasts gave very similar blot patterns indeed with MPM-13.

The stained bands of 3T3-15 cell proteins were quite similar to the bands of CO25 myoblast proteins on the gels. One protein, which was 24 kDa, was stronger than that for the CO25 cells on the gels. Otherwise they were qualitatively identical.

Primary chick heart fibroblast cells showed significantly fewer bands than the other samples under the same conditions. All the bands of primary chick heart fibroblast cell proteins were between 49 and 38 kDa. The other bands which stained with MPM-13 for 3T3-15 and CO25 cell extracts were not seen in chick heart fibroblasts. Three of the bands were identical to those seen for the other types but there was a fourth band, with a molecular weight of about 42 kDa, which was not present in the extracts of any of the other cell types.

FIG-37 (next page) : Proteins of different cell types run on 10% SDS polyacrylamide gel and immunoblotted with MPM-13 antibody. (A) Only first stage antibody was used on reduced proteins, (B) only second stage antibody was used, (C) first and second antibody was used together on unreduced and reduced proteins, and (D) Total proteins of the cells on the gel.

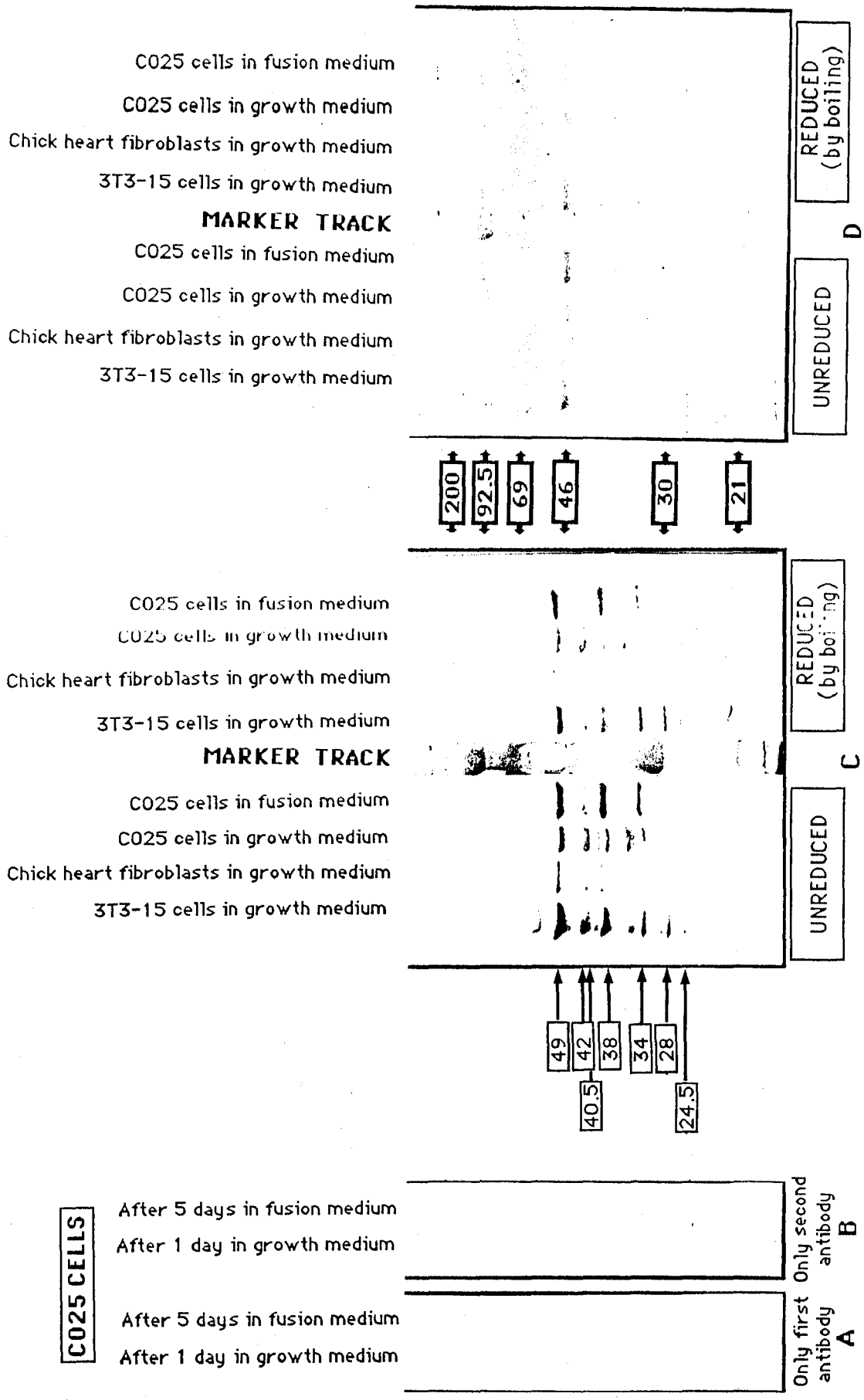
C025 cells in fusion medium
C025 cells in growth medium
Chick heart fibroblasts in growth medium
3T3-15 cells in growth medium
MARKER TRACK
C025 cells in fusion medium
C025 cells in growth medium
Chick heart fibroblasts in growth medium
3T3-15 cells in growth medium
REDUCED (by boiling)
UNREDUCED
D
200
92.5
69
46
30
21
C025 cells in fusion medium
C025 cells in growth medium
Chick heart fibroblasts in growth medium
3T3-15 cells in growth medium
MARKER TRACK
C025 cells in fusion medium
C025 cells in growth medium
Chick heart fibroblasts in growth medium
3T3-15 cells in growth medium
REDUCED (by boiling)
UNREDUCED
C
49
42
38
34
28
40.5
24.5
C025 CELLS
After 5 days in fusion medium
After 1 day in growth medium
Only second antibody
B
After 5 days in fusion medium
After 1 day in growth medium
Only first antibody
A

4.3.3. EFFECTS OF NOCODAZOLE ON THE DISTRIBUTION OF STRUCTURES IDENTIFIED BY MPM-13

After various preliminary experiments, I decided to use 1.5 μM nocodazole for 1 hour on the cells to obtain suitable results fairly quickly for the effects of nocodazole on CO25 cells.

After 1 hour of nocodazole treatment, when CO25 myoblast cells were stained using fluorescently labelled YL1/2, all microtubules disappeared. There were no polymerized microtubules present, and only cloudy fluorescence due to depolymerized tubulin and some dot-like staining were seen in the cell bodies (Fig. 38a). I could not use permeabilisation buffer on the cells, because CO25 cells were very sensitive to it, and the cells exploded. Because of this the depolymerized tubulin was retained. Also some MPM-13 bleed-through was visible in these cells. MPM-13 stained granules were seen to disperse into the cytoplasm in nocodazole treated cells (38b). No perinuclear crescent remained at all. After 1 hour of treatment in 1.5 μM nocodazole, cells were released from the drug by changing the medium. Microtubules rapidly started to regrow and elongate from centrosomes on the top of or beside the nuclei in the myoblasts after 3-5 minutes (arrow on Fig. 38c). The cytoplasm of the cells still showed much diffuse staining due to unpolymerized tubulin (Fig.38c). MPM-13 stained granules were no longer spread out in the cell body. They usually formed a variable sized group at one side of the nucleus after 3-5 minutes. No MPM-13 staining of the centrosome region was observed (Fig. 38d) altough small clusters of granules close to the centrosome were occasionally found (Fig. 38f). The granules were clearly not nucleation centres for newly regrown microtubules. Regrowth only occured from the centrosomes at this time (Fig.38c).

After 10 minutes growth following the withdrawal of nocodazole, the cell bodies were quite full with microtubules. Two possible nucleation centres were seen in these cells (Fig. 38e). The first one, clearly seen on the top of the nuclei, was the centrosome (thin arrow on Fig. 38e).However, not many microtubules were seen to radiate from the centrosome in cells such as that of Fig. 38e. Many microtubules seemed to originate from around the edges of the nuclei (thick arrows on Fig. 38e).

MPM-13 staining granules very quickly relocalized, predominantly around the nucleus in the same general area where

microtubule regrowth appeared (Fig. 38f). However in some cells, groups of MPM-13 staining granules were present in the cell bodies far from the nuclei. These granules were not nucleation centres for microtubules (arrow in Fig. 38f).

After 20 minutes recovery from nocodazole, microtubules were found to run all over the myoblast cell bodies (Fig. 38g). A region to one side of the nucleus usually stained more brightly than the other sides and was presumed to be a centrosomal MTOC (arrow on Fig. 38g). MPM-13 staining showed that a group of MPM-13 staining granules were localized very close to one side of the nucleus forming a crescent shape in most of the cells and the typical patterns had reformed (arrows show on Fig. 38h). The A2 perinuclear distribution was also seen in some of the cells (not shown, but see Fig. 35).

An identical treatment was given to myotubes after 1 hour nocodazole treatment, and no obvious microtubules were seen (Fig. 39a). But some strongly stained MPM-13 granules were visible in the tubulin channel because of bleed-through through the filters during the microscopy (Fig. 39a). Quite a few MPM-13 staining granules were localized around the nuclei (thin arrow shown on Fig. 39b), but some groups of MPM-13 granules were spread out in the myotubes (thick arrows shown on fig. 39b). The kind of staining patterns seen were in general very similar to those present in untreated controls (c.f. Fig. B5 and B6 in Fig. 36).

Fig.39c shows that, after 1-3 minutes withdrawal from nocodazole, many microtubules had started to appear around the nuclei in the myotubes. The areas around the nuclei were brightly stained forming microtubule nucleation centres showing a "basketwork"-like arrangement with YL1/2 staining. Most of them ran around the nuclei (arrows shown on Fig. 39c). Within 3 minutes, many microtubules had already re-grown and it was not easy to determine their origin (Fig.39c) as described previously in Chapter 3. MPM-13 staining showed that the granules still surrounded the nuclei (arrows shown on Fig. 39d), but many were dispersed in the cytoplasm of the nocodazole treated myotubes (Fig. 39d) as in controls. Fig. 39 also shows that during the regrowth of microtubules in the myotubes, the parallel arrangement was re-established in the myotubes at the same time. This parallel arrangement of microtubules did not show any correlation with the MPM-13 granule distribution (Fig. 39e, f).

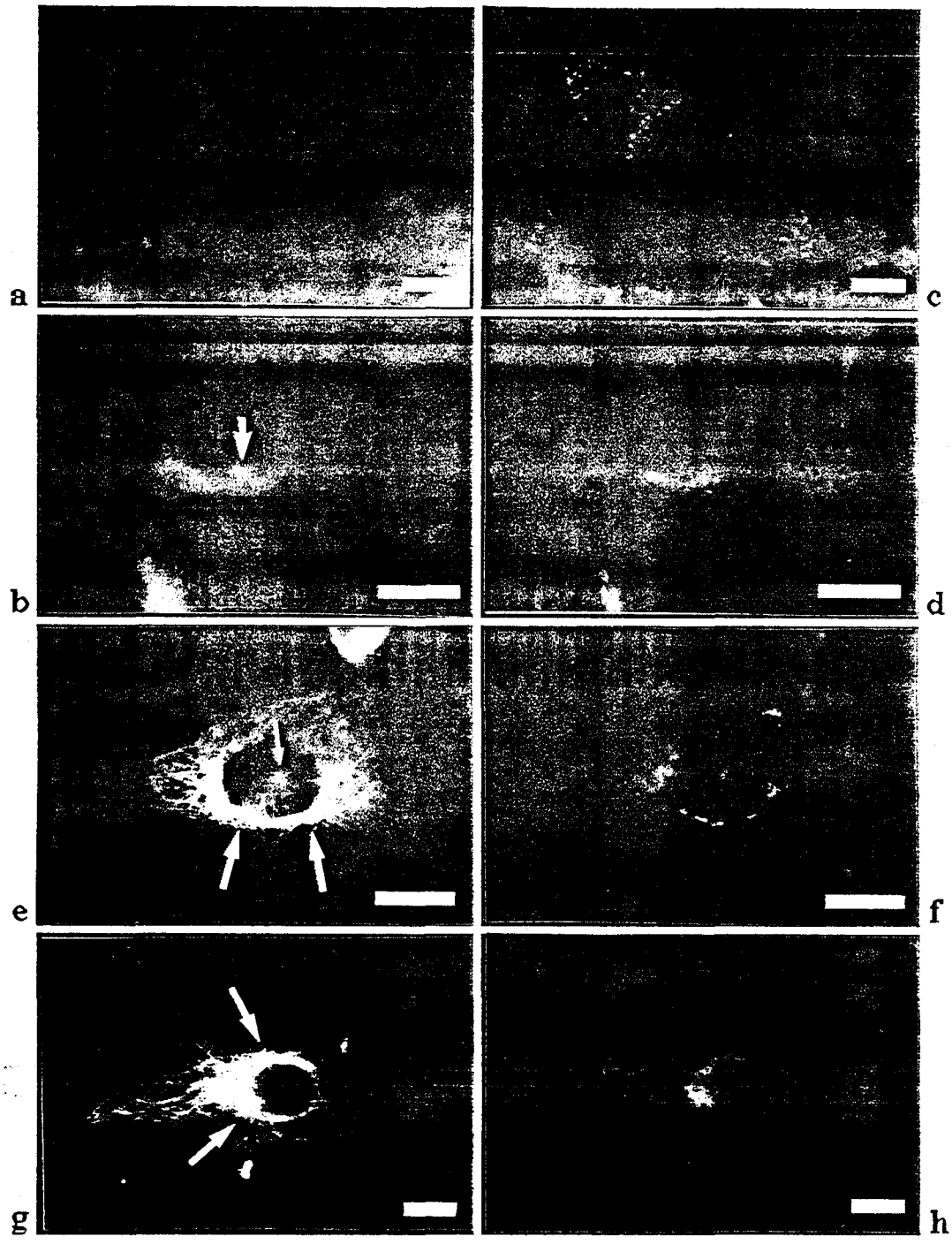

FIG-38 : CO25 cells stained by double immuno-fluorescence (a, b) after 1 hour nocodazole treatment left hand column YL1/2 staining, right hand column MPM-13 staining in all pairs, recovery from nocodazole, (c, d) 5 minutes, arrow, regrowing of microtubules from a centrosome, (e, f) 10 minutes, thin arrow (e) centrosome for regrowging of microtubules, thick arrows (e) origination of microtubules from the edges of nuclei, (g, h) 20 min., arrows (g) cresent shape of MTOC, (h) crescent shape of MPM-13 staining granules; Bars= 20 μm.

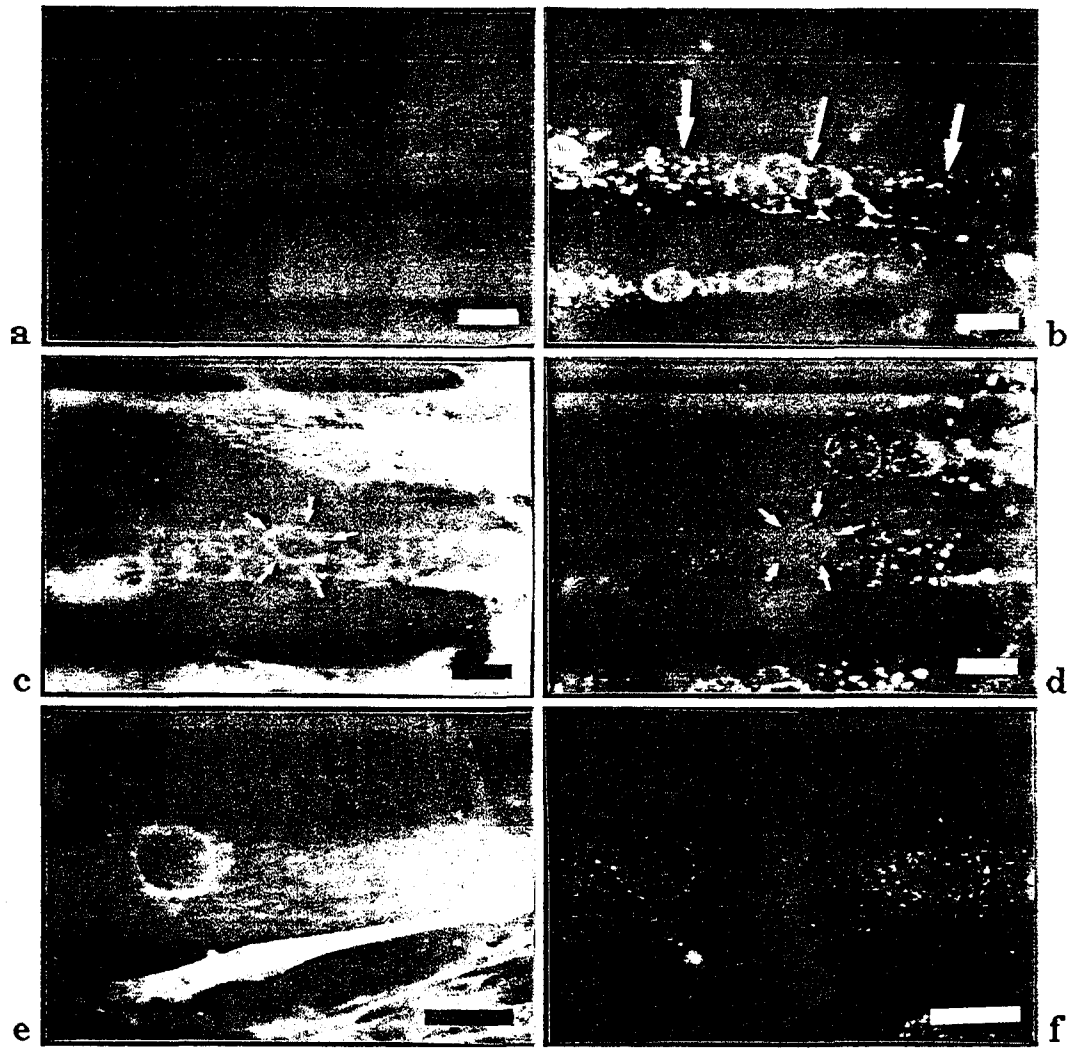

FIG-39 : (a and b) Fused CO25 cells (myotubes) stained by double immunofluorescence after 1 hour nocodazole treatment (a) YL1/2 staining, (b) MPM-13 staining, thin arrow, MPM-13 staining granules around nuclei in a myotube, thick arrows, spread MPM-13 staining granules in the myotube; (c and d) after 3 minutes recovery from nocodazole. Microtubule regrowth (c) YL1/2 staining, arrows, basketwork-like nucleation of microtubules around a nucleus, (d) MPM-13 staining, arrows, MPM-13 staining granules around a nucleus; (e and f) after 15 minutes recovery from nocodazole. Microtubule regrowth (e) YL1/2 staining, and (f) MPM-13 staining; Bars=20 µm.

The arrangement of microtubules in myotubes was completely reestablished after about 20 minutes (Fig. 40a, c). The number of microtubules and their length increased very quickly with the time of regrowth. The distribution of all the microtubules was parallel to each

other, and also they always ran along the long axis. This is true both of 1 week old myotubes (Fig. 40a) and also 3 week old myotubes (Fig. 40c). 20 minutes after withdrawal of nocodazole, MPM-13 surrounded the nuclei in 1 week old myotubes (Fig. 40b), but also was observed in the cytoplasm as in the controls (cf. Fig. 36 B5 and B6 for comparison). In the older myotubes, more of the MPM-13 stained granules were dispersed in the cytoplasm, as in untreated myotubes (Fig. 40 d).

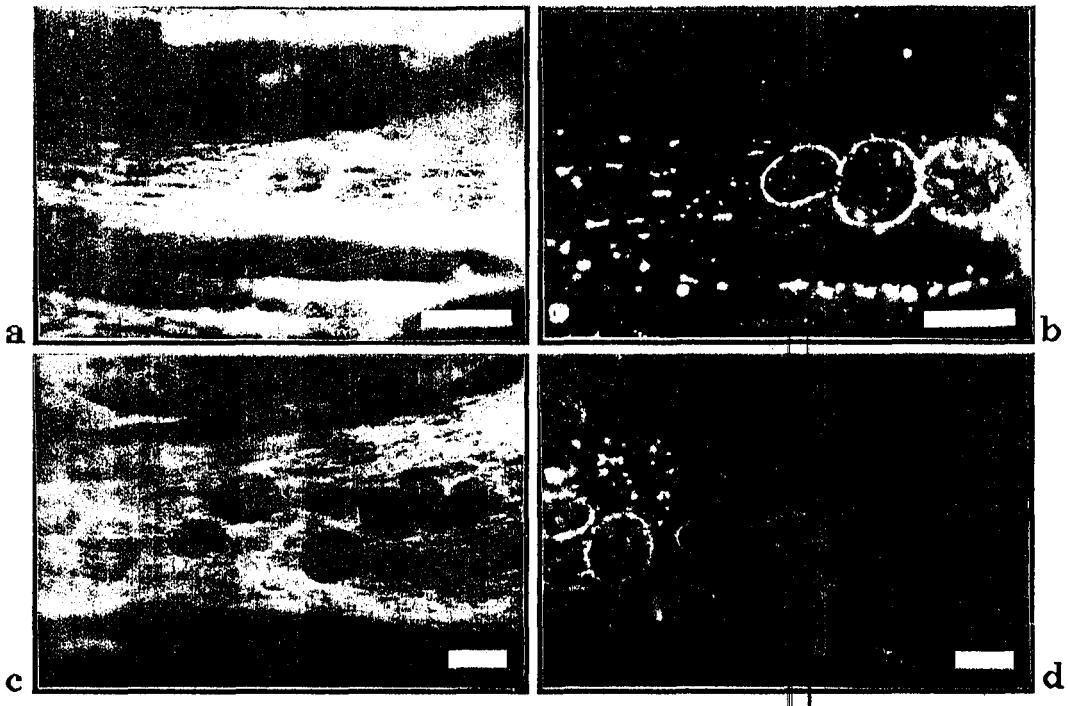

FIG-40 : CO25 myoblast cells 20 minutes recovery from nocodazole, (a, c) distribution of microtubules by YL1/2 staining, (b, d) localization of granules by MPM-13 staining. (a and b) 1 week old myotubes, (c and d) 3 weeks old myotubes. Bars= 20 µm.

4.3.4. EFFECTS OF TAXOL ON MPM-13 GRANULE DISTRIBUTION

After taxol treatment (as described in section 3.2.7.2) on CO25 cells, the distribution of the microtubules, and the localization of MPM-13 antigens were found to change in concert. The actual number of individual microtubules increased in the taxol treated myoblast cells, but they were much shorter than in control cells and formed short bundles frequently associated with the cell edges (Fig.41a, c, and e). The MPM-13 staining granules often formed a line which appeared to be

associated with the microtubule bundles (thin arrows show in Fig.41b, d, and f).

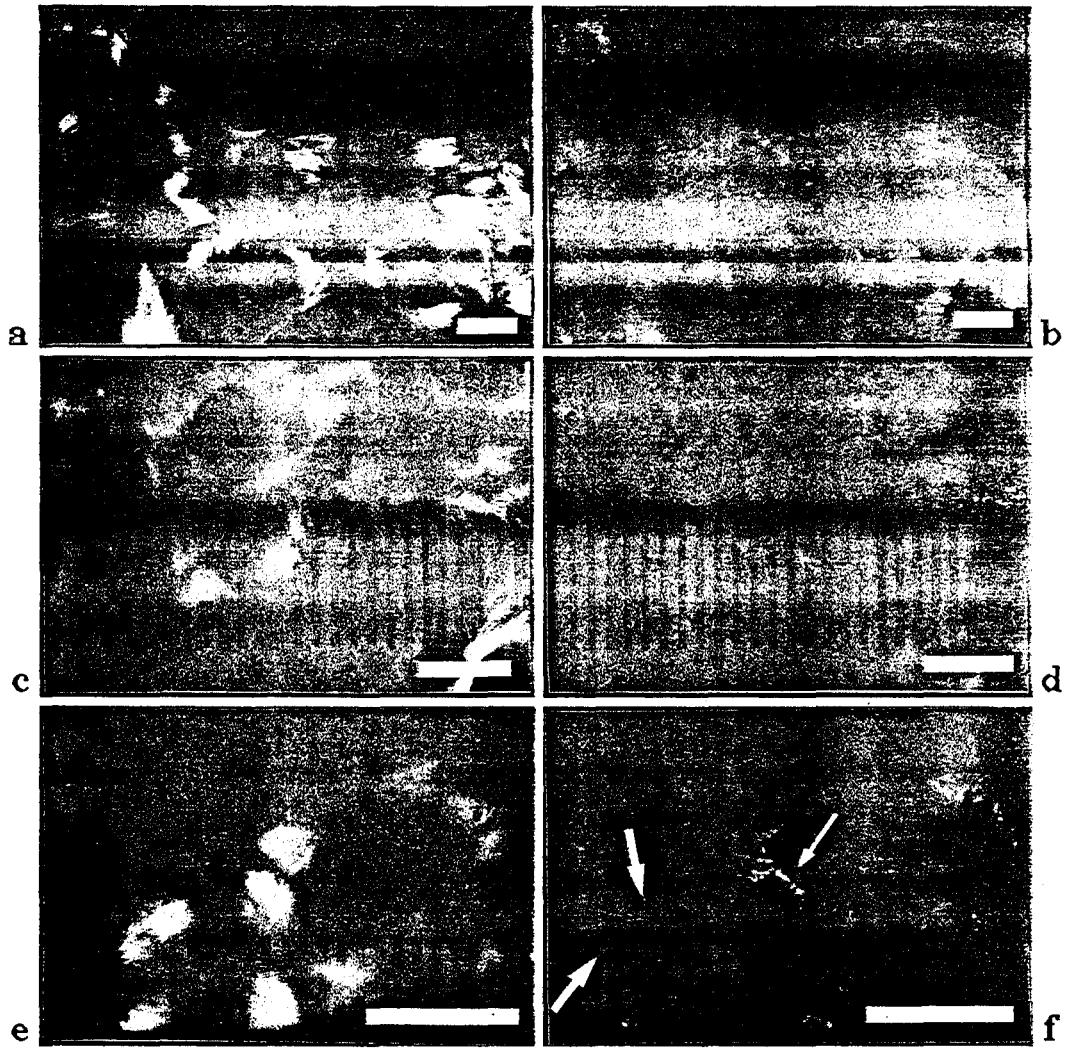

FIG-41 : CO25 cells stained by double imunofluorescence; after one day in growth medium (a) YL/12 staining, and (b) MPM-13 staining;after one week in fusion medium (c) YL1/2 staining, and (d) MPM-13 staining; after 2 weeks (e) YL1/2 staining, and (f) MPM-13 staining, thin arrows show line formed MPM-13 staining granules, thick arrows show absence of MPM-13 staining granule region; Bars= 20 μm.

Sometimes however the granules occurred in regions between bundles of microtubules (thin arrows show in Fig. 41d, f). Regions of microtubule bundles were also present lacking MPM-13 staining granules entirely (thick arrows show on Fig. 41b, d, f). The MPM-13 staining granules were usually seen as groups in different areas of the

cytoplasm. Occasionally, though, isolated granules were seen (Fig. 41b, d, f).

Treatment of myotubes with taxol again caused assembly of short microtubule bundles which were established as groups running along the long axis of the tubes (Fig. 42a, c). Their distribution was also localized mainly between the nuclei of the myotubes (Fig. 42a, c). Sometimes bundles of microtubules formed over the nuclei (Fig. 42a, c). The distribution of MPM-13 staining structures also changed significantly in taxol treated myotubes. The MPM-13 staining granular structures were distributed mainly around the nuclei in recently formed taxol treated myotubes (Fig. 42b), but older myotubes contained more dispersed MPM-13 staining granules in the cytoplasm of the myotubes in varying amounts (Fig.42d). Sometimes there was a correlation between MPM-13 staining granules and the ends of the bundles (thin arrows show on Fig. 42b, d), but sometimes not (thick arrow shows on Fig. 42b).

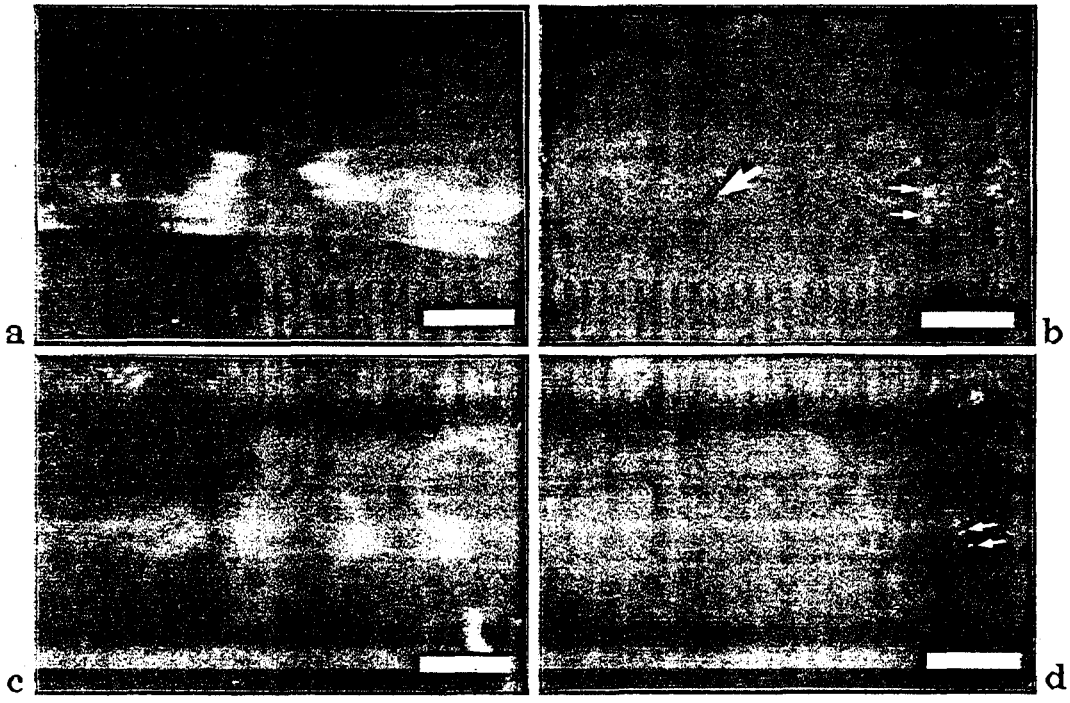

FIG-42 : Myotubes treated with taxol for 12 hours, (a, c) distribution of microtubules with YL1/2 staining, (b, d) localization of granules by MPM-13 staining. (a and b) 1 week old myotubes, (c and d) 2 weeks old myotubes, thin arrows, MPM-13 staining granules at the end of microtubule bundles, thick arrow, lacking of MPM-13 staining granules region; Bars= 20 μm.

4.3.5. CO-LOCATION OF THE GOLGI APPARATUS WITH MPM-13 STAINING

In some cases (e.g. Fig 35 A1) the pattern of staining with MPM-13 was very reminiscent of the pattern described with various antibodies specific for the Golgi apparatus (e.g. M3A5 Allan and Kreis, 1986). To investigate whether there was any co-localization of MPM-13 with the Golgi apparatus. I obtained a sample of M3A5 and used it with MPM-13 in a double immunostaining experiment. As can be seen in Fig. 43 the pattern of staining in both myoblasts (a and b) and myotubes (c and d) was identical. It was concluded that the MPM-13 staining granules were in fact elements of the Golgi apparatus. Localization of the two patterns of antibody staining was very variable in the cells as described before. Elements of the Golgi mostly localized very close to the nucleus in a crescent shape (Fig. 43a, c). Also in the variety of patterns previously described.

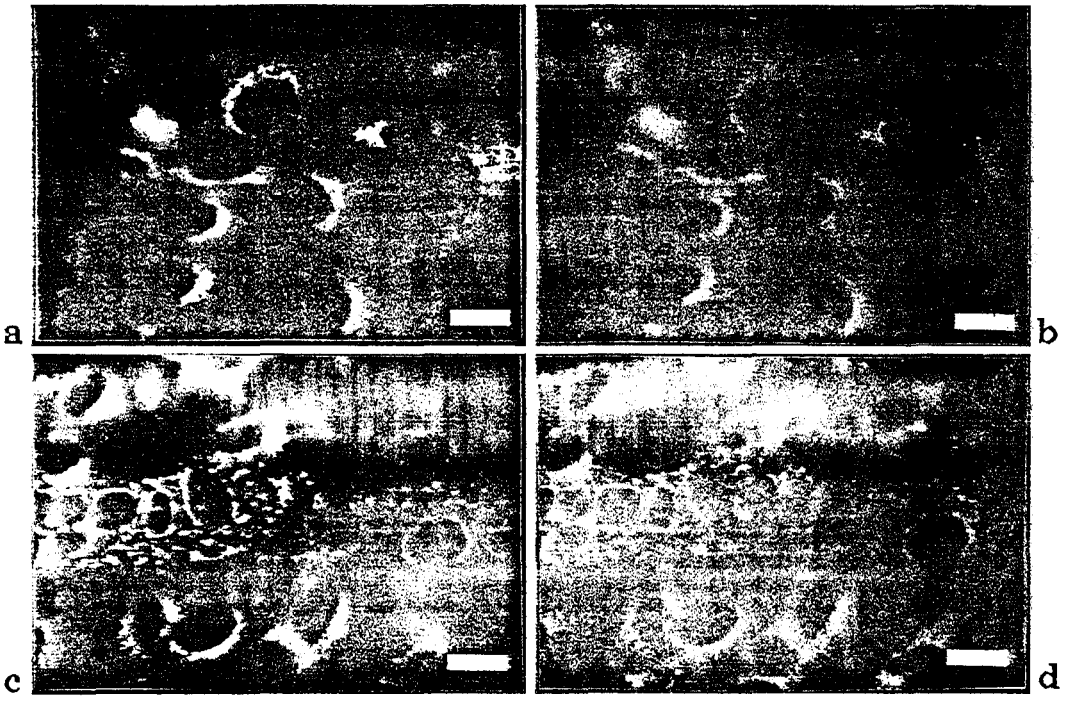

FIG-43 : CO25 cells showing a co-distribution of MPM-13 and M3A5 staining; (a and b) In myoblasts (a) MPM-13 staining, (b) M3A5 staining; (c and d) In myotubes (c) MPM-13 staining, (d) M3A5 staining; Bars= 20 µm.

4.4. DISCUSSION

4.4.1. IDENTIFICATION OF MPM-13 PROTEINS IN WESTERN BLOTS

Rao *et al.* (1989) reported that on immunoblots MPM-13 antibody recognized a major protein band at 43 kDa and a minor band of approximately 56 kDa by staining with a mixture of 5-bromo-4-choloro-3-indolyl phosphate disodium salt (BCIP) and p-nitro blue tetrazolium chloride (NBT). They also mentioned that some other low molecular weight peptides were detectable in all their blots but dismissed them as breakdown products. On my immunoblots, MPM-13 recognized many more bands than Rao *et al.*'s bands. I think the reason for this difference is that the enchanced chemiluminescence technique (ECL) is a much more sensitive method for protein detection on Western blots than the method described by Rao *et al.* (1989). In addition Rao *et al.* (1989) used an ultrasonic technique for the extraction of proteins from the cells, but I used a lysis buffer containing a detergent. The effect of the detergent is likely to extact more protein from the samples. The use of a cocktail of protease inhibitors would seem to rule out protein degradation as a cause of the additional bands. In addition reduction by boiling for 5 minutes produced little difference as compared with unboiled samples otherwise treated in the same way. Thus the difference in results is not likely to be due to the separation of sub-units. It is concluded that MPM-13 recognized a number of bands on Western gels for a variety of cell types.

I detected two strong bands in all the samples which were approximately 49 and 38 kDa. They may well correspond to Rao *et al.*'s 56 and 43 kDa proteins. Variations of 10 kDa or more are not uncommon in the molecular weight estimation of proteins on gels, due to the difficulties of accurate measurement. If a protein is glycosylated, even more variation may occur due to how much of the sugar moieties remain bound.

For both extracts of undifferentiated and differentiated CO25 myoblasts MPM-13 stained basically the same pattern of identical bands. MPM-13 antibody would seem to recognize a group of molecules with the same epitopes. Whether this reflects a down regulation of these proteins during differentiation is unclear. The major bands (49 and 38 kDa) of the differentiated CO25 cells were stronger than the major bands of the undifferentiated cells.

myotubes, particularly older myotubes, many of the granules were dispersed in the cytoplasm. Thus the relationship with established microtubule organizing centres was tenuous.Furthermore, drug studies showed that the MPM-13 granules were not MTOCs for regrowing microtubules after complete depolymerization. Also in taxol treated CO25 cells, the location of the MPM-13 staining proteins were not always the ends of the microtubule bundles. Thus even under conditions of taxol driven growth there was no relationship with microtubule growth. However, the MPM-13 staining granules clearly may have a relation with the microtubules. This is because they reformed into crescents close to the centrosomes as the microtubule network regrew, having dispersed when the network was destroyed by nocodazole.

My results showed that the staining pattern found with MPM-13 was identical to that obtained with M3A5, a specific antibody for the Golgi apparatus (Allan and Kreis, 1986). It has been previously reported that the Golgi apparatus is visualized by immunofluorescence microscopy to have a peri-centrosomal location (Rogalski and Singer, 1984). It was therefore very suprising that Rao *et al.*,(1989) did not even consider the Golgi as a possible structure stained by MPM-13. Lucocq *et al.* (1989) reported that when the interphase microtubules depolymerize and the mitotic spindle forms, elements of the Golgi apparatus were observed at the mitotic poles in line with Rao *et al.*'s (1989) results for the redistribution of MPM-13 antigens at mitosis. My results showed that the staining pattern obtained with an antibody which recognized the Golgi apparatus was identical to that obtained with MPM-13 during differentiation of CO25 cells. It is concluded that staining with MPM-13 identifies only the Golgi complex. After the granules stained by MPM-13 had been identified as components of the Golgi apparatus a survey of the literature revealed that Tassin *et al.* (1985b) had stained the Golgi apparatus of myoblasts and myotubes with wheat germ agglutin and antibodies against a Golgi specific enzyme (β-galactosyltransferase) obtaining very similar results to those observed here. The marked similarity further confirms that MPM-13 stains the Golgi in this material.

According to the results found in this work, MPM-13 does not bind to a single protein, but to a number. It is unlikely that some proteins were stained nonspecifically. A large increase in beckground staining was not seen and only elements of the Golgi were found to stain. Thus it is possible that several related proteins within the Golgi

were identified, all sharing a common epitope. A number of Golgi-specific proteins have been recognised (as introduced in section 4.1.3.) with different molecular weights.

4.4.3. THE RELATION OF THE GOLGI APPARATUS TO THE MICROTUBULE NETWORK

There is no known obligatory association between the Golgi apparatus and the microtubule network and it does not act as a MTOC (c.f. Burgess *et al.*, 1991). However there may well be a relation between them. As shown here for myoblasts treatment with microtubule depolymerizing drug causes a dispersion of the Golgi elements. Similar results have been found by Rogalski and Singer (1984). These authors have speculated that lateral association between Golgi elements and microtubules may exist with a preferential interaction of the Golgi for the minus ends of microtubules. However such a speculation does not really explain why elements of the Golgi associate near the MTOC of the cell or how they associate with microtubules. However in this context an intringuing finding of Allan and Kreis (1986) is that M3A5 also binds specifically to the neural MAP-2. Also Wiche *et al.* (1986) have reported that a MAP-2 antibody labelled the perinuclear region of mouse 3T3 cells. This may well be staining of a Golgi apparatus protein similar to MAP-2, a dimer with sub units of 54/39 kDa molecular weight, as reported by Valle (1984). These results suggest that MAP-2 and Golgi proteins may share an antigenic determinant. It may well be that the Golgi contain a microtubule binding protein similar to MAP-2. Furthermore MPM-13 identifies two proteins with similar molecular weights to MAP-2. It is therefore possible that MPM-13 identifies the sub-units of a MAP-2 like protein on Western blots. This intringuing possibility suggests MPM-13 might identify a Golgi MAP. It is not the same as that identified by M3A5, which has a different molecular weight.

CHAPTER 5

CHANGES IN MICROFILAMENT DISTRIBUTION DURING DIFFERENTIATION

5.1. INTRODUCTION

5.1.1. F-ACTIN MICROFILAMENTS

The discovery of cytoskeletal F-actin structures was first made by investigators studying muscular contraction. The fibrillar structures responsible for muscle contraction, the thin actin and the thick myosin filaments, were discovered, and described in early electron microscopic studies (Hanson and Huxley, 1953). Further studies using electron microscopy revealed actin-like filaments in stress fibres (a network of F-actin filaments) (Chang and Goldman, 1973; Goldman, 1975), and in lamellipodia (Small and Langager, 1981). Actin filament growth was correlated with changes in cell form (Heath and Holifield, 1991).

It is to be noted that stress fibres are more labile than myofibrils, undergoing cycles of assembly and disassembly during cell locomotion (Wang, 1984), during the cell cycle (Sanger, 1975), and in response to a variety of agents such as DMSO (Sanger *et al.*, 1980; Osborn and Weber, 1980), azide (Bershadsky *et. al*,1980) and cytochalasins (Weber *et al.*, 1976) which do not alter myofibril structure (Sanger, 1974).

5.1.1.1. THE ACTIN MOLECULE

Actin is highly conserved between species with only small differences in sequence between the polypeptides produced. The protein consists of 347-375 amino acid residues (Pollard and Cooper, 1986; Stewart, 1986). The 42-43 kDa monomers (G-actin) of all types of actin assemble into filaments with a very precise structure (Stewart, 1986). Most organisms have more than one isotype with diferences in one or a few amino acid residues. The filament is usually described as a right handed two-stranded helix with a repeat distance between crossover points (13 monomers form a crossover) of 36-40 μm (Egelman, 1985).

Polymerisation or depolymerisation of actin filaments is required for many types of cellular activity. Actin filaments can be depolymerised *in vitro* by lowering the ionic strength of the medium to well below physiological levels. Polymerisation *in vitro* can be induced by adding suitable concentrations of salts (e.g. 0.1 M KCl and/or 1 mM $MgCl_2$) to a solution of G-actin in water. Magnesium ions bind specifically to the protein, displacing calcium ions. The monomer, also requires bound nucleotide (usually ATP) in order to polymerise and during assembly ATP becomes hydrolysed to ADP (Carlier, 1989).

The importance of actin polymerisation and depolymerisation in cell movements is indicated by the effect of drugs that prevent changes

in the state of actin polymerisation which block such movements, e.g. the different cytochalasins-A, -B, and -D (Cooper, 1987; Stewart, 1986) (However in addition to binding actin, cytochalasins-A and -B inhibit monosaccharide transport across the plasma membrane). Cytochalasins are a group of closely related fungal metabolites that were found to specifically affect actin polymerisation (Casella *et al.*, 1981). Cytochalasins act like capping agents (Cooper, 1987). The principal action of cytochalasin is to bind specifically to the fast-growing plus ends of actin filaments, preventing the addition of actin molecules there (Cooper, 1987). Cytochalasin-D affects only the microfilament system, and has been widely used in experiments with cultured cells and other system to alter the state of actin microfilaments (Review, Cooper, 1987).

The other important drug which acts on actin is phalloidin. Phalloidin is a highly poisonous cyclic heptapeptide, produced by the deadly toadstool *Amanita phalloides* (Reviews, Stewart,1986; Cooper, 1987). It stabilizes actin filaments and inhibits their depolymerisation (Vandekerckhove *et al.*, 1985). The molecular mechanism of the specific action of phalloidin on actin is not yet clear. Fluorescent derivatives of the drug are often used instead of anti-actin antibodies to stain actin filaments in cells (Wulf *et al.*, 1979; Faulstich *et al.*, 1983).

5.1.1.2. DIFFERENT TYPES OF ACTIN

On the basis of amino acid sequence, at least six different actins have been identified in birds and mammals depending on species. Four classes are included among the α-actins :

1. Unique to striated skeletal muscle
2. Unique to cardiac muscle
3. Unique to smooth vascular muscle
4. Unique to smooth enteric muscles such as those that line the intestine.

Two further types of actins, termed β-actin and γ-actin, are found in the cytoplasm of muscle and non-muscle cells (Otey *et al.*, 1988; Rubenstein, 1990).

The organization and dynamics of microfilaments, in non-muscle cells is more complicated than in striated muscle cells. The individual subunits polymerise as in muscle actin but, for reasons not well understood, the filaments they form are a great deal less stable than the actin filaments of muscle (Carraway, 1990). There are some differences

between muscle and non-muscle actin, both in chemical composition and in the properties of the filaments formed from them (Rubenstein, 1990). The two proteins are, in fact, products of different genes.

Actin has now been found in all the major branches of the phylogenetic tree, including protozoa, lower and higher plants, and many cell types from higher animals. Non-muscle actins or their sequences closely resemble muscle actin in its sequence. They polymerize and depolymerize more readily, but in the filamentous form they look like muscle F-actin filaments and, when myosin is added, they act like actin.

5.1.1.2.1. ACTIN ISOFORM CHANGES DURING MYOGENESIS

During skeletal and cardiac muscle cell differention, nonmuscle isoactin synthesis gradually ceases (Rubenstein, 1990). It was reported by Pardo *et al.* (1983) that when the myoblasts fuse to form myotubes, α-actin synthesis increases to the extent that β- and γ-actins are barely detectable. Adult skeletal muscle examined by two-dimensional gel electrophoresis and Coomassie blue staining contains only α-actin (Lin *et al.*, 1987).

There is a big difference between muscle cells and nonmuscle cells in terms of the actin isoforms they express.. Nonmuscle cells have α-, β- and γ-actin and the actin filaments are anchored directly to the cell membrane. Cardiac muscle cells synthesize only α-actin, skeletal muscle cells have only α-actin, and smooth muscle cells have α- and γ-actin (Review, Rubenstein, 1990). Antin *et al.* (1986) observed that elongated myoblasts had a cortical meshwork of F-actin forming stress fibres. In contrast in the mature skeletal muscle fibres the actin filaments are anchored to flat protein structures called Z-discs or lines (zwischen=between), which separate each contractile unit. The contractile units are called sarcomeres. The shortest invertebrate muscle sarcomeres are 0.9 μm in length , the longest 30 μm (Chapman and Scully, 1962), with all vertebrate sarcomeres measuring approximately 2.3 μm at rest length (Sanger *et al.*, 1986). There is a prominent, periodic concentration of actin staining at the Z-band forming fine filaments parallel to the long axis of the myotubes. In contrast, staining for myosin is confined to the region between the Z-bands (Review, Muntz, 1990).

5.1.1.3. ACTIN-BINDING PROTEINS

F-actin filaments interact with many proteins called actin-binding proteins. The actin binding proteins regulate the degree of polymerisation of actin and the stability, length, and distribution of F-actin filaments. Actin-binding proteins all exhibit specific binding, but are involved in different functional activities with actin. A current list of actin binding proteins and their functions is as follows:

Protein name:	Molecular weight:	References:
MONOMER SEQUESTERING PROTEINS (Binding G-actin):		
Profilin	12-15 kDa	(Carraway, 1990; Pollard and Cooper, 1986)
Actobindin	12 "	(Preston *et al.*, 1990)
MONOMER SEQUESTERING AND FILAMENT SEVERING PROTEINS :		
Depactin	19-20 "	(Way and Weeds, 1990)
19 kD protein/ADF/Cofilin	19 "	(Preston *et al.*, 1990)
Destirin	19 "	(Way and Weeds,1990)
Actoforin	14 "	(Way and Weeds, 1990)
Vitamin D binding protein	5 "	(Preston *et al.*, 1990)
DNase-I	3 "	(Stewart,1986)
END-BLOCKING (Capping) AND NUCLEATING PROTEINS:		
Gelsolin	90 "	(Carraway, 1990; Sanger *et al*, 1987)
Villin	95 "	(Bazari *et al.*,1988; Friederich *et al.*, 1990)
Fragmin / Severin	40-45 "	(Sutoh and Hatano,1986)
Capping protein	28-31 "	(Bershadsky and Vasiliev, 1988)
Cap Z	32-34 "	(Preston *et al.*, 1990)
Acumentin	65 "	(Southwick and Hartwig,1982)
β-actinin	35-37 "	(Stewart, 1986)
Actophorin	15 "	(Preston *et al.*, 1990)
Brevin	93 "	(Preston *et al.*, 1990)
SIDE-BINDING PROTEINS:		
Tropomyosin	30-40 "	(Liu and Bretscher,1989; Stewart, 1986; Lin and Lin, 1986)

Troponin I,T,C	30	"	(Bretscher, 1986, Zot and Potter, 1987)
CROSS-LINKING PROTEINS:			
ISOTOPIC GELATIN PROTEINS:			
Myosin(s)	200	"	(Adams and Pollard, 1989; Carraway, 1990; Stewart, 1986)
Actin binding protein	2 X 270	"	(Bershadsky and Vasiliev, 1988)
Filamin	2 X 250	"	(Kobayashi and Tashima, 1989; Stewart, 1986)
Spectrin	α-240 - β-220	"	(Coleman *et al.*, 1989; Moon and McMahon, 1987)
TW 260/240	2 X 260 - 2 X 240	"	(Bershadsky and Vasiliev, 1988)
Caldesmon	2 X 150	"	(Fujii *et al.*, 1987)
ANISOTROPIC BUNDLING PROTEINS:			
α-actinin	2 X 95 - 2 X 100	"	(Terai *et al.*, 1989)
Actinogelin	2 X 115	"	(Preston *et al.*, 1990)
Fascin	53-58	"	(Bretscher, 1986)
Fimbrin	68	"	(Bretscher, 1986)
MEMBRANE ASSOCIATED PROTEINS:			
Ankyrin/Syndein	440	"	(Kunimoto *et al.*, 1991)
Band 4.1 protein	α-80 - β-78	"	(Preston *et al.*, 1990)
Vinculin	130	"	(Terai *et al.*, 1989)
Metavinculin	150	"	(Preston *et al.*, 1990)
Fodrin	235-260	"	(Coleman *et al.*, 1989)
MISCELLANEOUS:			
Gelactin	23-38	"	(Stewart, 1986)
MAP-2	300	"	(Lewis *et al.*, 1988)
Tau	50-68	"	(Hirokawa *et al.*, 1988)
Calpactins I,II (Annexin)	30-40	"	(Burgoyne, 1988; Glenney, 1987)
SECONDARILY ASSOCIATED (with F-actin):			
Calmodulin	17	"	(Bayley *et al.*, 1988)
Myosin light-chain kinase	130	"	(Adelstein *et al.*, 1982)
Talin	215	"	(Izzard, 1988)

Titin (connectin)	2000	"	(Terai *et al.*, 1989)
Nebulin	600	"	(Maruyama, 1987)

5.1.1.4. FUNCTIONS OF MICROFILAMENTS

The functions of actin filaments are well summarized and reported by Amos and Amos (1991):

1- a framework defining cell shape;

2- strengthening elements;

3- contractile muscle fibres;

4- extensile rods in microvilli;

5- fibrils for guiding transport;

6- the contractile ring for cytokinesis.

Microfilament-membrane interactions are commonly believed to be most important for regulating the shape and dynamics of animal cells (e.f. Carraway, 1990). In cultured cells, stress fibres composed of bundles of microfilaments, frequently run parallel to the primary axis of the cell. These stress fibres terminate at focal adhesions between the cell and substratum. Microvilli and other similar cell surface specializations contain a core of microfilaments as their supporting structural element. Ruffling membranes of motile cells are rich in actin-containing microfilaments in a sub-membrane network (Small and Langager, 1981). It is believed that F-actin bundles develop apparently at random within the actin network and then display a complicated pattern of extension and retraction, lateral motion, and fusion with one another (Izzard, 1988; Fisher *et al.*, 1988). Traction forces, created by microfilaments, also serve other important morphogenetic functions, in particular the reorganization and alignment of fibronectin and collagen matrices to form relatively large-scale anatomical structures (Harris *et al.*; 1981; Stopac and Harris, 1982). Cellular traction forces are known to be created as a result of acto-myosin dependent contraction (Cooke, 1986).

5.1.2. CYTOSKELETAL STRUCTURE OF MYOFIBRILS

The contractile units of striated muscle myofibrils are called sarcomeres. In the light microscope at high magnification a series of alternating broad light and dark bands can be seen in each sarcomere. Myosin thick filaments are the major constituents of the A (anisotropic) bands. On both sides of the I (isotropic) bands, the heads of the myosin molecules protrude as laterally forming cross-bridges with adjacent actin filaments. A dense line in the centre of each light band separates one

sarcomere from the next, and is known as the Z-band. F-actin filaments form the I-bands and are anchored to flat membrane/protein structures which form the Z-band, between every two contractile units. The actin filaments extend perpendicularly from both surfaces of the Z-band and run in opposite directions on opposite sides. The shortest intervertebrate muscle sarcomeres are 0.9 μm in length, the longest 30 μm (Chapman and Scully, 1962), with all vertebrate sarcomeres measuring approximately 2.3 μm at rest length (Sanger, et. al., 1986). Actin and myosin filaments overlap almost completely when the muscle fibre contracts so that the ends of the myosin filaments are close to the Z-bands. A major attachment protein for the actin filaments is α-actinin (19 kDa), which is a major component of Z-band in striated muscle (Davison and Critchley, 1988).

During the differentiation process, desmin is progressively integrated into vimentin filaments present in myoblasts, and both are progressively associated with the Z-bands during and after the assembly of the sarcomeres (Cossette and Vincent, 1991). Immunological localization of desmin in embryonic cardiac cells and skeletal myotubes *in vitro* indicates that desmin forms an intricate array of filaments in both of these cell types. In mature skeletal and cardiac muscle, desmin is found in the Z-bands of isolated myofibrils. When viewed in cross section, desmin is observed at the periphery of the each Z-band where it forms a transverse network encircling and interlinking adjacent Z-bands. Desmin forms an interconnecting network across each muscle fibre, perpendicular to the long axis of the fibre. Desmin fibres may also link Z-bands to the plasma membrane or to other cytoplasmic organelles. Gard and Lazarides (1980) reported that there must be a redistribution of desmin from free cytoplasmic filaments to the myofibril Z-band during the differentiation of both skeletal and cardiac muscle fibre.

Two distinct high molecular weight proteins, synemin (230 kDa) and paranemin (280 kDa), are associated with desmin filament in muscle cells and also with some, but not all vimentin filaments in muscle cells.

Vertebrate striated muscle contains elastic filaments composed of the high molecular weight protein titin (~3000 kDa) (Wang, et. al., 1979), also called connectin (Maruyama, 1986) which span the region from the M-line to the Z-bands and connect the thick filaments to the Z-band; these filaments are about 1-1.3 μm long (Furst, et. al., 1988).

Other large muscle proteins that have been identified are nebulin (~600 kDa) in vertebrate striated muscle Z-band (Wang and Williamson,

1980). Integrin is extracellularly accessible and is at the cell surface, also, integrin is localized in the Z-bands of the differentiated myotube (Volk, et. al ., 1990).

5.1.3. FOCAL CONTACTS

Most of the cell surface is separated from the substratum by gaps of more than 50 nm (Burridge *et al.*, 1988). In certain regions however the distance between the cells surface and the substration is reduced to 15-20 nm. These regions appear as dark areas in an interference reflection microscope and are termed "focal contacts" or "adhesion plaques". Immunostaining for actin filaments shown that focal contacts are closely related to the actin filament attachment sites in the plasma membranes of the cells (Geiger, 1979; Burridge, 1983). In cultured, cells close contacts are frequently made with the glass or plastic surface which forms the substrate. A dense plaque of material is observed at cytoplasmic surfaces where the cell membrane makes close contacts with the substrate. The plaques contain α-actinin, vinculin (which together bind to F-actin), and talin (which interacts strongly with vinculin) (Burridge *et al.*, 1988; Burridge and Fath, 1989; Geiger, 1989). It has been shown *in vitro* that talin (on the inside of the cell) also binds to integrins which localize to focal contacts in the membrane (Beckerle and Yeh, 1990). The extracellular domains of several integrins are receptors for several extracellular matrix proteins including laminin, fibronectin, and vitronectin (Hynes, 1987). These structures provide contact points where cell traction can be generated. Alternatively, in motile cells contact via focal contacts provides substrate adession points over which cells move.

5.2. MATERIALS AND METHODS

5.2.1. CELL CULTURE

5.2.1.1. CELL TYPE

As described in section 2.2.1.1.

5.2.1.2. PREPARATION OF CULTURE MEDIA

As described in section 2.2.1.2.

5.2.1.3. CELL CULTURE

As described in section 2.2.1.3.

5.2.1.4. TRYPSIN SOLUTION

As described in section 2.2.1.4.

5.2.1.5. PREPARATION OF PLASTIC DISCS

As described in section 2.2.1.5.

5.2.2. BUFFERS

5.2.2.1. PBS

As described in section 2.2.2.1.

5.2.2.2. PEM BUFFER

As described in section 3.2.2.3.

5.2.2.3. PERMEABILISATION BUFFERS

5.2.2.3.1. PERMEABILISATION BUFFER-1

As described in section 3.2.2.4.1.

5.2.2.3.2. MOPS PERMEABILISATION BUFFER

As described in section 3.2.2.4.2.

5.2.3. FIXATIVES AND FIXATION

5.2.3.1. PARAFORMALDEHYDE

As described in section 3.2.3.1.

5.2.3.2. 90% METHANOL

As described in section 3.2.3.2.

5.2.4. STAINING FOR FLUORESCENCE MICROSCOPY

5.2.4.1. PHALLOIDIN STAINING FOR F-ACTIN

Cells grown on plastic and/or glass coverslips were fixed with 4% paraformaldehyde (as decribed in section 3.2.3.1.). The cells were then stained with fluorescein labelled phalloidin (5 mg/ml; Wulf *et al.*, 1979) or rhodamine labelled phalloidin (1 mg/ml; Faulstich *et al.*, 1983) for 1 hour at 37 ^{o}C in a humid chamber. In both cases the labelled phalloidin was a gift from Prof. Th. Wieland. After final washing preparats were mounted in Citifluor (Citifluor Ltd., London). The cells were examined using epifluorescence microscopy (as described in section 3.2.5.1.).

5.2.4.2. IMMUNOSTAINING FOR VINCULIN

Cells to be stained for vinculin were first permeabilised for 30 seconds with 1% Nonidet P-40 in PIPES. The cells were then fixed with 4% paraformaldehyde (as described in section 3.2.3.1.), and then stained using the following protocol; Rabbit serum (Dako), 1:10; V284 mouse anti-vinculin (Asijee *et al.*, 1990; Serotec), 1:200; FITC rabbit anti-mouse (Dako), 1:100. All antibodies were applied for 1 hour at 37 ^{o}C in a humid chamber. After final washing preparats were mounted in Citifluor (Citifluor Ltd., London). The cells were examined using epifluorescence microscopy (as described in section 3.2.5.1.).

5.2.3. MICROSCOPY

5.2.3.1 EPI-FLUORESCENCE MICROSCOPY

As described in section 3.2.5.1.

5.2.4. LENSES AND FILTERS

5.2.4.1. LENSES AND FILTERS FOR EPI-FLUORESCENT MICROSCOPY:

As described in section 3.2.6.1.

5.2.5. PHOTOMICROSCOPY

5.2.5.1. CAMERAS

As described in section 3.2.8.1.

5.2.5.2. FILMS

As described in section 3.2.8.2.

5.2.5.3. PHOTOGRAPHIC SOLUTIONS

As described in section 3.2.8.3.

5.2.5.4. PHOTOGRAPHIC PAPER

As described in section 2.2.6.4.

5.3. RESULTS

5.3.1. ORGANIZATION OF MICROFILAMENTS

5.3.1.1. DISTRIBUTION OF MICROFILAMENTS DURING DIFFERENTIATION

Rhodamine labelled phalloidin (rh-phalloidin) was used for these experiments which reacted *in vitro* with only F-actin. Fig. 44a, b, and c show that CO25 cells in the 3 different media showed very different patterns of stress fibre organization.

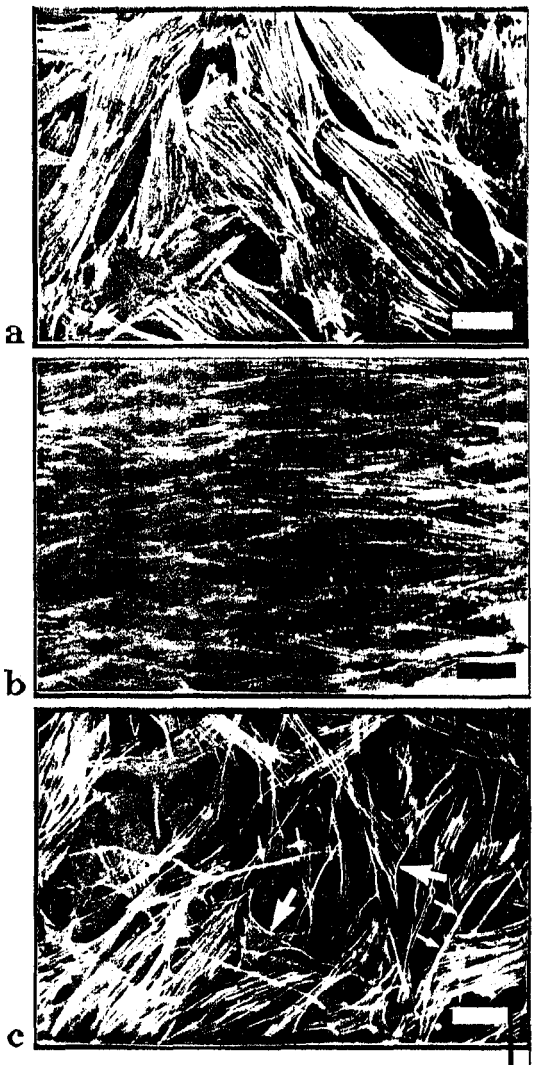

FIG.-44 : Rh-phalloidin stained CO25 cells in the different media after 2 days. (a) Cells in the growth medium, (b) cells in the fusion medium after 2 days, (c) cells in the fusion medium with (1 µM) dexamethasone after 2 days; thin arrows, localization of F-actin in the processes of transformed cells; thick arrows, localization of F-actin around the lateral edges of transformed cells; Bars= 20 µm.

Phalloidin staining showed the presence of large numbers of stress fibres within the undifferentiated myoblasts. Characteristically they displayed a high degree of organization; The majority of flattened mononucleated myoblasts displayed prominent parallel running microfilament bundles in the growth medium (Fig. 44a). This tendency for most of the microfilament bundles to run in parallel was much more apparent in fully formed myotubes (Fig. 44b). In contrast the actin bundles of cells transformed by dexamethasone were quite disorganized by comparison. Phalloidin brightly stained the edges and also the long processes of the smaller transformed cells (Fig. 44c).

Further experiments were done to observe in detail the changing distribution of microfilament bundles step by step during myogenesis. After the myoblast became obviously spindle-shaped, the stress fibres were increasingly orientated parallel to the long axis in each of the elongating myoblasts (Fig. 45b). Using rh-phalloidin staining the parallel alignment of the microfilament bundles can be seen during cell fusion (Fig. 45c, d). The microfilaments formed a network parallel to each other and frequently spaned the whole length of the cell. The high power detail in Fig 45d shows that only a small number of actin bundles were present in the fusion area. Actin cables ran throughout the body of all newly fused myotubes (Fig. 45e, f). Newly fused cells contained suprisingly few microfilament bundles (Fig. 45e, f). The lateral sides of newly formed myotubes stained very brightly and appeared to contain most of the stress fibre bundles (Fig. 45e, f).

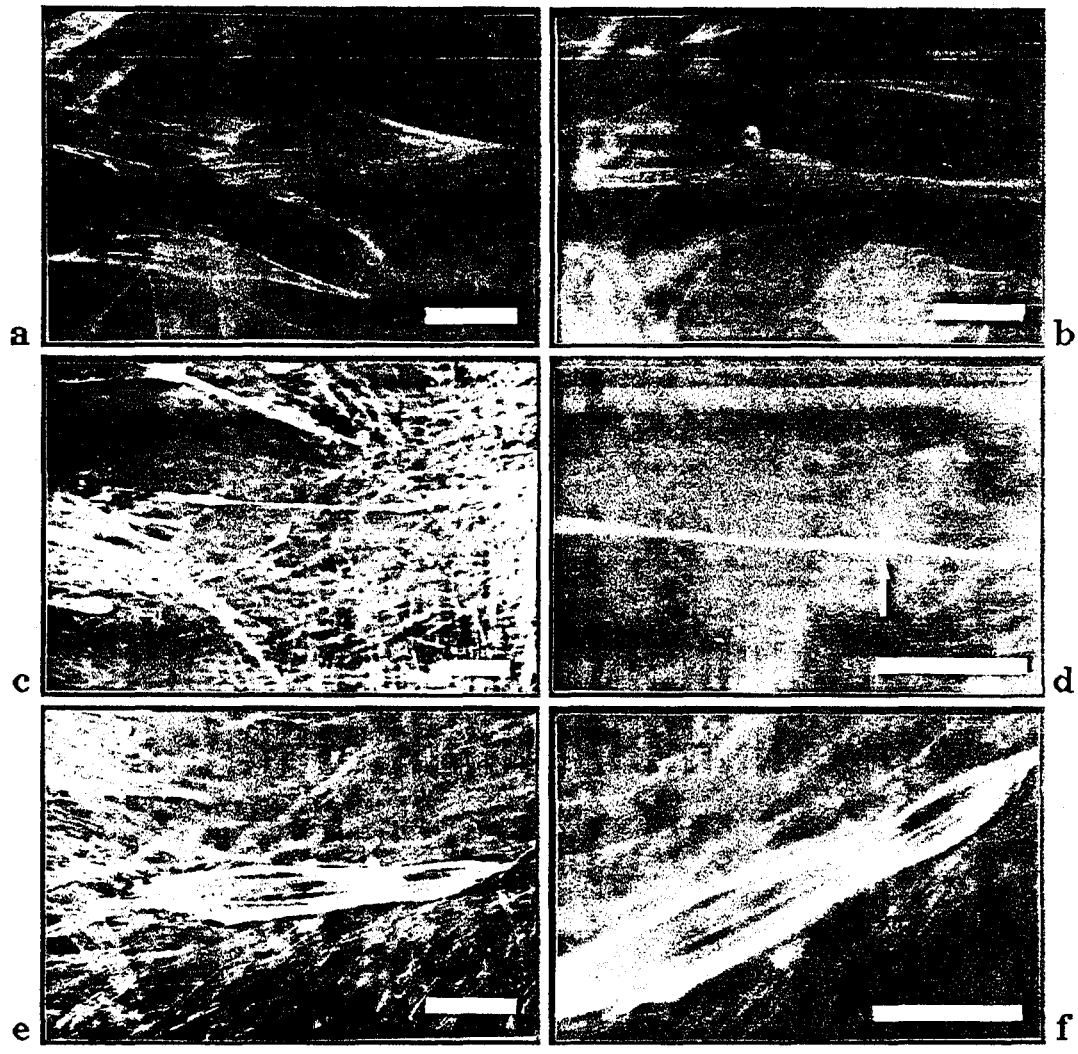

FIG.-45 : Distribution of F-actin in CO25 cells stained with Rh-phalloidin during myogenesis. (a) control cells before replacing with fusion medium, (b) first day after replacing with fusion medium, (c) cells starting to fuse after 2 days in fusion medium under the low power, arrow shows actin bundles in the fusion area, (d) fusion area of (c) under the higher power, (e) fused cells after 3 days under low power, and (f) fused cells under higher power; Bars= 20 µm.

The actin cables were all oriented at right angles to the long axis of the myotubes after a week in the fusion medium (Fig. 46a, b). Also the actin bundles seemed to increase in number in a week old myotubes as compared newly formed myotubes (Fig. 46a, b). After approximately 2 weeks, the stress fibres had either disappeared or become redistributed in a periodic organization in the myotubes (Fig. 46c, d). Some periodic sarcomere pattern was apparent (thick arrow shows on

Fig. 46d) and also some stress fibres were still present in the same myotube (thin arrow shows on Fig. 46d), demonstrating the replacement of stress fibres by sarcomeres.

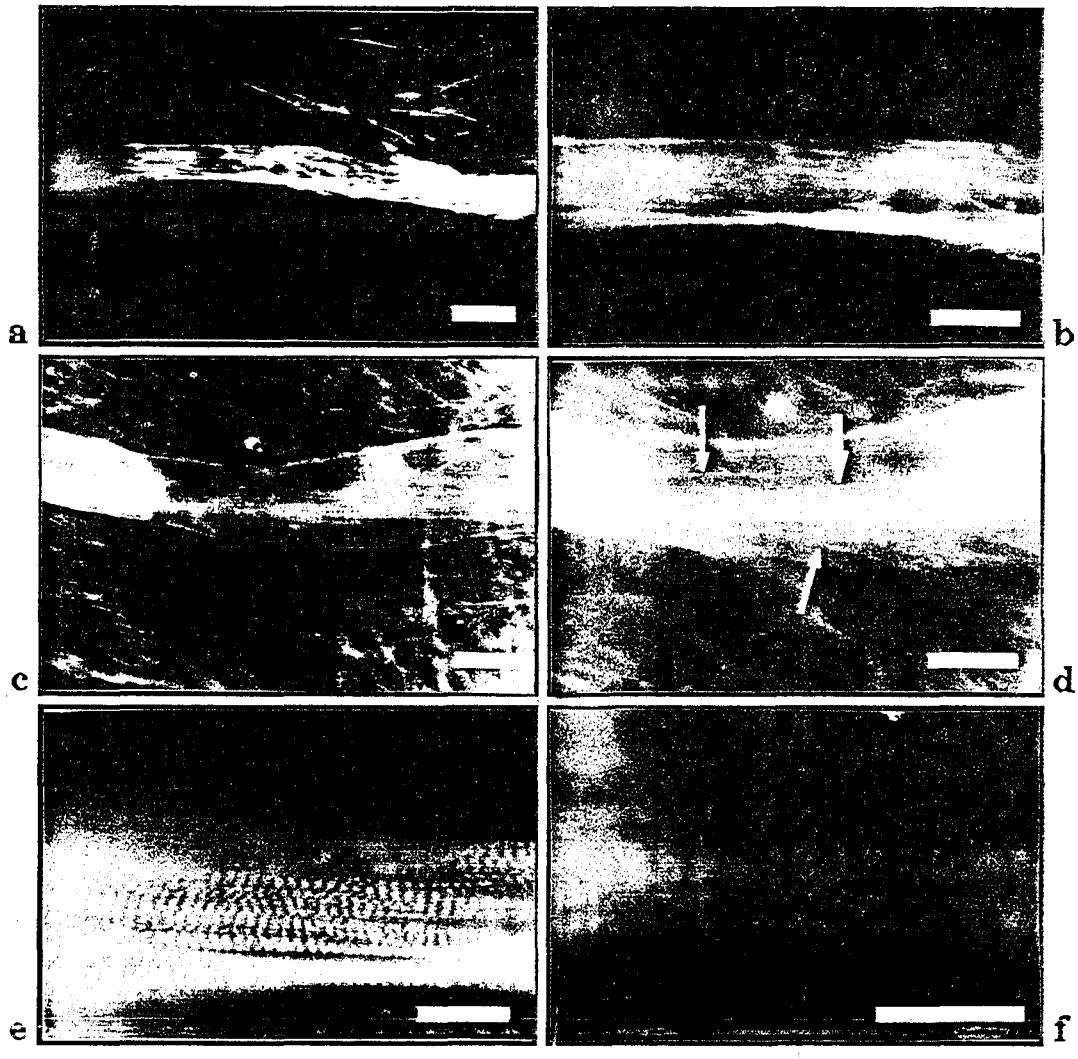

FIG.-46 : (a and b) F-actin distribution in a week old myotube (a) low power, (b) higher power; (c and d) After 2 weeks periodic actin pattern in the myotube (c) low power, (d) higher power, thin arrow shows the stress fibres, thick arrow shows the periodic organization of F-actin; (e and f) Sarcomeres after 3 weeks in fusion medium (e) low power, and (f) higher power; All rh-phalloidin stained; Bars= 20 μm.

After approximately 3 weeks, fully formed sarcomeres were seen by rh-phalloidin staining in CO25 myofibrils (Fig. 46e). Periodic F-actin I-bands were organized along the myofibrils (46e, f).

Usually myofibrils began to appear in fused CO25 cells after 2 weeks and began to show contractile behaviour after 3 weeks in culture.

Periodic contractions of the myofibrils formed by CO25 cells begun after 3 weeks (not shown).

5.3.1.2. DISTRIBUTION OF MICROFILAMENTS DURING TRANSFORMATION

The distribution of actin cables in CO25 cells was dramatically changed in cells transformed by dexamethasone. After 1 day, some parallel distributed actin cables were still present in the cell bodies (Fig. 47b). However the organization was begining to break down and clumps of F-actin were present. A dense concentration of F-actin became clearly visible in the processes and at the edges of the cells (thin arrows show on Fig. 44c; 47c).

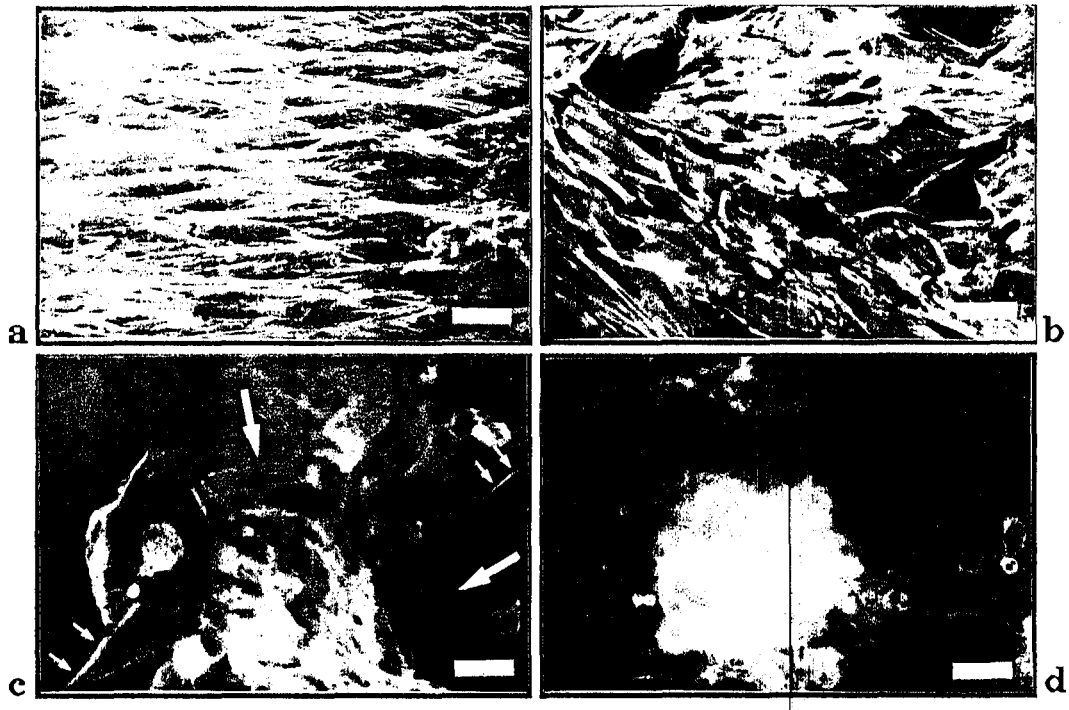

FIG.-47 : Rh-phalloidin stained CO25 cells in the fusion medium with (1μM) dexamethasone. (a)control cells before replacing with medium containing dexamethasone, (b) first day after replacing fusion medium with that containing dexamethasone, (c) second day after replacing fusion medium with that containing dexamethasone, thin arrows show localization of F-actin in the processes of transformed cells, thick arrows show localization of F-actin in the edges of transformed cells, and (d) after 4 days transformed cells have formed foci. Bars= 20 μm.

Stress fibres became largely replaced by a diffuse bright fluorescence, in the cells after 2 days treatment with dexamethasone and those that remained were much reduced in size as compared with cells grown in the absence of dexamethasone (Fig. 47c). Transformed cells in clumps had no detectable cables of stress fibres in the central area, and they showed only a bright diffuse fluorescence. In those cells which were at the bottom level of the clumps and attached foci to the substratum, cortical F-actin was present at the edges of cells (thick arrows show on Fig. 44a, 47c). Stress fibres were not at all obvious in the foci formed by the transformed CO25 cells after 4 days, but the cells were brightly stained by diffuse fluorescence (Fig. 47d).

5.3.2. FOCAL CONTACT ORGANIZATION

CO25 cells were grown in growth medium or fusion medium for periods of time, and were then stained with V284, a mouse anti-vinculin antibody, to investigate the localization of a major constituent of focal adhesion plaques. This experiment was to determine where the parallel bundles of F-actin bundles may attach during myotube formation. Undifferentiated cells had many focal adhesion plaques of varying sizes which were found to localize mainly around the periphery of the ventral surfaces of the undifferentiated cells (Fig. 48a, b).

After two days in the fusion medium, there was a significant change in the distribution of vinculin (Fig. 48c, d). The adhesion plaques were seen not only around the periphery of the cells, but along the ventral surfaces of the elongated cell bodies (Fig. 48d). During myotube formation, adhesion plaques were seen to redistribute forming a linear pattern (Fig. 49a, b). After myotube formation, the adhesion plaques were seen to localize mainly to the edges of the bottom surfaces of the myotubes (Fig 49b, d). A comparison of Figs. 48 and 49 shows that the adhesion and also possible decreased in number and became organised in a linear pattern during differentiation. Thus the adhesion plaques became more organized in distribution in the myotubes.

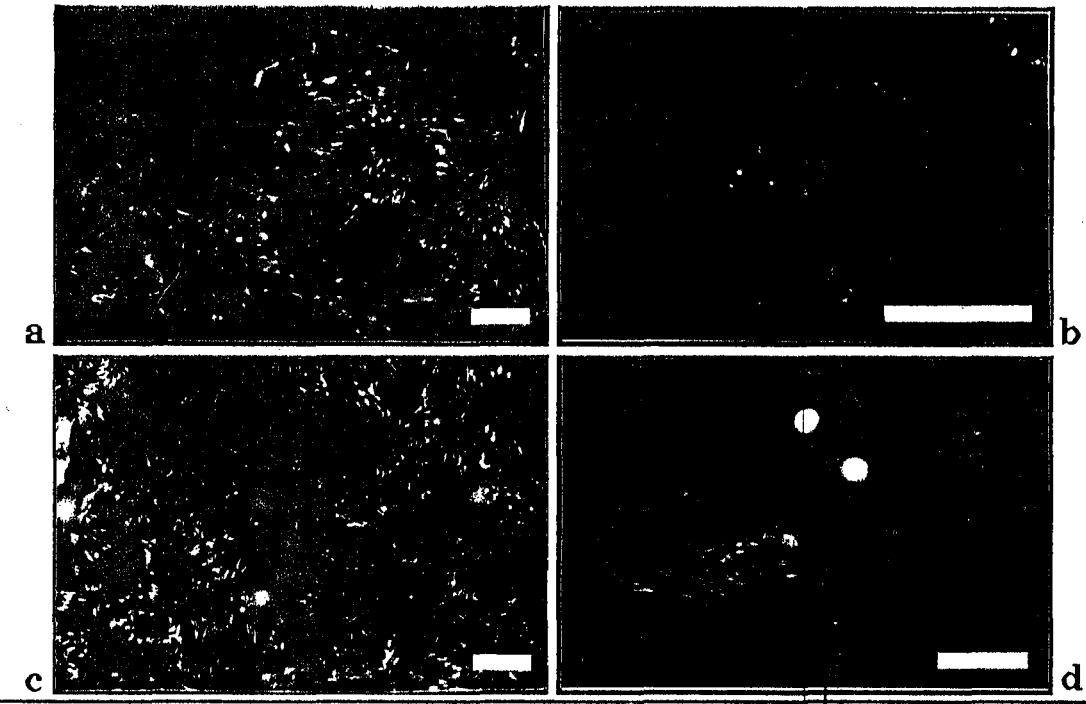

FIG.-48 : Vinculin localization of CO25 cells during differentiation. (a, b) After 1 day in growth medium, (a) level of focus close to substratum, (b) slightly higher level of focus as compared with (a), (c,d) after 2 days in the fusion medium, (c) low power, (d) higher power; Bars=20 μm.

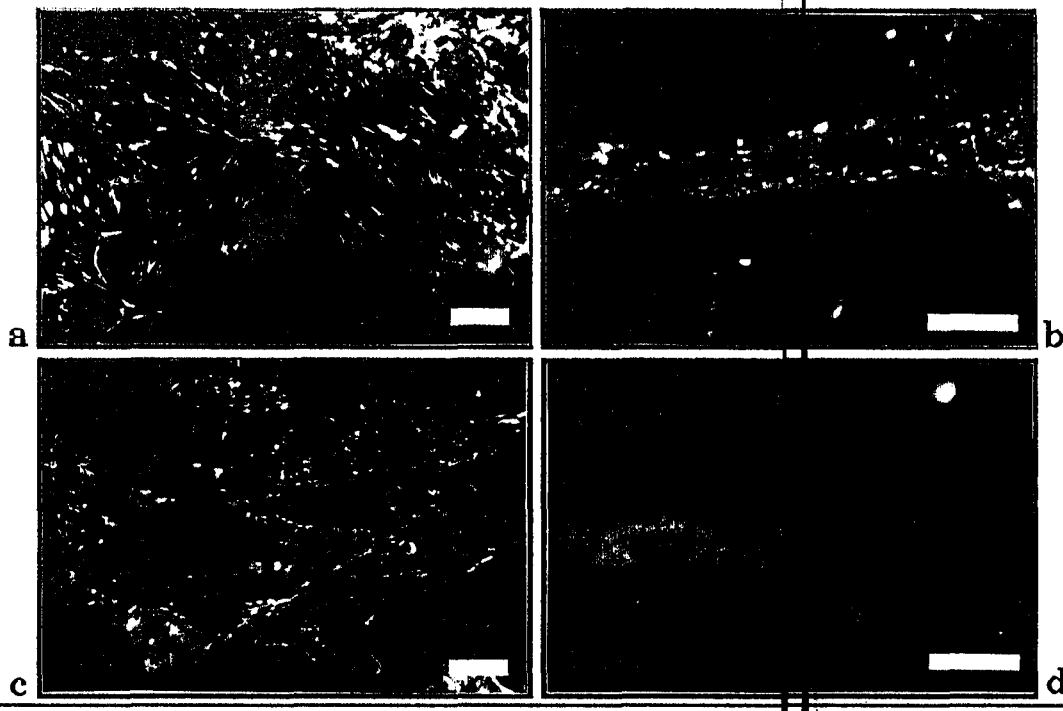

FIG.-49 : Vinculin localization of CO25 cells during myogenesis. (a, b) after three days in the fusion medium, (a) low power, (b) higher power, (c, d) after a week in the fusion medium, (c) low power, (d) higher power; Bars= 20 μm.

5.4. DISCUSSION

5.4.1. REDISTRIBUTION OF F-ACTIN DURING DIFFERENTIATION

This study demonstrated that the distribution and structure of the F-actin stress fibres of CO25 myoblast cells changed very significantly during differentiation.

The first significant change in actin distribution was the reorganization of stress fibres parallel to the long axis during elongation. Also, as elongation became apparent the number of stress fibres was reduced and there was an apparent increase in the intensity of fluorescence around the edges of the cells. However it is considered that the increase in brightness at the edges is at least partially an artefact due to the rounding up of the cells when they adopt a spindle form.

It is well known that in eukaryotic cells actin filaments and filament bundles are attached to the inner surfaces of the plasma membrane at focal contacts where a variety of actin binding proteins are localized (Geiger, 1979; Burridge, 1983). Therefore, these proteins have been suggested to have key roles in the attachment of actin filaments to the cell membrane. The distribution of actin filaments and also microtubules in the cells in general correlated well with the shape of the cells. The changing of myoblast shape from flat to spindle, appeared to be proceded by loss or change in the distribution of focal contacts present on the basal cell surfaces. The change in vinculin distribution along the long axis of the elongating cells may reflect a loss of anchorage. In turn the decrease in anchorage during myoblast differentiation, is likely to be closely correlated with a decrease in number of F-actin filaments in the cells. Thus, the reason for decreasing of F-actin during elongation and fusion stages may be loss of anchorages by changing of CO25 cell shape. When cell shape changed to spindle, the polarized parallel actin bundles may be generated between the two poles of the cells. Terai *et al.* (1989) reported similar results for polarization of vinculin and α-actinin in cardiac myocytes *in vitro*.

In early stage myotubes the number of stress fibres significantly increased again. It has been reported that proliferating skeletal myoblasts contain mostly β- and γ-actins (Vandekerckhove *et al.*, 1986), but begin to express α-actins in the multinucleate myotube (Buckingham, 1985). Olson and Capetanaki (1989) studied the expression of the mRNAs which encode the actin which forms microfilaments during myoblast differentiation, and they observed that

differentiation was accompanied by down-regulation of β- and γ-actins and accumulation of α-sarcomeric actins. Caplan *et. al.* (1983) also reported that there was a transient expression of α-smooth actin before α-sarcomeric actin appeared in L6 myoblast cultures. These results suggest one explanation of the increase in actin content and in the number of stress fibres may be due to the synthesis of new gene products as a result of genetic switch on as differentiation proceeds. The alternative hypothesis in that the stress fibres act as precursors and/or templates for myofibril formation.

As actin periodicity gradually appeared, the stress fibres gradually disappeared during the maturation of myotubes. The actin fibrils which resemble stress fibres in some way came to form the I-bands of the sarcomeres (Antin *et al.*, 1986; Sanger *et al.*, 1987; Otey *et al.*, 1988; Lin *et al.*, 1989; Eberhardt *et al.*, 1990). Thus the presence of pre-existing bundles of F-actin filaments which increase with myotube formation, may be precursors of myofibrils.

5.4.2. DISTRIBUTION OF F-ACTIN DURING TRANSFORMATION

It is commonly believed that a loss of F-actin stress fibres is a general marker for transformation. In this study, rh-phalloidin staining showed two kinds of F-actin structures in transformed CO25 cells in the same culture: a fairly normal but somewhat reduced distribution of F-actin in the cells which were attached on the substratum, and completely dispersed F-actin in the rounded up cells which were without attachment with the substratum. A comparison of normal cells and their transformed variants has been reported by Watt *et al.* (1978) and by Verderame *et al.* (1980). They found that some transformed cell lines had few or no actin cables but some others an essentially unaltered stress fibre pattern. These results suggest that the distribution of actin cables is not directly related to transformation but more to other factors such as shape of the cell and the adhesiveness to the substrate. Willingham *et al.* (1977) confimed this suspicion by demonstrating that the degree of development of stress fibres within cells can be manipulated by altering the adhesiveness of the cells to the culture dishes by various means. From such experiments it has been concluded that it is the degree of adhesion which determines whether stress fibres will form. It is concluded that a few transformed CO25 cells retain some residual substrate adhesiveness to the substratum. These cells also contain F-

actin mainly in the form of stress fibres. The majority of the cells have entirely lost any substratum adhesiveness but remain attached to those which do retain some thus forming foci. The cells not attached to the substratum lose all F-actin stress fibres as a consequence.

It is not known yet how activated *ras* gene product acts on the F-actin cytoskeleton in transformed cells. However it is reported that activated *ras* oncogene causes persistent activation of intracellular growth through GTPase activity (Sternberg *et al.*, 1989). In this way activated *ras* genes in CO25 cells act as internal growth factors causing continuous cell division (Gossett *et al*, 1988). Actin filaments change in form during the mitotic G2 phase of a normal cell cycle, and depolymerization of microfilament bundles occurs (Wang and Goldberg, 1976; Celis *et al.*, 1986). Thus continuous entry into mitosis may have some effect on the number of stress fibres present. The actin binding protein tropomyosin may be a major target of the changes which occur upon transformation resulting in a loss of stress fibres. It has been observed that tropomyosin is a component of stress fibres, and acts in stabilising F-actin polymers (Fattoum *et al.*, 1983; Urbancikova and Grofova, 1990). Several groups (Matsumura *et al.*, 1983; Hendricks and Weintraub, 1984; Cooper *et al.*, 1985) have demonstrated that changes in the pattern of tropomyosin isotypes and also their mRNA levels accompany cell shape changes occurring upon transformation. There is a down regulation of the higher molecular weight forms and an up regulation of the lower molecular weight forms. Given the known properties of tropomyosin as a actin polymer stabilizing agent it may well to that changes in tropomyosin isoform lead to a destabilization of the stress fibre.

An actin binding protein, profilin, which binds to phosphatidylinositol 4,5-biphosphate 1 (PIP2) on the inner surface of the plasma membrane forms a stable 1:1 complex with G-actin and keeps actin in the monomeric form (Goldschmidt -Clermont *et al.*, 1991). Expression of N-*ras* in 3T3 cells has been found to increase the hydrolysis of PIP2 (Bishop, 1988), and this causes the release of profilin from plasma membranes. It is therefore reasonable to speculate that the release of profilin may sequester actin as G-actin and thus prevent new stress fibre formation. This activation of profilin by *ras* may be an alternative mechanism by which changes in the actin cytoskeleton occur upon transformation.

REFERENCES

Adams,R.J. and Pollard,T.D. Binding of myosin I to membrane lipids: *Nature*; 1989; **340**; 565-568.

Adelstein,R.S., Pato,M.D., Sellers,J.R., de Lanerolle,P. and Conti, M.A. Regulation of actin-myosin interaction by reversible phosphorylation of myosin and myosin kinase: *Cold Spring Harbor Symposia on Quantitative Biology*; 1982; **46**; 921-928.

Afzelius,B.A. Cilia and flagella that do not conform to the 9+2 patern: *Journal of Ultrastructure Research*; 1963; **9**; 381-394.

Afzelius,B.A. Electron microscopy of sperm tail: *Journal of Biophysical and Biochemical Cytology*; 1959; **5**; 269-283.

Afzelius,B.A. The fine structure of the cilia from ctenophore swimming-plates: *Journal of Biophysical and Biochemical Cytology*; 1961; **9**; 383-390.

Ahkong,Q.F., Blow,A.M.J., Botham,G.M., Launder,J.M., Quirle, S.J. and Lucy,J.A. Proteinases and cell fusion: *FEBS LETTER*; 1978; **95(1)**, 147-152.

Albrecht-Buehler,G. The iris diaphragm model of centriole and basal body formation: *Cell Motility and the Cytoskeleton*; 1990; **17**; 197-213.

Albrecht-Buehler,G. and Bushnell,A. The ultrastructure of primary cilia in quiescent 3T3 cells: *Experimental Cell Research*; 1980; **123**; 427-437.

Allan,V.J. and Kreis,T.E. A microtubule-binding protein associated with membranes of the golgi apparatus: *Journal of Cell Biology*; 1986; **103(6)**; 2229-2239.

Amos,L.A. Structure of muscle filaments studied by electron microscopy:*Annual Review of Biophysics and Biophysical Chemistry* 1985; **14**; 291-313.

Amos,L.A., Jubb,J.S., Henderson,R. and Vigers,G. Arrangement of protofilaments in two forms of tubulin crystal induced by vinblastine: *Journal of Molecular Biology*; 1984; **178**; 711-729.

Amos,L.A., and Amos,W.B. Molecules of the cytoskeleton: *McMillian Education Ltd.*; 1991; London.

Anderson,R.G.W. Biochemical and cytochemical evidence for ATPase activity in basal bodies isolated from oviduct: *Journal of Cell Biology*; 1977; **74**; 547-560.

Anderson,R.G.W and Brenner,R.M. The formation of basal bodies (centrioles) in the rhesus monkey oviduct: *Journal of Cell Biology*; 1971; **50**; 10-34.

Anderson,R.G.W. and Floyd,A.K. Electrophoretic analysis of basal body (centriole) proteins: *Biochemistry*; 1980; **19**; 5625-5631.

Andres,A.C., Vandervalk,M.A., Schonenberg,C.A.S., Fluckiger,F., Lemeur,M. and Groner,B. Ha-ras and c-myc oncogene expression interferes with morphological and functional differentiation of mammary

epithelial cells in single and double transgenic mice: *Genes Development*; 1988; **2**; 1486-1495.

Antin,P.B., Tokunaka,S., Nachmias,V.T. and Holtzer,H. Role of stress fiber-like structures in assembling nascent myofibrils in myosheets recovering from exposure to etylmethhanesulfonate: *Journal of Cell Biology*; 1986; **102**; 1464-1479.

Asijee,G.M., Struk,A., Bruin,T., Wikinson,J.M. and Cate,W.T. Vinculin is a permanent component of the membrane skeleton and is incorporated into the (re)organizing cytoskeleton upon platelet activation: *European Journal of Biochemistry*; 1990; **189**; 131-136.

Ayer,L.M. and Fritzler,M.J. Anti centromere antibodies bind to trout testis histone 1 and a low molecular weight protein from rabbit thymus: *Molecular Immunology*; 1984; **21**; 761-770.

Baas,P.W., Black,M.M. and Banker,G.A. Changes in microtubule polarity orientation during the development of hippocampal-neurons in culture: *Journal of Cell Biology*; 1989; **109(6)**; 3085-3094.

Babai,F., Agham,J.M., Schurch,W., Royal,A., and Gabbiani,G. Coexpression of a-sarcomeric actin, a-smooth muscle actin and desmin during myogenesis in rat and mouse embryos I. skeletal muscle: *Differentiation*; 1990; **44**; 132-142.

Balczon,R. and West,K. The identification of mammalian centrosomal antigens using human autoimmune anticentrosome antisera: *Cell Motility and the Cytoskeleton*; 1991; **20**; 121-135.

Barnes,B.G. Ciliated secretory cells in the pars distal of the mouse hypophysis: *Journal of Ultrastructure Research*; 1961; **5**; 453-467.

Barra,H.S., Arce,C.A. and Carlos,E.A. Posttranslational tyrosination /detyrosination of tubulin: *Molecular Neurobiology*; 1988; **2**; 133-153.

Bar-Sagi,D. and Framisco,J.R. Microinjection of the ras oncogene protein into PC12 cells induces morphological differentiation: *Cell*; 1985; **42**; 841-848.

Bar-Sagi,D. and Feramisco,J.R. Induction of membrane ruffling and fluid-phase pinocytosis in quiescent fibroblasts by ras protein: *Science*; 1986; **233**; 1061-1068.

Bayley,P., Martin,S. and Jones,G. The conformation of calmodulin: A substantial enviromentally sensitive helical transition in Ca2+-calmodulin with potential mechanistic function: *FEBS*; 1988; **187**; 160-166.

Bazari,W.L., Matsudaira,P., Wallek,M., Smeal,T., Jakes,R. and Ahmed,V. Villin sequence and peptide map identifying six homologous domains: *Proseedings of the National Academy of Sciences USA*; 1988; **85**; 4986-4990.

Beckerle,M.C. and Yeh,R.K. Talin: Role at sites of cell-substratum adhesion: *Cell Motility and the Cytoskeleton*; 1990; **16**; 7-13.

Bergen,L.G. and Borisy,G.G. Tubulin-cochicine complex inhibits microtubule elongation at both plus and minus end: *Journal of Biological Chemistry*; 1983; **258(7)**; 4190-4194.

Bergmann,J.E., Kupfer,A. and Singer,S.J. Membrane insertion at the leading edge of motile fibroblast: *Proceeding of the National Acadamy of Sciences of U.S.A.*; 1983; **80**; 1367-1371.

Bernhard,W. and De Harwen,E.L. Ultrastructure du centriole et dautres elements de l'appareil achromatique: *In vierter Internationaler Kongress fur Elektronenmikroskopie, Berlin, Springer*; 1960; **2**; 217-223.

Bershadsky,A.D., and Vasiliev,J.M. Cytoskeleton: *Plenum Press*; 1988; NewYork and London.

Bershadsky,A.D., Gelfand,V.I., Svitkina,T.M. and Tint,I.S. Destriction of microfilament bundles in mouse embryo fibroblasts treated with inhibitors of energy metabolism: *Experimental Cell Research*; 1980; **127**; 421-429.

Bischoff,R. Proliferation of muscle satellite cells on intact myofibers in culture: *Developmental Biology*; 1986; **115**; 129-139.

Bishop,J.M. Molecular themes in oncogenesis: *Cell*; 1991; **64**; 235-248.

Bloodgod,R.A. and Miller,K.R. Resoption of organelles containing microtubules: *Cytobios*; 1974; **9(35)**; 143-152.

Bloom,G.S. and Brashear,T.A. A novel 58-kDa protein associates with the golgi apparatus and microtubules: *Journal of Biological Chemistry*; 1989; **264(27)**; 16083-16092.

Borisy,G.G., Markham,J.M., Olmsted,J.B., Murphy,D.B. and Johnson,K.A. *Annals of the New York Academy of Sciences*; 1975; **253**; 107-132.

Bradford,M.M. A rapid and sensitive method for the quantitation of microgram quantities of protein utilizing the principle of protein-dye binding: *Analytical Biochemistry*; 1976; **72**; 248-254.

Bre,M.H., Kreis,T.E. and Karsenti,E. Control of microtubule nucleation and stability in Madin-Darby canine kidney cells: The occurence of noncentrosomal stable detyrosinated microtubules: *Journal of Cell Biology*; 1987; **105**; 1283-1296.

Bretscher,A. Thin filament regulatory proteins of smooth and non-muscle cells: *Nature*; 1986; **321**; 726-727.

Brinkley,B.R. Microtubule organizing center: *Annual Review of Cell Biology*; 1985; **1**; 145-172.

Bruce,B., Schrevel,J. and Gros,D. Evulation of the surface of mouse myocardial-cell during ontogenesis 3. quantitative changes of Con-A and WGA receptor sites: *Biology of the Cell*; 1983; **47(3)**; 291-300.

Brunke,K.J., Young,E.E., Buchbind,B.U. and Weeks,D.P. Coordinate regulation of the 4 tubulin genes of *Chlamydomonas-reinhardi*: *Nucleic Acid Research*; 1982; **10(4)**; 1295-1310.

Buckingham,M.E. Actin and myosin multigene families. Their expression during the formation of skeletal muscle: *Essays in Biology*; 1985; **20**; 77-109.

Buehler,G.A. The iris diaphragm model of centriole and basal body formation: *Cell Motility and the Cytoskeleton*; 1990; **17**; 197-213.

Buendia,D., Bre,M.H., Griffiths,G. and Karsenti,E. Cytoskeletal control of centrioles movement during the establishment of polarity in mardin-darby canine kidney cells: *Journal of Cell Biology*; 1990; **110**; 1123-1135.

Bulinski,J.C. and Gundersen,G.G. Stabilization and post-translational modification of microtubules during cellular morphogenesis.: *BioEssays*; 1991; **13(6)**; 285-293.

Burgess,T.L., Skoufias,D.A. and Wilson,L. Disruption of the golgi apparatus with brefeldin A does not destabilize the associated detyrosinated microtubule network: *Cell Motility and the Cytoskeleton*; 1991; **20**; 289-300.

Burgoyne,R.D. Calpactin in exocytosis: *Nature* ; 1988; **331**; 820-822.

Burridge,K. Studies on α-actinin and vinculin: proteins of the adhesion plaque: *Anatomical Record Supplies*; 1983; **1**; 51-65.

Burridge,K., Fath,K., Kelly,T., Nuckolls,G. and Turner,C. Focal adhession: Transmembrane junction between the extracellular matrix and the cytoskeleton: *Annual Review of Cell Biology*; 1988; **4**; 487-525.

Burridge,K. and Fath,K. Focal contacts: Transmembrane links between the extracellular matrix and the cytoskeleton: *BioEssays*; 1989; **10(4)**; 104-108.

Byers,H.R. and Fujiwara,K. Stress fibers in cell *in situ* : immuno-fluorescence visualization with anti-actin, anti-myosin, and anti-alpha-actinin: *Journal of Cell Biology*; 1982; **93**; 804-811.

Campion,D.R. The muscle satellite cell: *International Review of Cytology*; 1984; **87**; 225-251.

Cande,W.Z. Centrosomes: Composition and reproduction: *Current Opinios in Cell Biology*; 1990; **2**; 301-305.

Caplan,A.I., Fiszman,M.Y. and Eppenberger,H.M. Molecular and cell isoforms during development: *Science*; 1983; **221**; 921-927.

Carlier,M.F. Role of nucleotide hydrolysis in the dynamics of actin filaments and microtubules: *International Review of Cytology*; 1989; **115**; 139-170.

Carlson,B.M. and Faulkner,J.A. The regeneration of skeletal muscle fibers following injury: *Medicine and Science in Sports and Exercise*; 1983; **15(3)**; 187-198.

Carraway,K.L. Membranes and microfilaments: Interactions and role in cellular dynemics: *BioEssay*; 1990; **12(2)**; 90-92.

Cartwright,J. and Goldstein,M.A. Microtubules in soleus muscle of the postnatal and adult rat: *Journal of Ultra Research*; 1982; **79(1)**; 74-84.

Casella,J.F., Flanagan,M.D. and Lin,S. Cytochalasin D inhibits actin polymerisation of actin filaments formed during plattelet shape change: *Nature*; 1981; **293**; 302-305.

Celis,J.E., Gesser,B., Small,J.V., Nielsen,S. and Celis,A. Changes in the levels of human tropomyosin IEF52, 55 and 56 do not correlate with the loss of actin cables observed in SV-40 transformed MRC-5 fibroblast: *Protoplasma*; 1986; **38**; 135-146.

Chang,C.M. and Goldman,R.D. The localization of actin-like fibers in cultured neuroblastoma cells as revealed by heavy meromyosin binding: *Journal of Cell Biology*; 1973; **57**; 867-875.

Chapman,E.M. and Scully,R.E. Muscle weakness and Gangrene of fact: *New England Journal of Medicine* ; 1962; **267**; 663-666.

Charles,W.B. Modern Embriology: *Holt Rinehart and Winston Inc.*; 1968; NewYork, Sanfrancisco, Toronto, London.

Chevrier,V., Komesli,S., Schmit,A.C., Vantard,M., Lambert,A.M. and Job,D. A monoclonal antibody, raised against mammalian centrosomes and screened by recognition of plant microtubule organizing centers, identifies a pericentriolar component in different cell types: *Journal of Cell Science*; 1992; **101**; 823-835.

Chicheportiche,Y., Vassali,P., and Tartakoff,A.M. Characterization of cytoplasmically oriented Golgi proteins with a monoclonal antibody: *Journal of Cell Biology*; 1984; **99**; 2200-2210.

Clayton,L., Black,C.M. and Lloyd,C.W. Microtubule nucleating sites in higher plant cells identified by an auto-antibody against pericentriolar material: *Journal of Cell Biology*; 1985; **101**; 319-324.

Cleveland,D.W. Autoregulated control of tubulin synthesis in animal cells: *Current Opinion in Cell Biology*; 1989; **1**; 10-14.

Coleman,T.R., Fishkind,D.J., Mooseker,M.S. and Morrow,J.S. Functional diversity among spectrin isoforms: *Cell Motility and the Cytoskeleton*; 1989; **12**; 225-247.

Connolly,J.A., Kiosses,B.W. and Kalnins,V.I. Centrioles are lost as embryonic myoblasts fuse into myotubes *in vitro*: *European Journal of Cell Biology*; 1985; **39**; 341-345.

Cooke,R. The mechanism of muscle contraction: *CRR Critical Reviews in Biochemistry*; 1986; **21**; 53-118.

Cooper,J.A. Effect of cytochalasin and phalloidin on actin: *Journal of Cell Biology*; 1987; **105**; 1473-1478.

Cooper,H.L., Feuerste,N., Noda,M. and Bassin,R.H. Suppression of tropomyosin synthesis a common biochemical feature of oncogenesis by structurally diverse retroviral oncogenes: *Molecular Cell Biology*; 1985; **5(5)**; 972-983.

Cossette,L.J. and Vincent,M. Expression of a developmentally regulated cross-linking intermediate filament-associated protein (IFAPa-400) during the replacement of vimentin for desmin in muscle cell differentiation: *Journal of Cell Sciences*; 1991; **98**, 251-260.

Cox,J.V., Schenk,E.A. and Olmsted,J.B. Human anticentromere antibodies: Distribution characterization of antigens and effect on microtubule organization: *Cell*; 1983; **35**; 331-339.

Daniels,K. and Sandra,A. Cytoskeletal organization and synthesis in substrate-independent and -dependent myogenesis in chick embryos: *The Anatomical Record*; 1990; **227**; 254-263.

Darnell,J., Lodish,H. and Baltimore,D. Molecular cell biology: *Scientific American Books Inc.* NewYork.; 1990.

Davison,M.D., and Critchley,D.R. a-actinins and the DMD protein contain spectin-like repeats: *Cell*; 1988; **52**; 159-160.

Debec,A. A Drosophila melanogaster cell line lacking centriole: *Biology of the Cell*; 1982; **44**; 133-138.

DeBrabander,M., Geuens,G., DeMey,J. and Joniau,M. In microtubules and microtubule inhibitors (Eds. DeBrabander,M. and DeMay,J.): *Elsevies*, Amsterdam; 1980.

Dinsmore,J.H. and Sloboda,R.D. Microenjection of antibodies to a 62kD mitotic apparatus protein arrests mitosis in dividing sea-urchin embryos: *Cell*; 1989; **57(1)**; 127-134.

Dirksen,E.R. and Crocker,T.T. Centriole replication in differentiating ciliated cells of mammalian respiratory epithelium: *Journal de Microscopie*; 1965; **5**; 629-637.

Dowben,R.M. Cell biology: *Harper and Row, Publishers* , NewYork, Evanston, San Francisco, London; 1971.

Dowrick,P.G. and Warn,R.M. The cellular responce to factors which induce motility in mammalian cells: *Cell Motility Factors*; ed. by Goldberg,I.D., Birkhäuser Verlag Basel/Switzerland; 1991; 89-108.

Dustin,P. Microtubules: *Springer-Verlag*, Berlin, Heidelberg and New York; 1978.

Dustin,P. Microtubules: 2.Ed. *Springer-Verlag*, NewYork; 1984.

Earnshaw,W.C., Halligan,N., Cooke,C. and Rothfield,N. The kinetochore is part of the methaphase chromosome scaffold: *Journal of Cell Biology*; 1984; **98**; 352-357.

Eberhardt,M.E., Flamme,I., Kurer,V. and Eppenberger,H.M. Reexpression of alpha-smooth muscle actin isoform in cultured adult rat cardiomyocytes: *Developmental Biology*; 1990; **139**; 269-278.

Egelman,E.H. The structure of the actin thin filament: *Journal of Muscle Research and Cell Motility*; 1985; 6; 129-151.

Eichenlaub-Ritter,U. and Tucker,J.B. Microtubules with more than 13 protofilaments in the dividing nuclei of ciliates: *Nature*; 1984; **307**; 60-62.

Eipper,B. Prufication of rat-brain tubulin: *Transactions of the New York Academy of Science*; 1974; **36(6)**; 596-603.

Erickson,H.P. and Pantaloni,D. The role of subunit entropy in cooperative assembly, nucleation of microtubules and other two-dimensional polymers: *Biophysics*; 1981; **34**; 297-309.

Evans,L., Mitchison,T. and Kirschner,M. Influence of the structure of nucleated microtubules: *Journal of Cell Biology*; 1985; **100**; 1185-1191.

Fattoum,A., Hartwig,J.H. and Stossel,T.P. Isolation and some structural and functional-properties of macrophage tropomyosin: *Biochemistry*; 1983; **22(5)**; 1187-1193.

Faulstich,H, Trischmann,H. and Mayer,D. Preparation of tetramethylrhodaminyl-phalloidin and uptake of the toxin into short term cultured hepatocytes by endocytosis: *Experimental Cell Research*; 1983; **144**; 73-82.

Feldman,J.L., and Stockdale,F.E. Skeletal muscle satellite cell diversity: Satellite cells form fibres of different types in cell culture: *Developmental Biology*; 1991; **143**; 320-334.

Feramisco,J.R., Gross,M., Kamata,T., Rosenberg,M. and Sweet,R.W. Microinjection of the oncogene form of the human H-ras (T-24) protein results in rapid proliferation of quiescent cells: *Cell*; 1984; **38(1)**; 109-117.

Field,D.J., Collins,R.A. and Lee,J.C. Heterogenity of vertebrate brain tubulins.: *Proceeding of the National Academy of Sciences USA*; 1984; **81**; 4041-4045.

Fine,R.E. and Taylor,L. Decreased actin and tubulin synthesis in 3T3 cells after transformation by SV40 vius: *Experimental Cell Research* ; 1976; **102(1)**; 162-168.

Fisher,G.W., Conrad,P.A., DeBiasio,R.L. and Taylor,D.L. Centripetal transport of cytoplasm, actin and the cell surface in lamellipodia of fibroblasts: *Cell Motility and the Cytoskeleton*; 1988; **11**; 235-247.

Frash,M., Glower,DM. and Saumwebe,H. Nuclear antigens follow different patways into daughter nuclei: during mitosis in early *Drosophyla* embryos: *Journal of Cell Biology*; 1986; **82**; 155-172.

Friederich,E., Pringault,E., Arpin,M. and Louvard,D. From the structure to the function of villin, an actin-binding protein of the brush border: *BioEssay*; 1990; **12**; 403-408.

Fujii,T., Imai,M., Rosenfeld,G.C. and Bryan,J. Domain mapping of chicken gizzard caldesmon: *Journal of Biological Chemistry;* 1987; **112**; 2757-2763.

Furst,D.O., Osborn,M., Nave,R. and Weber,K. The organization of titin filaments in the half-sarcomere revealed by monoclonal antibodies in

immunoelectron microscopy: A map of ten nonrepetitive epitopes starting at the Z line extends close to the M line: *Journal of Cell Biology*; 1988; **106**; 1563-1572.

Gallagher,B.C. Primary cilia of the corneal endothelium.: *American Journal of Anatomy*; 1980; **159**; 475-484.

Gard,D.L. and Kirschner,M.W. A polymer-dependent increase in phosphorylation of β-tubulin accompanies differentiation of a mouse neuroblastoma cell line: *Journal of Cell Biology*; 1985; **100**; 764-774.

Gard,D.L. and Lazarides,E. The synthesis and distribution of desmin and vimentin during myogenesis *in vitro*: *Cell*; 1980; **19**; 263-275.

Geiger,B. A 130 K protein from chicken gizzard: its localization at the termini of microfilament bundles in cultured chicken cells: *Cell*; 1979; **18**; 193-205.

Geiger,B. Cytoskeleton-associated cell contacts: *Current Opinion Cell Biology*; 1989; **1**; 103-109.

Gerald,K., and Berrill,N.C. Development. Second Ed.: *McGraw-Hill Book Com.*; 1981; NewYork, St. Luis, London, Madrit, Sydney, Tokyo, Toronto.

Gething,M.J., McCammon,K. and Sambrook,J. Expression of wild-type and mutant forms of influenza hemagglutinin-the role of folding in intracellular-transport: *Cell*; 1986; **46(6)**; 939-950.

Gibbons,I.R. Dynein ATPases as microtubule motors.: *Journal of Biological Chemistry*; 1988; **263**; 15837-15840.

Glenney,J.R. Calpactins-calcium-regulated membrane skeletal proteins: *Biochemical Society Transactions* ; 1987; **15(5)**; 798-800.

Goedert,M., Spillantini,M.G., Potier,M.C., Ulrich,J. and Crowther,R.A. Cloning and sequencing of the cDNA encoding an isoform of microtubule-associated protein tau containing four tandem repeats: Differential expression of tau protein mRNAs in human brain.: *EMBO Journal*; 1989; **8**; 393-399.

Goldberg,G.A., Marmer,B.L., Grant,G.A., Eisen,A.Z., Wilhelm,S. and He,C.S. Human 72-kilodalton type IV collagenase forms a complex with a tissue inhibitor of metalloproteases diagnated: *Proceeding of National Academy of the Sciences of the U.S.A.*; 1989; **86(21)**; 8207-8211.

Goldman,R.D. The use of heavy meromyosin binding as an ultrastructural cytochemical method for localizing and determining the possible functions of actin-like microfilaments in non-muscle cells: *Journal of Histochemistry and Cytochemistry*; 1975; **23**; 529-535.

Goldschmidt-Clermont,P., Kim,J.W., Machesky,L.M., Rhee,S.G. and Pollard,T.D. Regulation of phospholipase C-γ 1 by profilin and tyrosine phosphorylation: *Science*; 1991; **251**; 1231-1233.

Golstein,J.L., Anderson,R.G.W. and Brown,M.S. Coated pits, coated vesicles, and receptor-mediated endocytosis: *Nature*; 1979; **279**; 679-685.

Goodman,S.R. and Shiffer,K. The spectrin membrane skeleton of normal and abnormal human erytrocytes: *American Journal of Phychology* ; 1983; **244**; c121-141.

Gospodarowicz,D.J., Weseman,J., Moran,J.S. and Linastrom,J. Effect of fibroblast growth factor on the division and fusion of bovine myoblasts: *Journal of Cell Biology*; 1976; **70**; 394-405.

Gossett,L.L., Zhang,W., and Olson,E.N. Dexamethasone-dependent inhibition of differentiation of C2 myoblasts bearing steroid-inducible N-ras oncogenes: *Journal of Cell Biology*; 1988; **106**; 2127-2137.

Gould,R.P. The basal bodies of Chlamydomonas reinharti: Formation from probasal bodies isolation and partial characterization: *Journal of Cell Biology*; 1975; **65**; 65-74.

Gould,R.P. and Borisy,G.G. The pricentriolar material in chinese hamster ovary cells nucleates microtubule formation: *Journal of Cell Biology*; 1977; **73**; 601-615.

Grant,P., and Tseng,Y. Embryonic and regenerating Xenopus retinal fibres are instrinsically different: *Developmental Biology*; 1986; **114**; 475-491.

Gray. Grays anatomy. Ed. Williams,P.L., Warrich,R., Dyson,M. and Bannister,LH. *Churchill Livingstone*. London; 1989.

Guldner,H.H., LaKonsek,H.J. and Bautz,F.A. Human anticentromere sera recognize a 19.5 Kd nonhistone chromosomal protein from HeLa cells: *Clinical and Experimental Immunology*; 1984; **58**; 13-20.

Gundersen,G.G. and Bulinski,J.C. Distribution of tyrosinated and nontyrosinated alpha-tubulin during mitosis: *Journal of Cell Biology*; 1986; **102(3)**; 1118-1126.

Gundersen,G.G., Kalnoski,M.H. and Bulinski,J.C. Distine populations of microtubules: Tyrosined and non tyrosined alpha-tubulin distributed differently in vitro.: *Cell*; 1984; **38**; 779-789.

Gundersen,G.G., Khawaja,S. and Bulinski,J.C. Effects of microtubule antagonists on the distribution of tyrosinated and nontyrosinated tubulin *in vivo*: *Cell Motility*; 1986; **6(2)**; 224-230.

Gundersen,G.G., Khawaja,S. and Bulinski,J.C. Generation of a stable posttranslationally modified microtubule array is in early event in myogenic differentiation.: *Journal of Cell Biology*; 1989; **109**; 2275-2288.

Gurdon,J.B. Egg cytoplasm and gene control in development: *Proceedings of the Royal Society B*; 1977; **198**; 211-247.

Gurdon,J.B. From egg to embryo: The initiation of cell differentiation in Amphibia: *Proceedings of the Royal Society B.*; 1989; **237**; 11-25.

Hagag,N., Diamond,L., Palermot,R. and Lyubsky,S. High expression of *ras* p21 correlates with increased rate of abnormal mitosis in NIH3T3 cells: *Oncogene*; 1990; **5**; 1481-1489.

Hanson,J. and Huxley,H.E. Structural basis of the cross-striations in muscle: *Nature*; 1953; **172**; 530-532.

Harris,A.K., Stopac D. and Wild,P. Fibroblast traction as a mechanism for collagen morphogenesis: *Nature*; 1981; **290**; 249-251.

Hauser,M. Taxol affects both the microtubular arrays of heliozoan axonemes and their microtubule-organizing center: *European Journal of Cell Biology*; 1986; **42**; 295-304.

Heath,J.P. and Holifield,B.F. Cell locomotion: New research test old ideas on membrane and cytoskeletal flow: *Cell Motility and the Cytoskeleton*; 1991; **18**; 245-257.

Hendricks,M. and Weintraub,F. Multiple tropomyosin polypeptides in chicken-embryo fibroblasts, differential repression of transcription by rous-sarcoma virus transformation: *Molecular Cell Biology*; 1984; **4(9)**; 1823-1833.

Hinterberger,T.J. and Barald,K.F. Fusion between myoblasts and adult muscle fibers promotes remodeling of fibers into myotubes in vitro: *Developmental Biology*; 1990; **109**; 139-148.

Hiraoka,L. Golden,W. and Magnuson,T. Spindle pole organization during early mouse development: *Developmental Biology*; 1989; **133(1)**: 24-36.

Hirokawa,N., Shiomura,Y. and Okabes,S. Tau proteins-the molecular-structure and mode of binding on microtubules: *Journal of Cell Biology* ; 1988; **107(4)**; 1449-1459.

Hollenbeck,P.J. The transport and assembly of the axonal cytoskeleton: *Journal of Cell Biology*; 1989; **108(2)**; 223-227.

Holtzer,H., Schaudies,S., Dlugosz,A., Antin,P. and Dupyac,G. Interactions between IFs, microtubules, and myofibrils in fibrogenic and miyogenic cells: *Annual NewYork Academy Sciences*; 1985; **455**; 106-125.

Horridge,G.A. Macrocilia with numerous shafts from the lips of the ctenophore Beroe: *Proceedings Royal Society (London), Ser.B.*; 1965; **162**; 351-359.

Hynes,R.O. Integrins: A family of cell surface receptors: *Cell*; 1987; **48**; 549-554.

Izzard,C.S. A precursor of the focal contact in cultured fibroblasts: *Cell Motility and the Cytoskeleton*; 1988; **10**; 137-142.

Jensen,C.G., Davison,E.A., Bowser,S.S. and Rieder,C.L. Primary cilia cycle in PtK1 cells: Effects of colcemid and taxol on cilia formation and resorpsion: *Cell Motility and the Cytoskeleton*; 1987; **7**; 187-197.

Johnson,U.G. and Porte,K.R. Fine structure of cell division in *Chlamydomonas reinhardi*. Basal bodies and microtubules: *Journal of Cell Biology*; 1968; **38**; 403-425.

Joshi,H.C., Palacios,M.J., McNamara,L. and Cleveland,D.V. Gamma-tubulin is a centrosomal protein required for cell cycle-dependent microtubule nucleation: *Nature*; 1992; **356**; 80-82.

Kalderon,N. and Gilula,N.B. Membrane events involved in myoblast fusion: *Journal of Cell Biology*; 1979; **181**; 411-425.

Kano,Y., Fujimaki,N. and Ishikawa,H. The distribution and arrangement of microtubules in mammalian skeletal muscle fibers: *Cell Structure and Function*; 1991; **16**; 251-261.

Karsenti,E., Kobayashi,S., Mitchison,T. and Kirschner,M. Role of the centrosome in organizing the interphase microtubule array: Properties of cytoplasts containing or lacking centrosomes: *Journal of Cell Biology*; 1984; **98**; 1763-1776.

Karsenti,E. and Maro,B. Centrosomes and the spatial distribution of microtubules in animal cells: *Trends in Biochemical Sciences*; 1986; **11**; 460-466.

Katz,B. Terminations of afferent nerve fibre in muscle sipindle of frog: *Philosophical Transastion of the Royal Society of London B Biological Sciences*; 1961; **243**; 221-229.

Kilmartin,J.V., Wright,B. and Milstein,C. Rat monoclonal antitubulin antibodies derived by using a new nonsecreting rat cell line: *Journal of Cell Biology*; 1982; **93**; 576-582.

Kim,H., Binder,L.I. and Rosenbaum,J.L. The periodic association of MAP 2 with brain microtubules *in vitro*: *Journal of Cell Biology*; 1979; **80**; 266-276.

Kirschner,P. Microtubule assembly and nucleation: *International Review of Cytology*; 1978; **54**; 1-71.

Knudsen,K.A. and Horwitz,A.F. Tandem events in myoblast fusion; *Developmental Biology*; 1977; **58**; 328-338.

Kobayashi,R. and Tashima,Y. Filamin and vinculin expressions during avian myogenesis *in vitro*: *Biomedical Research*; 1989; 10(4); 307-313.

Komesli,S., Tournier,F., Paintrand,M., Margolis,R.L., Job,D. and Bornens,M. Mass isolation of calf tymus centrosomes-identification of a specific configuration: *Journal of Cell Biology*; 1989; **109(6)**; 2869-2878.

Kreis,T.E. Microtubules containing detyrosinated tubulin are less dynamic: *EMBO Journal*; 1987; **6(9)**; 2597-2606.

Kreis,T.E. Role of microtubules in the organization of the Golgi apparatus: *Cell Motility and Cytoskeleton*; 1990; **15**; 67-70.

Kreis,T.E., Lanz,J. and Birchmeier,W. Stress fiber sarcomeres of fibroblasts are contractile: *Cell*; 1980; **22**; 555-561.

Kuang,J., Zhao,J.V., Wright,D.A., Saunders,G.F. and Rao,P.N. Mitosis-specific monoclonal-antibody MPM-2 inhibits xenopus oocyte maturation and depletes maturation promoting activity: *Proceedings of the National Academy of Sciences USA*; 1989; **86(13)**; 4982-4986.

Kumar,N. and Flovin,M. Preferential action of a brain detyrosilating carbocypeptidase on polymerized tubulin: *Journal of Biological Chemistry*; 1981; **256**; 7678-7686.

Kunimoto,M., Otto,E. and Bennett,V. A new 440 kD isoform is the major Ankyrin in neonatal rat-brain: *Journal of Cell Biology*; 1991; **115(5)**; 1319-1331.

Kuriyama,R. and Borisy,G.G. Identification of molecular-components of the centrosphere in the mitotic spindle of sea-urchin eggs: *Journal of Cell Biology*; 1985; **111(2)**; 524-530.

Leifer,D., Lipton,S., Barnstable,C.J. and Masland,R.H. Monoclonal antibody to Thy-1 enhances regeneration of processes by rat retina ganglion cells in culture: *Science*; 1984; **224**; 303-306.

Lewis,J. and Wolpert,L. Diploidy, evulation and sex: *Journal of Theoretical Biology*; 1979; **78**; 425-438.

Lewis,S.A., Wang,D. and Cowan,N.J. Microtubule-associated protein MAP 2 shares a microtubule binding motif with tau protein: *Science*; 1988; **242**; 936-939.

L'Hernault,S.W. and Rosenbaum,J.L. Reversal of the post-translational modification on Clamydomonas flagellar alpha-tubulin occur during flagellar resorption: *Journal of Cell Biology*; 1985; **100**; 457-462.

Lin,J.C. and Lin,J.L. Assembly of different isoforms of actin and tropomyosin into the skeletal tropomyosin-enriched microfilaments during differentiation of muscle cells *in vitro*: *Journal of Cell Biology*; 1986; **103**; 2173-2183.

Lin,Z., Eshelman,J.R., Schaudies,S.F., Duran,S., Lessard,J.L., and Holtzer,H. Sequential disassembly of myofibrils induced by myritate acetate in cultured myotubes: *Journal of Cell Biology*; 1987; **105**; 1365-1376.

Lin,Z., Eshleman,J., Grund,C., Fischman,D.A., Masaki,T., Franke,W.W. and Holtzer,H. Differential response of myofibrillar and cytoskeletal proteins in cells treated with phorbol myristate acetate: *Journal of Cell Biology*; 1989; **108**; 1079-1091.

Linkhart,T.A., Clegg,C.H. and Hauschka,S.D. Myogenic differentiation in permanent clonal mouse myoblast cell-lines-regulation by macromolecular growth-factors in the culture medium: *Developmental Biology*; 1981; **86**; 19-30.

Linse,K. and Mandelkow,E.M. The GTP-binding peptide of beta-tubulin: *Journal of Biological Chemistry*; 1988; **263**; 15205-15210.

Linstead,P., Jennings,B., Prescott,A., Hawley,P., Warn,R. and Gibson, I. Scanning electron microscopy and the transformed phenotype: *Micron*; 1988; **19(3)**; 155-162.

Lis,H. and Sharon,N. Lectins as molecules and tools: *Annual Review of Biochemistry*; 1986; **55**; 35-67.

Liu,H. and Bretscher,A. Distruption of the single tropomyosin gene in yeast results in the disappearance of actin cables from the cytoskeleton: *Cell*; 1989; **57**; 233-242.

Lloyd,C.W. and Seagull,R.W. A new spring for plant cell biology: microtubules as dynemic helixes: *Trends in Biochemical Sciences*; 1985; **10**; 476-478.

Lu,R.C. and Elzinga,M. Primary structure of tubulin sequences of carboxyl terminus and 7 other cyanogen-bromide peptides from a-chain: *Biochimica et Biophysica Acta*; 1978; **537(2)**; 320-328.

Lucocq,J.M., Berger,E.M. and Werren,G. Mitotic Golgi fragments in HeLa cells in their role in the reassembly pathway: *Journal of Cell Biology*; 1989; **109**; 463-474.

Maccioni,R.B., Serrano,L., Avila,J. and Cann,J.R. Characterization and structural aspects of the enhanced assembly of tubulin after removal of its carboxyl terminal domain: *European journal of Biochemistry*; 1986; **156**; 375-381.

Manfredi,J.J., Parness,J. and Horwitz,S.B. Taxol binds to cellular microtubules: *Journal of Cell Biology*; 1982; **94(3)**; 688-696.

Maniotis,G. and Schliwa,M. Microsurgical removal of centrosomes blocks cell reproduction and centriole generation in BSC-1 cells: *Cell*; 1991; **67**; 495-504.

Margolis,R.L. and Rauch,C.T. Characterization of rat brain crude extract microtubule assembly: Correlation of cold stability with the phosphorylation state of a microtubule-associated 64 K protein: *Biochemistry*; 1981; **20**; 4451-4458.

Maro,B. and Bornens,M. The centriole-nucleus association-effects of cytochalasin-B and nocodazole: *Biologie Cellulaire*; 1981; **39(3)**; 287-290.

Maruyama,K. Connectin, an elastic filamentous protein of striated muscle: *International Review of Cytology* ; 1986; **104**; 81-114.

Massague,J., Cheifetz,T.S., Endo,T. and Nadal-Ginard,B. Taype β transforming growth factor is an inhibitor of myogenic differentiation: *Proceeding National Academy of Sciences U.S.A.*; 1986; **83**; 8206-8210.

Matsumura,F., Yamashir,S. and Lin,J.J.C. Isolation and characterization of tropomyosin-containing microfilaments from cultured cell: *Journal of Biological Chemistry*; 1983; **258(10)**; 6636-6644.

Mauro,A., and Adams,W.R. Structure of sarcolemma of frog skeletal muscle fibre: *Journal of Biophysical and Biochemical Cytology*; 1961; **10**; 177-183.

McIntosh,A.A.G. Further-studies on the extinsion of cytosol macromolecules by cultured chick embryo fibroblasts: *International Journal of Biochemistry*; 1985; **61(3)**; 307-397.

McNiven,M.A. and Porter,K.R. Organization of microtubules in centrosome-free cytoplasm: *Journal of Cell Biology*; 1988; **106**; 1593-1604.

Mitchison,T. and Kirschner,M. Microtubule assembly nucleated by isolated centrosomes: *Nature*; 1984; **312**; 232-237.

Mitchison,T., Evans,L., Schulze,E. and Kirschner,M. Sites of microtubule assembly and disassembly in the mitotic spindle: *Cell*; 1986; **45**; 515-527.

Moestrup,O. Flagellar structure in algae: 1982; *Phycological Review 7. Phycologia*; **21**; 427-528.

Mogensen,M.M. and Tucker,J.B. Evidence for microtubule nucleation at plasma membrane-associate sites in *Drosophila*: *Journal of Cell Sciences*; 1987; **88**; 95-107.

Mogensen,M.M., Tucker,J.B. and Stebbings,H. Microtubule polarities indicate that nucleation and capture of microtubules occurs at cell-surfaces in *Drosophila*: *Journal of Cell Biology*; 1989; **108(1)**; 1445-1452.

Moon,R.T. and McMahon,A.P. Composition and expression of spectrin-based membrane skeletons in non-erythroid cells: *BioEssays*; 1987; **7**; 159-164.

Mori,Y., Akedo,H., Tanigaki,Y., Tanaka,K. and Okada,M. Ciliogenesis in tissue-cultured cells by the increased density of cell population: *Experimental Cell Research*; 1979; **120**; 435-439.

Moudjou,M., Paintrand,M., Vigues,B. and Bornens,M. A human centrosomal protein is immunologically related to basal body-associated protein from lower eucaryotes and is involved in the nucleation of microtubules: *Journal of Cell Biology*; 1991; **115**; 129-140.

Muntz,L. Cellular and biochemical aspects of muscle differentiation: *Comperative Biochemistry and Physiology*; 1990; **97(B)**; 215-225.

Muroya,K., Hattori,S. and Nakamura,S. Nerve growth factor induces rapid accumulation of the GTP-bound form of p21 ras in rat pheochromocytoma PC12 cells: *Oncogene*; 1992; **7**; 277-281.

Murphy,D.B., Johnson,K.A. and Borisy,G.G. Role of tubulin-associated proteins in microtubule nucleation and elongation: Journal of Molecular Biology; 1977; 177; 33-52.

Murphy,D.B. and Wallis,K.T. Erytrocyte microtubule assembly *in vitro* - tubulin oligomers limit the rate of microtubule self-assembly: *Journal of Biological Chemistry*; 1986; **261(5)**; 2319-2324.

Nathanson,M.A. Transdifferentiation of skeletal muscle into cartilage: Transformation of differentiation: *Current Topics in Developmental Biology*; 1986; **20**; 39-62.

Nathanson,M.A. Differentiation of musculoskeletal tissues: *International Review of Cytology*; 1988; **116**; 89-164.

Neff,N.F., Thomas,J.H., Grisati,P. and Botstein,D. Isolation of the β-tubulin gene from yeast and demonstration of its essential function *in vitro*: *Cell*; 1983; **23**; 211-219.

Nenci,I. and Marchetti,E. Concerning the localization of steroids in the centrioles and basal bodies by immunofluorescence: *Journal of Cell Biology*; 1978; **76**; 255-260.

Nishikai,M., Okand,O., Yamashita,H. and Watanabe,M. Characterization of centromere (kinetochore) antigen reactive with sera of patients with a scleroderma variant (CREST syndrome): *Annals of the Rheumatic Diseases*; 1984; **43**; 819-824.

Novikoff,A.B. and Holtzman,E. The cell: *Holt, Rinehart and Winston, Inc.* London, NewYork, Sydney, Toronto.; 1970.

Oakley,C.E. and Oakley,B.R. Identification of gamma-tubulin, a new member of the superfamily encoded by mipA gene of Aspergillus nidulans: *Nature*; 1989; **338**; 662-664.

Ohta,K., Toriyama,M., Endo,S. and Sakai,H. Localization of mitotic-apparatus-associated 51-kD protein in unfertilized and fertilized sea urchin eggs: *Cell Motility and the Cytoskeleton*; 1988; **10**; 496-505.

Olmsted,J.B. Microtubule-associated proteins: *Annual Review of Cell*; 1986; **2**; 4221-4257.

Olmsted,J.B. and Borisy,G.G. Ionic and nucleotide requirements for microtubule polymerization *in vitro*: *Biochemistry*; 1975; **14**; 3996-4004.

Olson,E.N., and Capetanaki,Y.G. Developmental regulation of intermediate filament and actin mRNAs during myogenesis is distrupted by oncogenic ras genes: *Gene*; 1989; **4**; 907-913.

Olson,E.N., Spizz,G., and Tainsky,M.A. The oncogenic forms of N-ras or H-ras prevent skeletal myoblast differentiation: *Molecular and Cellular Biology*; 1987; **7(6)**; 2104-2111.

Olson,E.N., Stenberg,E., Hu,S., Spizz,G. and Wilcox,C. Regulation of myogenic differentiation by type beta transforming growth factor: *Journal of Cell Biology*; 1986; **103**; 1799-1805.

Osborn,M. and Weber,K. Dimethyl sulfoxide and the ionophore A23187 affect the arrangement of actin and induce nuclear actin paracrystals in PtK2-cells: *Experimental Cell Research*; 1980; **129(1)**; 103-114.

Otey,O.A., Kalnosky,M.H. and Bulinsky,J.C. Immunolocalization of muscle and nonmuscle isoforms of actin in myogenic cells and adult skeletal muscle: *Cell Motility and the Cytoskeleton*; 1988; **9**; 337-348.

Pantel,J. and De Sinety,R. Les cellular de lignee male chez le Notonecta glauca L. avec des details plus etendus sur la periode d'accroissement et sur celle de transformation: *Cellule*; 1906; **23**; 87-93.

Paper,D.A. and Brinkley,B.R. Microtubule initiation at kinetochores and centrosomes in lysed mitotic cells: Inhibition of site specific nucleation by tubulin antibody: *Journal of Cell Biology*; 1979; **82**; 585-591.

Pardo,J.V., Pittenger,M.F. and Craig,S.W. Subcellular sorting of isoactins: Selective association of gamma actin with skeletal muscle mitochondria: *Cell*; 1983; **32**; 1093-1103.

Parysek,L.M., Wolosewick,J.J. and Olmsted,J.B. MAP4: A microtubule-associated protein specific for a subset of tissue microtubules: *Journal of Cell Biology*; 1984; **99**; 2287-2296.

Pasternak,J., Karel,F. and Oswald,J. Surface and volume excitation energy-transfer and recombination processes in ALN-MN: *Journal of Luminescence*; 1979; **18(9)**; 805-808.

Pavlath,G.K., Rich,K., Webster,S.G. and Blan,H.M. Localization of muscle gene-products in nuclear domains: *Nature*; 1989; **337(6207)**; 570-573.

Penman,S., Fulton,A., Capco,D., Ben,Z.A., Wittelsberger,S. and Tse, C.F. Cytoplasmic and nuclear architecture in cells and tissue: Form, functions and mode of assembly: *Cold spring Harbor symposia on Quantitative Biology*; 1982; **46(2)**; 1013-1027.

Phillips,D.M. Substructure of flagellar tubules: *Journal of Cell Biology*; 1966; **31**; 635-642.

Piperno,G., Dizet,M.L. and Chang,X.J. Microtubules containing acetylated alpha-tubulin in mammalian cell in culture: *Journal of Cell Biology*; 1987; **104**; 289-302.

Pollack,R. Osborn,M. and weber,K. Patterns of organization of actin and myosin in normal and transformed cultured cells: *Proceeding of National Acadamy of the Sciences of the U.S.A.*; 1975; **72(3)**; 994-998.

Pollard,T.D. and Cooper,J.A. Actin and actin-binding proteins. A critical evulation of mechanisms and functions: *Annual Review in Biochemistry*; 1986; **55**; 987-1035.

Ponstingl,H., Krauhs,E., Little,M. and Kempf,T. Complete amino acid sequence of a-tubulin from porcine brain: *Proceeding of the National Academy of Sciences USA*; 1981; **78**; 2757-2761.

Ponstingl,H., Weber,R. and Krauhs,E. Linkage of amino-acid exchanges and establishement of a disulfide bridge in b-tubulin by reversed phase peptide-mapping: *Biology of the Cell*; 1982; **45(S1)**; 259.

Prensier,G., Vivier,E., Goldstein,S. and Schrevel,J. Motile flagellum a "3+0" ultrastructure: *Science*; 1980; **207**; 1493-1494.

Prescott,A.R., Vestberg,M. and Warn,R.M. Microtubules rich in modified alpha-tubulin characterize the tail processes of motilite fibroblasts: *Journal of Cell Science*; 1989; **94**; 227-236.

Prescott, A.R., Webb, S.F., Rawlins, D., Shaw, R.J. and Warn, R.M. Microtubules rich in post translationally modified alpha-tubulin form distinct arrays in frog lens epithelial cells: *Experimental Eye Research*; 1991; **52**; 743-753.

Prescott, A.R., Dowrick, P.G. and Warn, R.M. Stable and slow-turning-over microtubules characterize the processes of motile epithelial cells treated with scatter factor: *Journal of Cell Science*; 1992; **102**; 103-112.

Preston, T.M., King, C.A. and Hyams, J.S. The cytoskeleton and cell motility: *Blackie and Son Ltd.* NewYork; 1990.

Quinn, L.S., Ong, L.D. and Roeder, A.R. Paracrine control of myoblast proloferation and differentiation by fibroblast: *Developmental Biology*; 1990; **140**; 8-19.

Raff, E.C. Genetics of microtubule systems: *Journal of Cell Biology*; 1984; **99**; 1-10.

Rahilly, M.A. and Fleming, S. A tumor promoter induces alterations in vinculin and actin distribution in human renal epithelium: *Journal of Pathology*; 1992; **166**; 283-288.

Rao, J.Y., Hurst, R.E., Bales, W.D., Jones, P.L., Bass, R.A., Archer, P.B., Bell, P.B. and Hemstreet, G.P. Cellular F-actin levels as a marker for cellular transformation: relationship to cell division and differentiation: *Cancer Research*; 1990; **50**; 2215-2220.

Rao, P.N., Zhao, H.Y., Ganju, R.K. and Ashorn, C.L. Monoclonal antibody against the centrosome: *Journal of Cell Sciences*; 1989; **93**; 63-69.

Rappaport, L. and Samuel, J.L. Microtubules in cardiac myocytes: *International Review of Cytology*; 1988; **113**; 101-143.

Rash, J.E., Shay, J.W. and Biesele, J.J. Cilia in cardiac differentiation: *Journal of Ultrastructure Research*; 1969; **29**; 470-484.

Rathke, P.C., Osborn, M. and Weber, K. Immunological and ultrastructural characterization of microfilament bundles: Polygonal nets and stress fibers in an established cell line: *European Journal of Cell Biology*; 1979; **19**; 40-48.

Reaven, E.P., and Reaven, G.M. Evidence that microtubules play a permissive role in hepatocyte very low density lipoprotein secretion: *Journal of Cell Biology*; 1980; **84**; 28-39.

Rieder, C.L. Ribonucleoprotein staining of centrioles and kinetochores in new lung cell spinales: *Journal of Cell Biology*; 1979; **80**; 1-9.

Roach, A., Bane, S. and Luduena, R.F. The effects of colchicine analogs on the reaction of tubulun with iodic-14-acetamine and N-N'-ethylenebis ((iodoacetamide): *Journal of Biological Chemistry*; 1985; **260(5)**; 3015-3023.

Robinson, L. and Engelborghs, H. Fluorescence stopped flow study of the binding of S6-GTP to tubulin-colchicine and microtubule protein: *Biology of the Cell*; 1982; **45(S1)**; 259.

Rogalski, A.A. and Singer, S.J. Associations of elements of the Golgi apparatus with microtubules: *Journal of Cell Biology*; 1984; **99**; 1092-1100.

Rossman, M.D., Maida, B.T. and Douglas, S.D. Monocyte-derived macrophage and alveolar macrophage fibronectin production and cathepsin-D activity: *Cellular Immunology*; 1990; **126(2)**; 268-277.

Rothman, J.E. The golgi-apparatus-2 organalles in tendem: *Science*; 1981; **213(4513)**; 1212-1219.

Rowinsky, E.K., Cazenave, L.A. and Donehower, R.C. Taxol: A novel investigational antimicrotubule agent: Journal of the National Cancer Institute; 1990; 82; 1247-1259.

Rubenstein, P.A. The functional importance of multible action isoforms: *BioEssay*; 1990; **12(7)**; 309-315.

Sanchez, F., Natzle, J.E., Cleveland, D.W., Kirschner, M.W. and McCarthy, B.J. A dispersed multigene family encoding tubulin in *Drosophila melanogaster*: *Cell*; 1980; **22**; 845-854.

Sanderson, P.D., Fitch, J.M., Linsenmayer, T.R. and Mayne, R. Fibroblast promote the formation of a continuous basal lamina during myogenesis *in vitro*: *Journal of Cell Biology*; 1986; **102**; 740-747.

Sanger, J.W. Changing patterns of actin localization during cell division: *Proceedings of the National Academy of Sciences USA*; 1975; **72**; 1913-1916.

Sanger, J.W., Gwinn, J. and Sanger, J.M. Dissolution of cytoplasmic actin bundles by dimethyl-sulfoxide: *Journal of Experimental Zoology*; 1980; **213(2)**; 227-230.

Sanger, J.M., Mittal, B., Pochapin, M. and Sanger, J.W. Observation of microfilament bundles in living cell microinjection with fluorescently labelled contractile proteins: *Journal of Cellular Biochemistry Supplement*; 1986; **5** 17-44.

Sanger, J.M., Mittal, B., Wagner, A., Jockunsch, B.M. and Sanger, J.W. Differentiatial response of stress fiber and myofibrils to gelsolin: *European Journal of Cell Biology*; 1987; **43**; 421-428.

Sanger, J.W. The use of cytochalasin B to distinguish myoblasts from fibroblasts in cultures of developing chick striated muscle: *Proceedings of the National Academy of Sciences USA*; 1974; **71**; 3621-3625.

Sawin, K. and Mitchson, T. Motoring in the spindle: *Nature*; 1990; **345**; 22-23.

Sawyer, J.T. and Akenson, R.A. Clonal myoblast and myotubes show differences in lectin-binding patterns: *Experimental Cell Research*; 1983; **145(1)**; 1-13.

Schaper, J., Hein, S., Brand, T., and Schaper, W. Contractile proteins and the cytoskeleton in isolated rat myocytes: *Journal of Applied Cardiology*; 1989; **4**; 423-429.

Schatten,G., Simerly,C. and Schatten,H. Microtubule configurations during fertiliation mitosis and early development in the mouse and the requirement for egg microtubule-mediate motility during mammalian fertilization: *Proceedings of the National Academy of the Sciences USA*; 1985; **82**; 4152-4156.

Schatten,H., Schatten,G., Mazaia,D., Balczon,R. and Simerl,C. Behavior of centrosomes during fertilization and cell division in mouse oocytes and in sea urchin eggs: *Proceedings of the National Academy of Sciences USA*; 1986; **83**; 105-109.

Schliwa,M. The cytoskeleton: An introductory survey. In cell biology monographs: *Springer/Verlag, NewYork Inc.* NewYork; 1986.

Schliwa,M. Head and tail: *Cell*; 1989; **56**; 719-720.

Schroer,T.A., Schnapp,B.B.J., Reese,T.S. and Sheetz,M.P. The rule of kinesin and other solube factors in organalle movement along microtubules: *Journal of Cell Biology*; 1988; **107**; 1785-1792.

Schroeder, H.C., Wehland,J. and Weber,K. Purification of brain tubulin-tyrosine ligase by biochemical and immunological methods: *Journal of Cell Biology*; 1985; **100**; 276-281.

Schulze,E.S, Asai,D.J., Bulinski,J.C. and Kirschner,M. Posttransla-tional modification and microtubule stability: *Journal of Cell Biology*; 1987; **105**; 2167-2177.

Schulze,E.S. and Kirschner,M. Distribution and dynamics of stable microtubules in interphase cells: *Journal of Cell Biology*; 1986; **103(5)**; A432.

Schulze,E.S. and Kirschner,M. Microtubule dynamics *in vivo*: *Journal of Cell Biology*; 1987; **S11B**; 133.

Seremetis,S., Inghirami,G., Ferrero,D., Newcomb,E.W., Knowles,D.M., Dotto,G.P. and Dalla-Favera,R. Transformation and plasmacytoid differentiation of EBV-infected human B lymphoblasts by ras oncogene: *Science*; 1989; **243**; 660-663.

Shapiro,J.E., Hershenov,B.R. and Tulloch,G.S. The fine structure of Haematolaechus spermatozoon tail: Journal of Biophysical and *Biochemical Cytology*; 1961; **9**; 211-222.

Shpetner,H.S. and Vallee,R.B. Identification of dynamin, a novel mechanochemical enzyme that mediates interactions between microtubules: *Cell*; 1989; **59**; 421-432.

Shyamala,M., Segarini,P.R., Atcheson,C.L. and Kasamatsu,H. Expression of a centriolar antigen in TC7 cells: *Journal of Cell Biology*; 1982; 95(2); A25.

Silveira,M. and Porter,K.R. The spermatozoids of flatworms and their microtubular systems: Protoplasma; 1964; 59; 240-248.

Singer,S.J. and Kupfer,A. The directed migration of eukaryotic cells: *Annual Review of Cell Biology*; 1986; **2**; 337-365.

Skoufias,D.A., Burgess,T.L., and Wilson,W. Spetial and Temporal colocalization of the Golgi apparatus and microtubules rich in detyrosinated tubulin: *Journal of Cell Bilogy*; 1990; **111**; 1929-1937.

Small,J.V. and Langager,G. Organization of actin in the leading edge of cultured cells: Influence of osmium tetroxide and dehydration on the ultrastructure of actin meshwork: *Journal of Cell Biology*; 1981 **91**; 695-705.

Smith,Z.D.J., Eugenio-Gumkowski,F., Yanagisawa,K., and Jamieson,J.D. Endrogenous and monoclonal antibodies to the rat pankreatic acinar cell Folgi complex: *Journal of Cell Biology*; 1984; **98**; 2035-2046.

Snyder,J.A. Evidence for a ribonucleoprotein complex as a template for microtubule initiation *in vivo*: *Cell Biology Int. Rep.*; 1980; **4**; 859-868.

Sorokin,S.P. Centrioles and the formation of rudimentary cilia by fibroblasts and smooth muscle cells: *Journal of Cell Biology*; 1962; **15**; 363-377.

Sorokin,S.P. Reconstructions of centriole formation and ciliogenesis in mammalian lungs: *Journal of Cell Sciences*; 1968; **3**; 207-230.

Southwick,F.S. and Hartwig,J.H. Acumentin, a protein in macrophages which caps the "pointed" end of actin filaments: *Nature*; 1982; **297**; 303-307.

Spizz,G., Roman,D., Strauss,A. and Olson,E.N. Serum and fibroblast growth factor inhibit myogenic differentiation through a mechanism depent on protein synthesis and independent of cell proliferation: *The Journal of Biological Chemistry*; 1986; **26(20)**; 9483-9488.

Stacey,D.W. and Kung,H.F. Transformation of NIH-3T3-cells by microinjection of Ha-ras p21-protein: *Nature*; 1984; **310(5977)**; 508-511.

Sternberg,E.A., Spizz,G., Perry,M.E. and Olson,E.N. A ras-dependent pathway abolishes activity of a muscle-specific enchancer upstream from the muscle creatine kinase gene: *Molecular and Cellular Biology*; 1989; **9**; 594-601.

Stearns,T., Evans,L. and Kirschner,M. Gamma-tubulin is a highly conserved component of the centrosome: *Cell*; 1991; **85**; 825-836.

Stewart,U.G. Immunochemistry of cytoplasmic contractile proteins: *International Review of Cytology*; 1986; **65**; 192-254.

Stopac,D. and Harris,A.K. Connective tissue morphogenesis by fibroblast traction: *Developmental Biology;* 1982; **90**; 383-398.

Sullivan,K.F. Structure and utilization of tubulin isotypes: *Annual of Review of the Cell*; 1988; **4**; 687-716.

Sullivan,K.F., Havercroft,J.C. and Cleveland,D.W. Primary structure and expression of a vertebrate b-tubulin gene family. In molecular biology of the cytosksleton: *Cold Spring Harbor*, NewYork.; 1984.

Sullivan,I.M. and Quigley,J.P. An anti catalytic monoclonal antibody to avian plasminogen-activator its effects on behavior of RSV-transformed chick fibroblasts: *Cell*; 1986; **45(6)**; 905-915.

Sutoh,K. and Hatano,S. Actin-fragmin interactions as revealed by chemical cross-linking: *Biochemistry*; 1986; **25**; 435-440.

Takahashi,K., Heine,U.I., Junker,J.L., Colburn,N. and Rice,J.M. Role of cytoskeleton changes and expression of the H-*ras* oncogene dirung promotion of neoplastic transformation in mouse epidermal JB6 cells: *Cancer Research*; 1986; **46(11)**; 5923-5932.

Tartakoff,A.M. Simplifying the complex Golgi: *Trends of Biological Science*; 1982; **7**; 174-176.

Tassin,A.M., Maro,B. and Bornens,M. Fate of microtubule organizing centers during myogenesis *in vitro*: *Journal of Cell Biology*; 1985a; **100**; 35-46.

Tassin,A.M., Paintrant,M., Berger,E.G. and Bornens,M. The golgi apparatus remaines associated with microtubule organizing centers during myogenesis: *Journal of Cell Biology*; 1985b; **101**; 630-638.

Terai,M., Komiyama,M. and Shimada,Y. Myofibril assembly is linked with vinculin, alpha-actinin, and cell-substrate contacts in embryonic cardiac myocytes *in vitro*: *Cell Motility and the Cytoskeleton*; 1989; **12**; 185-194.

Theriot,J.A. and Mitchison,T.J. Actin tracks: *Nature* ; 1991; **354**; 363-364.

Thyberg,J. and Moskalewski,S. Microtubules and the organization of the Golgi complex: *Experimental Cell Research*; 1985; **159**; 1-16.

Tomasz,M., Lipman,R., Chowdary,J., Pawlak,J., Verdine,G.L., and Nakanishi,K. Isolation and structure of a covalent cros-link adduct between mitomycin C and DNA: *Science*; 1987; **235**; 1204-1208.

Toriyama,M., Ohta, Endo,S. and Sakai,H. 51 kD protein, a component of microtubule-organizing granules in the mitotic apparatus involved in aster formation *in vitro*: *Cell Motility and the Cytoskeleton*; 1988; **9**; 117-128.

Toshia,A., Shibata,Y., and Yamamoto,T. Three-dimensional visiualization of basal structures ans some cytoskeletal components in the apical zone of tracheal ciliated cell: *Journal of Ultrastructural Research*; 1985; **93(1)**; 61-70.

Tousson,A., Zeng,C., Brinkley,B.R. and Valdivia,M.M. Centrophilin: A novel mitotic spindle protein involved in microtubule nucleation: *Journal of Cell Biology*; 1991; **112**; 427-440.

Troutt,L.L. and Burnside,B. The unusual microtubule polarity in teleost retinal-pigment epithelial cells: *Journal of Cell Biology*; 1988; **107(4)**; 1461-1464.

Tucker,R.W. and Pardee,A.B. Centriole ciliation is related to quiescence and DNA synthesis in 3T3 cells: *Cell*; 1979; **17**; 527-535.

Tucker,J.B., Paton,C.C., Richardson,G.P., Mogensen,M.M. and Russel,I.J. A cell surface-associated centrosomal layer of microtubule-organizing material in the inner pillar cell of the mouse cochlea: *Journal of Cell Science*; 1992; **102**; 215-226.

Turksen,K., Aubin,J.E. and Kalnins,V.I. Identification of a centriole-associated protein by antibodies present in normal rabbit sera: *Nature*; 1982; **298**; 763-765.

Urbancikova,M. and Grofova,M. Immunofluorescent detection of actin cytoskeleton in spontaneously transformed and B77-supertransformed cells using antibody to tropomyosin: *Neoplasma*; 1990; **37(6)**; 703-711.

Valdivia,M.M. and Brinkley,B.R. Kinetochore/centromere of mammalian chromosomes. In molecular biology of the cytoskeleton: *Cold Spring Harbor*, NewYork; 1984.

Valle,R.B. MAP2 (microtubule-associated protein 2), in cell and muscle motility. Vol.5, The Cytoskeleton (Ed. J.W. Shay): *Planum Press*. NewYork; 1984.

Vandekerckhove,J., Debobin,A., Nassal,M. and Wieland,T. The phalloidin binding site of F-actin: *EMBO Journal*; 1985; **4**; 2815-2818.

Vandekerckhove,J., Bugaisky,G. and Buckingham,M. Simultaneous expression of skeletal muscle and heart actin proteins in various striated muscle tissues and cells: *Journal of Biological Chemistry*; 1986; **261**; 1838-1843.

Verderame,M., Alcorta,D., Egnor,M., Smith,K. and Pollack,R. Cytoskeletal F-actin patterns quantitated with fluorescein isothiocyanate-phalloidin in normal and transformed cells: *Proceedings of the National Academy of Sciences of the U.S.A.*; 1980; **77(11)**; 6624-6628.

Volk,T., Fessler,L.I. and Fessler,H. A role for integrin in the formation of sarcomeric cytoarchitecture: *Cell*; 1990; **63**; 525-536.

Vorobjev,I.A. and Chentsov,Y.S. Centriols in the cell cycle 1. Epithelial cells: *Journal of Cell Biology;* 1982; **98**; 938-949.

Wakelam,M.J.O. and Pete,D. Myoblast fusion calcium and receptor occupation: *Abstract of FEBS meeting 15*; 1983.

Wang,Y.L. Reorganization of actin filament bundles in living fibroblasts: *Journal of Cell Biology*; 1984; **99(4)**; 1478-1485.

Wang,E. and Goldberg,A.R. Changes in surface-thography and microfilament organization upon transformation of chick-embryo fibroblasts with rous-sarcoma virus: *Journal of Cell Biology*; 1976; **70(2)**; A122.

Wang,K., McClure,J. and Tu,A. Titin: Major myofibrillar components of striated muscle: *Proceedings of the National oAcademy of Sciences of the U.S.A.*; 1979; **76(8)**; 3698-3702.

Wang,K. and Williamson,C.L. Identification of an N2 line protein of striated muscle: *Proceedings of the National Academy of Sciences of the U.S.A.*; 1980; **77(6)**; 3254-3258.

Wang,Y. Reorganization of actin filament bundles in living fibroblast: *Journal of Cell Biology*; 1986; **99**; 1478-1485.
Watkins,S.C., Samuel,J.L., Marotte,F., Bertiers,B. and Rappaport,L. Microtubules and desmin filaments during on set of heart hypertrophy in rat - a double immunoelectron microscopy study: *Circulation Research*; 1987; **60(3)**; 327-336.

Watt,F.M., Harris,H., Weber,K. and Osborn,M. The distribution of actin cables and microtubules in hybrids between malignant and non-malignant cells and in tumours derived from them: *Journal of Cell Sciences*; 1978; **32**; 419-432.

Way,M. and Weeds,A. Actin-binding proteins: Cytoskeletal ups and downs: *Nature*; 1990; **344**; 292-294.

Weber,K., Rathke,P.C., Osborn,M. and Franke,W.W. Distribution of actin and tubulin in cells and in glycerinated cell models after treatment with cytochalasin B (CB): *Experimental Cell Research*; 1976; **102**; 285-297.

Wehland,J., Willingham,M.C. and Sandoval,I.V. A Rt monoclonal antibody reacting specifically with the tyrosylated form of alpha-tubulin: *Journal of Cell Biology*; 1983; **97**; 1467-1475.

Wehland,J. and Weber,K. Turnover of carboxy-terminal tyrosine of alpha-tubulin and means of reaching elevated levels of detyrosination in living cells: *Journal of Cell Science*; 1987; **88**; 185-203.

Weil,D., Boyle,K. and Diamond,L. Effects of phorbol esters on human-melanoma cell-lines: *Proceedings of the American Association for Cancer Research*; 1986; **27(March)**; 47.

Whatley,G. Cell biology monographs. Vol II. (Alfert,M. Ed.): *Springer Varlag*; 1975.

Wheatley,D.N. Cilia in cell-cultured fibroblasts I. on their occurrence and relative frequencies in primary culture and established cell lines: *Journal of Anatomy;* 1969; **105**; 351-362.

Wheatley,D.N. The centriole: A central enigma of cell biology: *Elsevier*, NewYork; 1982.

White,J., Kielian,M. and Heleius,A. Membrane fusion proteins of enveloped animal viruses: *Quarterly Reviews of Biophysics*; 1983; **16**; 151-195.

Wiche,G., Herrmann,H., Dalton,J.M., Foisner,R., Leichtfried,F.E., Lassmann,H., Koszka,C. and Briones,E. Molecular aspects of MAP-1 and MAP-2: Microheterogenety, *in vitro* localization and distribution in neuronal and non-neuronal cells: *Annual NewYork Academy of Sciences*; 1986; **466**; 180-198.

Willingham,M.C., Yamada,K.M., Yamada,S.S., Pouyssegur,J. and Pastan,I. Microfilament bundles and cell shape are related to adhesiveness

to substratum and are dissociable from growth control in cultured fibroblasts: *Cell*; 1977; **10**; 375-380.

Wulf,E., Deboben,A., Bautz,F.A., Faulstich,H. and Wieland,T. Fluorescent phalloidin, a tool for the visualization of cellular actin: *Proceedings of the National Academy of Sciences of the U.S.A.*; 1979; **76(9)**; 4498-4502.

Yablonka-Reuveni,Z., Balestreri,T.M. and Bowen-Pope,D.F. Regulation of proliferation and differentiation of myoblast derived from adult mouse skeletal muscle by specific isoforms of PDGF: *The Journal of Cell Biology*; 1990; **111**; 1623-1629.

Yarbrough,L.R. and Fishback,J.L. Kinetics of interaction of 2-amino-6-mercapto-9-b-ribofuranosylpurine-5'-triphosphate with bovine brain tubulin: *Biochemistry*; 1985; **24(7)**; 1708-1714.

Yaffe,D. Tissue culture: Methods and applications. Kruse,P.P. and Patterson,M.K. Eds.: *Academic Press*, New York; 1973.

Yaffe,D., and Saxel,O. Serial passaging and differentiation of myogenic cells isolated from dystrophic mouse muscle: *Nature*; 1977; **270**; 725-727.

Zalin,R. The cell cycle myoblast differentiation and prostaglandin as a developmental signal.: *Developmental Biology*; 1979; **71**; 274-288.

Zheng,Y., Katherine,J. and Oakley,R. Gamma-tubulin is present in Drosophila melanogaster and homo sapiens and is associated with the centrosome: *Cell*; 1991; **85**; 817-823.

Zot,A.S. and Potter,J.D. Structural aspects of troponin-tropomyosin regulation of skeletal muscle contraction: *Annual Review of Biophysics and Chemistry*; 1987; **16**; 535-559.